Groundwater, Pore Pressure and Wall Slope Stability

– a model for quantifying pore pressures

in current and future mines.

A thesis submitted in partial fulfilment of the requirements for the

degree of

Master of Science in Engineering Geology

in the

University of Canterbury

by

Richard J. Brehaut

University of Canterbury

2009

TABLE OF CONTENTS

TABLE OF FIGURES

LIST OF TABLES

Frontispiece

The South East Prongs, Tom Price – June 2008.

Acknowledgements

First of all I would like to say a big thanks to my supervisor David Bell for all the hard work and guidance you have given me over the past eighteen months. Your experience and judgement has been sincerely appreciated, not to mention your sense of humour and hospitality on the many field trips we took together.

A massive thank you goes out Rio Tinto Iron Ore and especially to my co-supervisors George Domahidy and Phil de Graaf for the ongoing support, enthusiasm and valuable revisions of work throughout the duration of this thesis. Without your input both through advice and generous use of resources my project would not have been able to get off the group let alone over the obstacles along the way. Further thanks must go to the other members of the Resource Development team in Perth that kindly offered their knowledge and advice during this project.

To the Tom Price Technical Services team, I really appreciate you putting up with me as I tagged along during my time on site. I would especially like to thank Lindsey Campbell, Chris New, Tim Kendrick, Leigh Nicholas and Dave Sepe for their assistance as I worked the details of my project and answered my endless questions. Peter Croft from Brockman Solutions Ltd, your understanding of all things structural was magic, thanks heaps for helping me off to a great start.

Yet another big thanks to David Lucas and colleagues at MiningOne Consultants, Melbourne. Your ongoing correspondence and knowledge was invaluable not to mention your assistance with the geotechnical component of my study. Thank you also to Mark Eggers and colleagues from PSM Sydney that assisted me during the initial stages of my research.

I would like to acknowledge the generous support that both Geo-Slope International and Rocscience Inc have given me in providing licences to their specialist software for the duration of my study. Special thanks must be extended to Curtis Kelln of Geo-Slope for his ongoing advice and comprehensive audit of my seepage model.

I would like to thank all my friends and fellow students from the department that have made my post graduate experience so enjoyable over the last couple of years. Finally, Mel thanks for the all of the hours you have spent encouraging and supporting me as well as the endless revisions during my write up, I couldn't have done it without you.

Abstract

The Hamersley Province, located approximately 1200 km north of Perth, Western Australia forms part of the southern Pilbara craton, an extensive area of Band Iron Formations (BIF). The area has a high economic significance due to several enrichment stages of the country rock (BIF) resulting in several large high-grade iron ore deposits. Mount Whaleback near Newman and Mount Tom Price are the largest deposits, where reserves have been estimated at 1400 Mt and 900 Mt respectively. These ore bodies have been quantified as being high grade resources at approximately 64 % iron, with a high lump to fines ratio, and low impurities. The Mount Tom Price ore body is a hematite-rich ore, associated with a variety of shale and some dolomitic units (MacLeod et al., 1963, MacLeod, 1966, Taylor et al., 2001, Morris, 1980).

The local hydrogeology of the Mount Tom Price area involves two main aquifer systems. The Dales Gorge member of the Brockman Iron Formation with contributions from the upper mineralised section of Footwall zone make up the main semi confined aquifer within the area. The underlying low permeability Mount McRae Shale and Mount Sylvia Shale lithologies separate a secondary aquifer which is located within the Wittenoom Formation. A dewatering program within Mount Tom Price has been ongoing since installation in 1994.

Within the open pit mining industry, pits depths are increasingly being deepened as the easily accessible surface ore has been removed. This involves excavating pit walls below the existing groundwater table, which can lead to instabilities within pit walls. Added to this is the timing and economic considerations which need to be accounted for in a working mine. As dewatering and depressurisation are pivotal to the extraction of ore resources below the groundwater table, there can often be considerable time pressures to maintain planned mine developments (Hall, 2003).

The South East Prongs pit, located within the Mount Tom Price mine, holds some of the most valued low impurity, high grade hematite ore. Structurally the South East Prongs is unique as the deposit lies in the base of a steeply dipping double plunging syncline, intersected by the Southern Batter Fault which runs parallel in strike to the Turner Syncline.

The current pit floor of South East Prongs is located at 600 mRL. The long term development plan for the western end of this pit includes a further 30 m of excavation to a final depth of

570 mRL. This currently poses a number of stability issues that require resolution before any development can be undertaken.

A conceptual understanding of flow dynamics within structurally complex wall rock environment has been generated through the utilisation of finite element numerical modelling. The complex structural setting within the northern wall of the South East Prongs has shown to interact with high conductivity lithologies to promote preferential flow of groundwater from the underling Wittenoom Formation aquifer. Recharge to the semi confined DG aquifer occurs as groundwater travels up shear zones within the South East Prongs Fault Zone before migrating along Brunos Band.

An investigation into alternative methods of depressurisation has been recommended to ensure the ongoing management of pore water pressures within the northern pit wall during planned pit cut backs. Limiting recharge from the WF to the pit through stated preferential flow paths has been identified as a potential issue when the remaining DG aquifer is removed. Maintaining the proposed dewatering buffer will be difficult to achieve using the current system.

The ability to design optimal pit shells for access and ore recovery as well as an effective dewatering and depressurisation system relies heavily on the a sound geological model. Further to this, time allocations to ensure forward planning deadlines are met can be significantly interrupted if adjustments to initial plans are required.

Chapter 1: Introduction

1.1 Preamble

The Hamersley Province (Figure 1-1), situated approximately 1200 km north of Perth, forms part of the southern Pilbara craton. The Hamersley Province covers an area of approximately 80,000 km^2. The Mount Bruce Supergroup is the primary stratigraphic succession within the area, containing the ~2.5 km thick stratified assemblage known as the Hamersley Group which is the focus of this study.

The Hamersley Province has a world renowned reputation as having some of the most extensive examples of Banded Iron Formations (BIF) on earth. BIF represent the largest volumes of iron on the Earth's surface. Formed during the late Archean and Paleoproterozoic, BIF are characterised by well developed, thin laminations of iron rich material interbedded with iron poor material (Robb, 2005, Simonson, 2003).

BIF of the Hamersley Province are a classic example of "Superior BIF". These formations were generally deposited on stable continental shelf platforms away from the influence of wave action. At times these deposits interacted with the wave base, and cross beds are seen within some of the Hamersley units (Robb, 2005, Simonson, 2003).

BIF were formed in unique atmospheric, hydrospheric, lithospheric and biospheric conditions. These conditions were particularly sensitive to the acidity and redox state of the depositional environment. The typical mineral assemblages of BIF are iron oxides (haematite or magnetite), carbonates, silicates and sulphides. Cherts and carbonaceous shales often occur together with iron minerals (Robb, 2005, Simonson, 2003).

Groundwater within the Pilbara region is primarily derived from three main aquifer types. Shallow unconfined aquifers are present in recent alluvial deposits which can include calcrete. Semi confined aquifers can be found in palaeovalley fill deposits throughout the region. Finally, confined aquifers are located in the fractured and cavernous bedrock that makes up the majority of the region.

The Hamersley region is of high economic significance due to several enrichment stages of the country rock (BIF) resulting in several large high-grade iron ore deposits. Mount Whaleback near Newman and Mount Tom Price are the largest deposits, where reserves have been estimated at 1400 Mt and 900 Mt respectively. These ore bodies have been quantified as

being high grade resources at approximately 64 % iron, with a high lump to fines ratio, and low impurities. The Mount Tom Price ore body is a hematite-rich ore, associated with a variety of shale and some dolomitic units (MacLeod et al., 1963, MacLeod, 1966, Taylor et al., 2001, Morris, 1980).

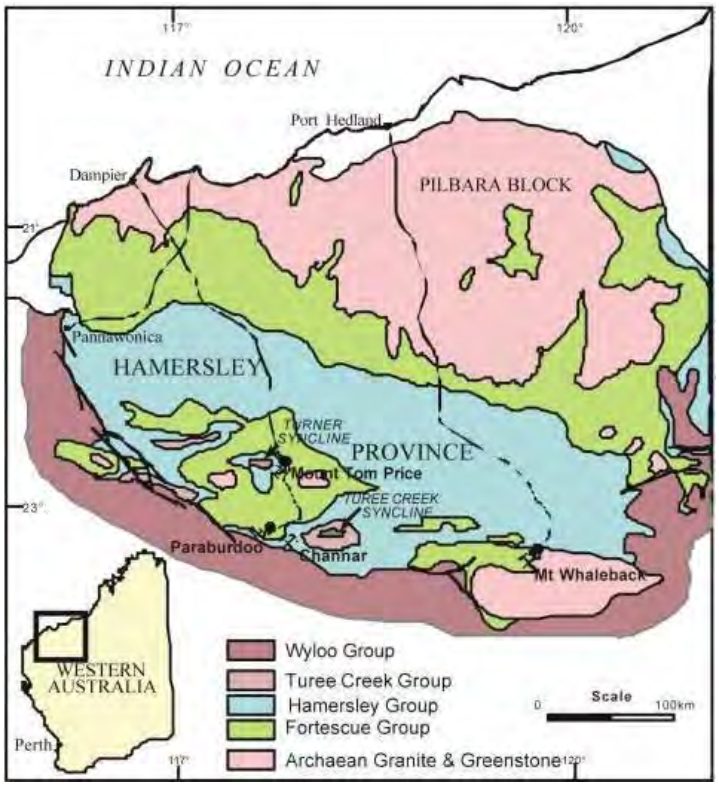

Figure 1-1 - Location and extent of the Hamersley Province (Taylor et al., 2001).

Open pit mining is one of the most financially viable mining methods. It allows for a high grade of mechanisation and large production volumes. Very low grade deposits, which would be uneconomic to mine by underground methods, are feasibly mined through open pit mining. Depths of open pits have increased in recent decades and commonly exceed over 500 m (Mandzic, 1992, Powers et al., 2007).

A complicating factor of deeper pits is the increased risk of large scale stability issues. These issues often result from geological and hydrogeological interactions. This effect can also be exasperated by the economic and design considerations of the mining operation. One of the most significant issues in mining today is the control of groundwater and the associated problems it creates, such as a reduction in the effective stress of a rockmass. Problems with water in mining situations tend to be unique, especially in hard rock deposits where the geology and hydrogeology are often complex (Atkinson, 2001). Dewatering and

depressurisation are two methods commonly used to mitigate the effects of groundwater levels interacting with large excavations. However, there is much more to lowering the groundwater table than simply installing a pumping well. (Harmen et al., 2007)

As dewatering and depressurisation are pivotal to the extraction of ore resources below the groundwater table, there can often be considerable time pressures to maintain planned mine developments (Hall, 2003).

The South East Prongs (SEP) pit, located within the Mount Tom Price mine, holds some of the most valued high grade hematite ore with low impurities of the entire eleven mine network based in the Pilbara. Maximum recovery of this resource is therefore a fundamental component contributing towards the ongoing success of the Rio Tinto Iron Ore (RTIO) product.

Primarily ore recovery was carried out above the groundwater table requiring relatively little hydrogeological related investigation. A sustainable water supply for the mining towns of Tom Price, Paraburdoo and Panawonica was the primary reason for the initial hydrogeological studies (Hedley and Domahidy, 2007)

However as current operations at the SEP are far below the pre mining groundwater table and with pit walls to be steepened, to access the remaining ore within the deposit, the ongoing management of the hydrogeology within this pit is pivotal to the success of the Mount Tom Price operation.

A number of small pit wall failures and one large failure have occurred during the development of the SEP pit. As developments continue in line with the long term mine plan, sensitivities within the rock mass will require careful management to ensure the integrity of the pit walls is maintained. This will contribute towards both a safe operational environment and increased economic returns through maximisation of ore recovery.

1.2 Thesis Objectives

The aim of this study is to combine an understanding of the localised hydrogeological conditions within South East Prongs, with knowledge of the geotechnical characteristics of the rock mass to determine whether the current level of depressurisation within the pit is adequate in providing suitable pit slope stability for ongoing operations within the area.

The principal hypotheses of this thesis are that:

- There will be a measurable decline in pit wall piezometric pressures following installation of the horizontal drainage systems.
- This will also be reflected by an increase in the two dimensional factor of safety based on available geological and geotechnical models.
- A predictive model can be developed to improve slope stability (and hence mine safety) by strategically planned drainage measures in advance of pit floor lowering.

1.3 Research Methods

- An extensive literature review has been undertaken to outline fundamental concepts associated with rock mass characterisation and hydrogeology. These ideas have been incorporated into best practice procedures for the successful undertaking of dewatering, depressurisation and slope design. In addition to this, an introduction into the engineering applications of numerical analysis has been included.
- Field work was completed over a five week period (May to June) during 2008. Throughout this time, interviews were conducted with personnel from specific departments (Perth based resource development team and Mount Tom Price technical services group) to gain an initial understanding of the mines operations from a number of perspectives. This was followed by a program of data acquisition. Structural geology mapping data was supplied by Brockman Solutions Ltd who had recently completed a comprehensive field study of the SEP pit. Groundwater levels were acquired through the RTIO hydrogeological database as well as weekly piezometer monitoring runs while on site.

  An introduction to the specific geotechnical characteristics of the SEP was gained while at the Mount Tom Price operation. In addition to this, a five day visit to MiningOne Consultants Ltd in Melbourne provided a comprehensive insight into the rockmass model and associated geotechnical database that was to be utilised in the stability analysis of the SEP.
- Finite element numerical modelling was utilised to create a conceptual groundwater model to simulate the effectiveness of the currently installed passive horizontal drain hole depressurisation system. Steady-state analysis provided equilibrium solutions while a progressive transient analysis conceptually illustrated the time dependant response of the ground water table to horizontal drainage.

- A geotechnical stability analysis was undertaken using a limit equilibrium numerical model. This study aimed to identify sensitivities within the rockmass through a number of trials and to ultimately determine the effectiveness of the horizontal depressurisation system. Two rockmass strength characteristics were simulated in combination with the progressively lowering phreatic surface outputs obtained from the previous hydrogeological drawdown analysis.
- The resulting Factor of Safety outputs from the geotechnical stability analysis were utilised as a means of quantifying the effectiveness of the horizontal drainholes. This provided a means of predicting future drainage requirements for the SEP pit to ensure the ongoing stability of the pit slopes.

Chapter 2: Literature Review

2.1 Introduction

One of the most cost effective mining methods is open pit; this allows a high grade of mechanisation and large production volumes. Very low grade mineral deposits, which would be uneconomic to mine underground, are able to be mined using open pit methods. The depths of open pits have increased steadily over the last few decades with pit depths of over 500 metres common.

A complicating factor of increasing the depth of pits is the increased risk of large scale stability issues. These issues are the result of interactions between geological, hydrogeological factors and planning around the design and economics of mining operations (Sjoberg, 1996).

One of the most significant issues in mining today is the control of groundwater and the associated problems it creates. Problems with water in mining situations tend to be unique, especially in hard rock deposits where the geology and hydrogeology are often complex (Atkinson, 2001). For this reason it is of the utmost importance to have a comprehensive understanding of a sites subsurface conditions, before the design phase of a project is initiated.

This chapter aims to outline the fundamental principles that are necessary to understanding the principle factors involved in a open pit slope stability assessment. This includes rockmass characterisation, failure mechanisms, slope design criteria, hydrogeological regimes, dewatering and depressurisation planning and infrastructure. In addition to this an insight into methods of forward prediction and analysis has been included through the utilisation of numerical models for ground water and geotechnical sensitivity.

2.2 Rock Mass Characteristics

When assessing the stability of a slope for construction or a potential development site a sound understanding of rock mass discontinuities is of key importance. Structures present in the rock mass (i.e. bedding planes, faults ,defect sets joints and cleavage) contribute towards the overall integrity of the slope (Bell and Pettinga, 1983, Wyllie and Mah, 2006, Cornforth, 2005). The relationship between the orientation of a proposed slope and the identified discontinuities is significant when establishing whether failure is possible. Day lighting of

discontinuities can allow rock to slide or topple when the slope is excavated (Wyllie and Mah, 2006).

2.2.1 Defects in Rock Masses

Defects or discontinuities with a rock mass are simply defined as a break in the continuity of a body of rock or soil substance. These create complexities when establishing potential stability with a slope and promote anisotropic strength characteristics. Table 2-1 outlines the main types of defects recognised in structural geology (Fell et al., 2005, Wyllie and Mah, 2006).

Table 2-1 - Common rockmass defects.

Defect Type	Definition and Description
Bedding	Layered or parallel arrangement of grains, developed during deposition as sediment.
Foliation	Layered or parallel arrangement of grains (often tabular or flakey in shape) developed either by viscous flow (in igneous rocks) or by pressure and heat (metamorphic rocks).
Cleavage	Foliation in which many surfaces have developed along which the substance splits readily
Lineation	Linear arrangement of (often elongated) grains, developed by viscous flow (in igneous rocks) or pressure with or without heat (in metamorphic rocks); the lines of grains may or may not lie within surfaces or layers of foliation.
Joints	Joints are usually defined as an almost planar surface or crack, across which the rock has little tensile strength. The presence of joint sets in a rock makes it less stiff and strong while being more permeable than the equivalent body of rock that is not jointed. Joint sets can be open (air filled) or conduits to water flow. Where water has been able to flow, weathering processes are often present. Alternatively joints can be soil, clay or rock filled. The joint surface can also range from rough to smooth and if displacement or movement has occurred along the joint surface slickenside can be evident. Size of joints can also range from less than a metre to tens of metres.
Faults (Sheared or crushed zones)	Regardless of the nature of displacement (normal, reverse, oblique and strike slip) a fault may show a zone of shearing or crushed material or a combination. Shearing and crushing of rocks within the plane of a fault is a good indicator of the rocks deformation properties. This can range from brittle to pseudo ductile. Fault zones often act as conduits to flow due to their highly fractured nature and corresponding high level of secondary permeability. Their orientation often intersects a number of lithologies that may also be water bearing units within the local strata. This allows interconnection of permeable units and water to flow through what would otherwise have a low hydraulic conductivity. Alternatively fault zones can be filled with clay or gouge fill, effectively forming barriers to flow. Rock located adjacent to fault zones where water is present can be exposed to preferential weathering processes, subsequently creating a weaker boundary layer of rock around the fault (Fell et al., 2005, Wyllie and Mah, 2006)

2.2.2 Effective stress

Terzaghi first illustrated the principle of effective stress experimentally in 1923. However this concept is only applicable to fully saturated soils comprised of a skeleton of particles encapsulating a multitude of void spaces. Effective normal stress σ' (often referred to as intergranular stress) is defined by Woodward (2005: pg 22) as "the stress transferred through the soil due to the intergranular contact and also controls the deformation occurring within a saturated soil". In addition, the internal stress acting within a materials grain structure can be measured using effective stress (Barnes, 2000).

2.2.3 Pore Pressure and Matric Suction

When external stress is applied to a soil above the water table, the air in the pores readily compresses under load. Below the water table, applied stress increases the level of pore water pressure in the saturated soil. Volume reduction in the soil then occurs as pore water drains. The rate at which this occurs is dependent on the permeability of the material and drainage conditions present (Woodward, 2005).

Negative pore pressure (or matric suction) within slopes can play a critical role in the stability of earthworks. This is a characteristic that has been identified but is not greatly understood and therefore often ignored during the design process by many geotechnical engineers (Rahardjo et al., 2003).

It has been noted that there is often variation within insitu soils, as they are exposed to unequal levels of horizontal and vertical stress. This tends to affect the stress conditions within the pore water of the soil and therefore is required to be accounted for in the associated soil mechanics. Matric suction is used by authors to represent a pressure deficiency measured from a small sample of soil free from external stress. The term negative pore water pressure is reserved for any pressure deficiency present within insitu soils or in a laboratory with the soil subject to the stress regime associated particular loading conditions under consideration (Croney and Coleman, 1960)

Blight, (1980) as in (Fredlund and Rahardjo, 1993) outlines a number of influential conditions which can act to vary the suction profile with a material:

Environmental: The matric suction profile below the ground surface is very susceptible to change, especially when environmental influences such as dry (matric suction increases) or wet seasons (matric suction decreases) are present. The suction profile deeper within the ground surface is more constant than that of one within the uncovered surface. An example

of this would be the suction profile beneath a house or pavement compared to that in an open paddock (Blight, 1980).

In the dry season when evaporation rates are high there is a net loss of water in the soil and hence a higher level of suction at these times. The opposite of this occurs during the wet season with a net of water due to precipitation and other infiltration into the soil.

Vegetation can also have an effect on the levels of matric suction within a soil as pressure on the ground surface can apply a tension to the pore pressure (of up to 1-2 MPa) through the evapotranspiration process. This results in a net loss of water in the soil causing higher levels of suction to occur (Blight, 1980).

Water Table affects the level of matric suction in the ground. The deeper the water table is the higher the potential suction. The closer to the surface the water table is the more significant of an affect it will have (Blight, 1980).

Permeability of the soil profile also plays a role of suctions levels as it defines the ability of the soil to change its level of matric suction resulting from environmental changes. Matric suction is a hydrostatic or isotropic pressure as it has an equal magnitude in all directions. Of special note is that the level of matric suction in a soil can be significant greater than that of the net normal stress acting on it (Blight, 1980). Figure 2-1 gives illustrative table of comparisons between matric and normal forces.

Equation 2-1

$$\textbf{Matric suction} = \mu_a - \mu_p$$

Where:

μ_a = Pore Air Pressure

μ_p = Pore water pressure

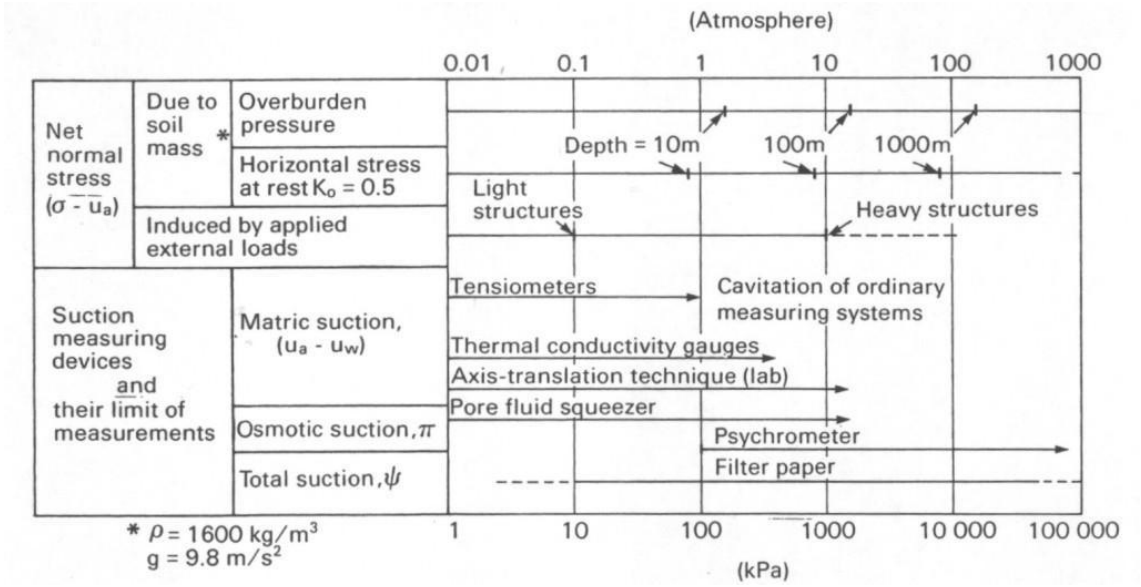

Figure 2-1 - Typical magnitudes of normal stress in relation to matric suction (Fredlund and Rahardjo, 1993).

2.3 Slope Design

After primary investigations into rock structure and defect orientation have been completed more specific geotechnical classifications of the rock mass are required such as shear strength and cohesion when developing an initial slope design. Wyllie and Mah (2006) discuss the relationships between sample size and rock strength characteristics. They note shear strengths taken at a single joint scale (for example) may not be applicable to the overall slope. To combat such misrepresentation, Wyllie and Mah (2006) have established three sub categories:

- Discontinuities – Single bedding planes, joints or faults. Properties that effect shear strength include shape and roughness of surfaces otherwise known as asperities. These can be either fresh or weathered. Infilling of joints and discontinuities can range from low strength to cohesive materials.
- Rock Mass – The factors that influence the overall shear strength of a jointed rock mass includes compressive strength (measures in laboratories using UCS system) and friction angles of the intact rock. Spacing and dilation of discontinuities as well as condition of infilling is also important to note.
- Intact Rock - Shear strength of intact rock can be measured during initial investigation and design however this has the possibility of reducing as the rock undergoes degradation over its design life.

Water has been shown to diminish the shear strength of discontinuities as a result of a reduction in the effective normal stress acting on the surface. The effective normal stress is defined as the difference between the weight of the overlying rock and the uplift pressures produced by the water as discussed in more detail below (Wyllie and Mah, 2006).

When planning a large mining pit/slope excavation there are a number of primary considerations that need to be taken into account. Overall slope height, geology, rock strength, influence of groundwater pressures and likely degradation of the rock mass through blasting are all key aspects of the site that require careful evaluation during the planning phase. Wyllie and Mah (2006) break down slope angle considerations into three main categories; overall slope angle, inter ramp angle and finally actual face angle of each batter. An annotated diagram of this has been included in Figure 2-2.

When determining respective slope angles the scale of defects needs to be accommodated. For example, the overall rock mass of the slope can have significantly different influential defects than the corresponding batter faces. On a single batter the length of a discontinuity can easily extend the entire distance of the face which will determine the appropriate rock mass strength to use for the inter ramp design (Wyllie and Mah, 2006).

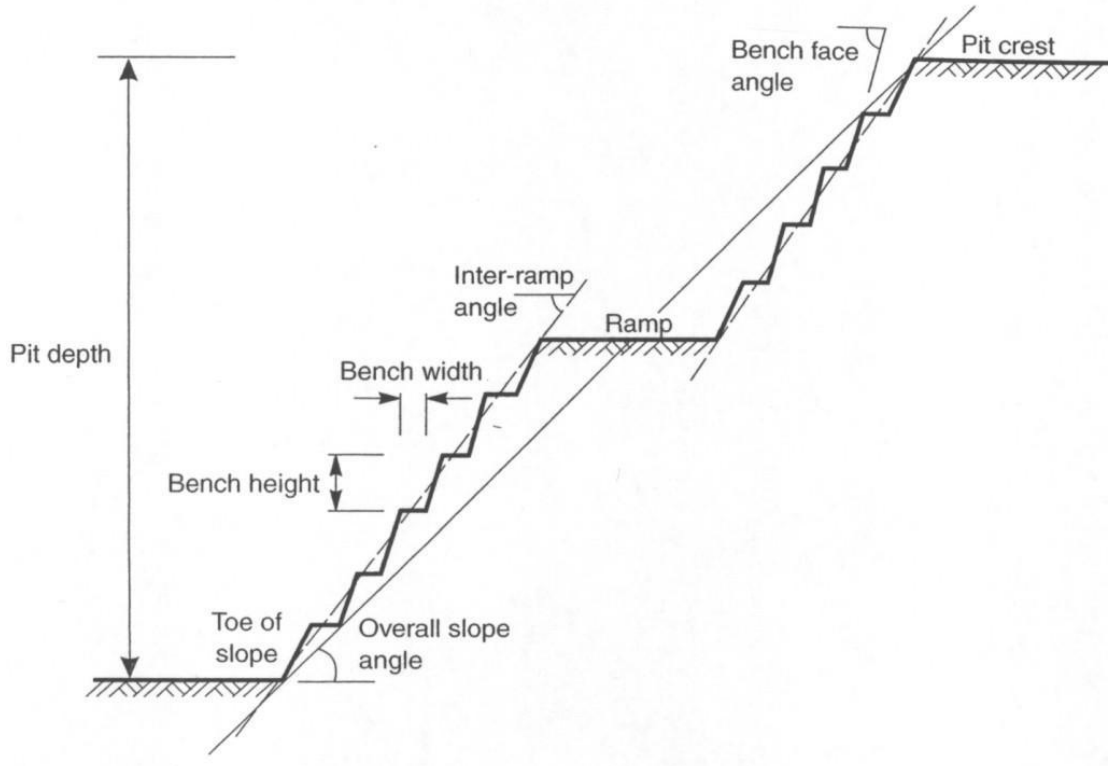

Figure 2-2 - Outline of pit slope design terminology and features after Wyllie and Mah (2006)

Identification of rock mass shear strength versus defect/discontinuity shear strength is a key consideration to be made when assessing the risk of potential slope instabilities (Wyllie and Mah, 2006). The processes that were responsible for creating the geological structures present at the site could still have an active component in complex landscapes such as those where mining and civil projects are often sighted. The likelihood of these processes continuing (such as faulting) could put the development at risk and therefore need to be fully constrained (Fell et al., 2005).

Wyllie and Mah (2006) note that the design life of mining slopes are set on much shortened time scales than equivalent civil projects as failure or even rock fall is much more tolerable than in the civil sector.

2.3.1 Fundamental Failure Mechanisms

"Assessment of rock slope failure mechanisms require an understanding of structural geology, groundwater and climate, rock mass strength and deformability, in situ stress conditions and seismicity. Stress relief associated with mining excavation leads to elastic rebound and ground relaxation displacements that dissipate with time, a process that is often referred to as time-dependent deformation" (Rose and Hungr, 2007: pg 308)page .

Planar Failure

Planar or translational failures are primarily bedding or defect controlled in nature. The plane on which sliding will occur needs to strike sub parallel (within approximately ± 20°) to the slope face. The slide plane must "daylight" within the slope which occurs when the dip angle of the plane is less than that of the slope ($\Psi p < \Psi f$). The dip of the plane must be greater than that of the materials friction angle of the designated plane. Finally the top of the plane must intersect the top of the slope or end in a tension crack at the head of the slope to allow release of the material. If the weight of the sliding block is offset equally or greater by an uplifting force of water pressure the potential for movement will be greatly increased. This is related to the cohesion and respective shear strength of the material in question. A schematic block diagram (Figure 2-3) outlines this failure concept (Wyllie and Mah, 2006).

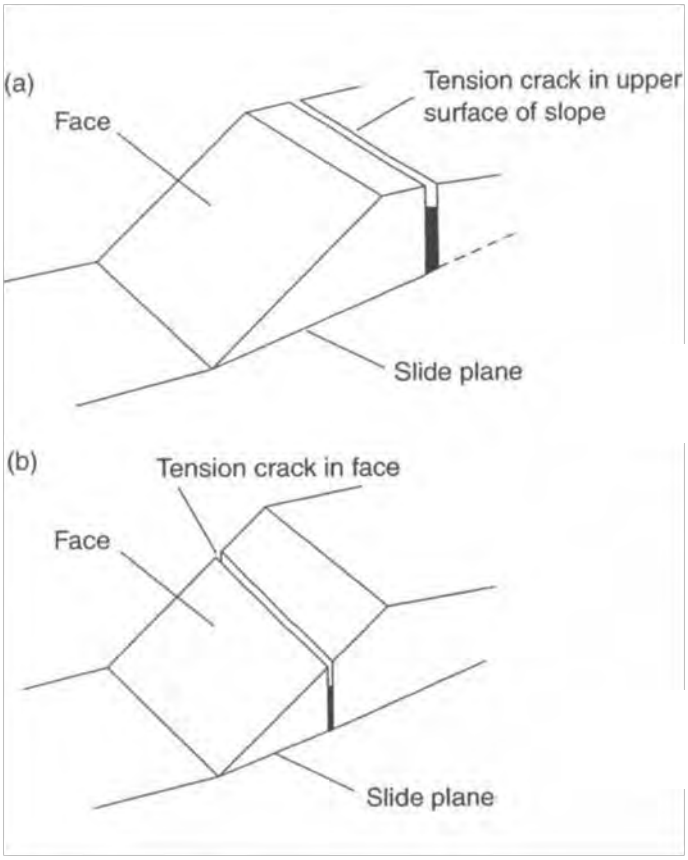

Figure 2-3 Break down of planar failure components. A) Identifies bench scale collapse with head scarp on surface. Part B) outlines possible breakout along from a tension crack. (Wyllie and Mah, 2006)

Wedge Failure

Wedge failures occur when discontinuities strike obliquely to a slope where sliding of a wedge of rock takes place alone lines of intersection. Wedge failures can occur over a much wider range of both geological and geometric conditions than the previously mentioned planar failures. As a result of this, prevention of wedge failures through rock slope engineering takes a comprehensive understanding of the rockmass characteristics. Typical geometry for a wedge failure to occur can be seen in Figure 2-4 where the cut slope has two continuous planar discontinuities and the line of intersection of these two planes daylights at the toe of the rock face. If the friction angle of the material is less than the angle of the line of intersection between the discontinuities, a release is likely to occur. If one of these factors is not present then it is not likely that a failure will occur. If a comprehensive structural data set for a given slope has been prepared, the prediction of potential wedge failure can be investigated through Stereonet analysis (Wyllie and Mah, 2006).

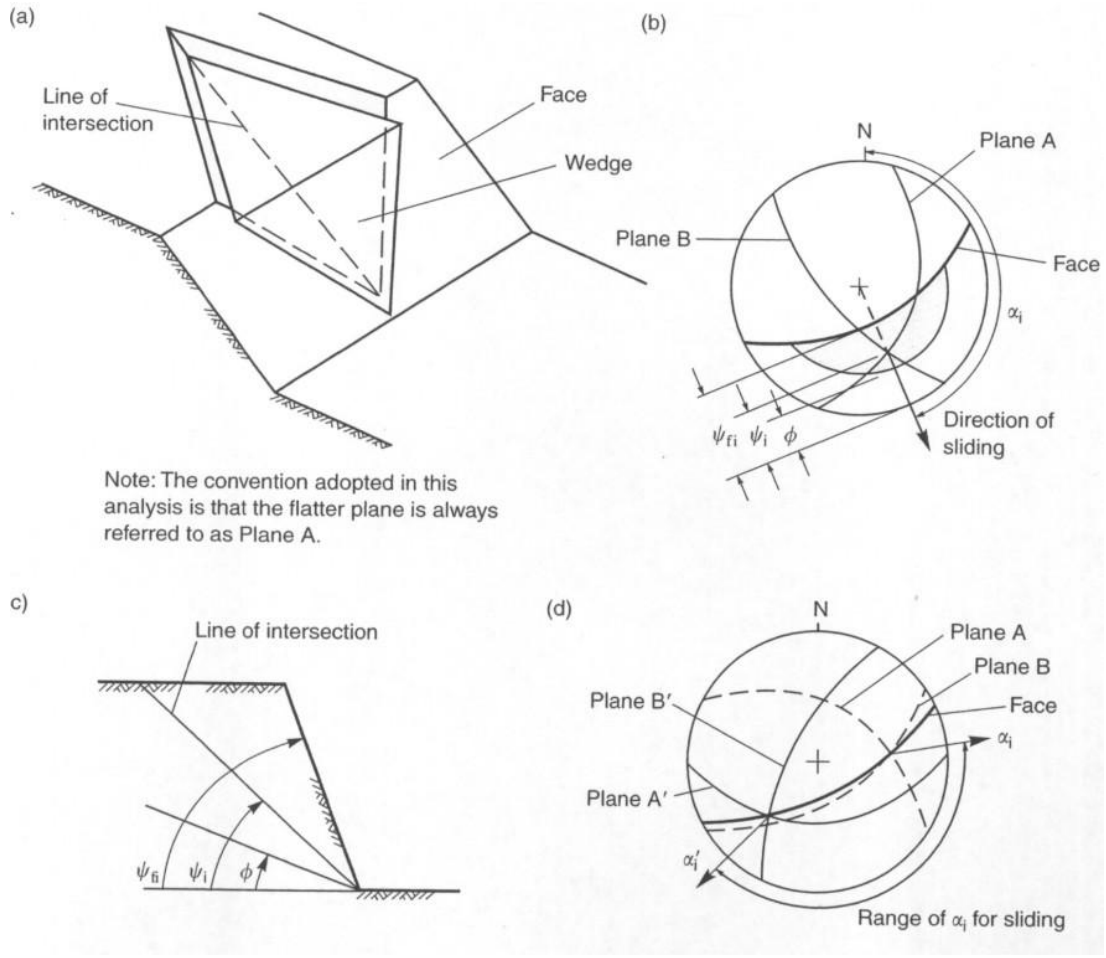

Figure 2-4 - Break down of wedge failures components. A) & C) show schematic illustrations of defect orientations in slope. B) & D) show respective stereo net plots of defect analysis for wedge failure (Wyllie and Mah, 2006).

Circular Failure

Circular failures most commonly occur in weaker slopes composed of soils rather than rock. Areas of hard rock that have extensive discontinuities or highly levels of weathering can act like a weak soil as can waste dumps on mine sites or other unconsolidated stockpiles. Circular failures are not limited to intersecting discontinuities or planes daylighting on slope; these have been shown to follow a path of least resistance which commonly forms a circular failure profile in the slope. Specific failure profiles are dependent on the material properties present within a slope. A homogeneous weak rock mass or rock fill is most likely to form a shallow large radius failure profile often extending from a tension crack at the head of the slope/scarp. In contrast a material with high cohesion and low friction angles such as clay rich soils are more likely to form deep small radius failure profiles. These failures also have the potential to extend below the toe of the slope and cause heave in the outlying ground especially when they occur in an engineered slope. Groundwater profiles with a particular

slope play a very important role in the propagation of circular failures. Figure 2-5 illustrates the geometry of a circular slope failure and the contributing forces present (Wyllie and Mah, 2006).

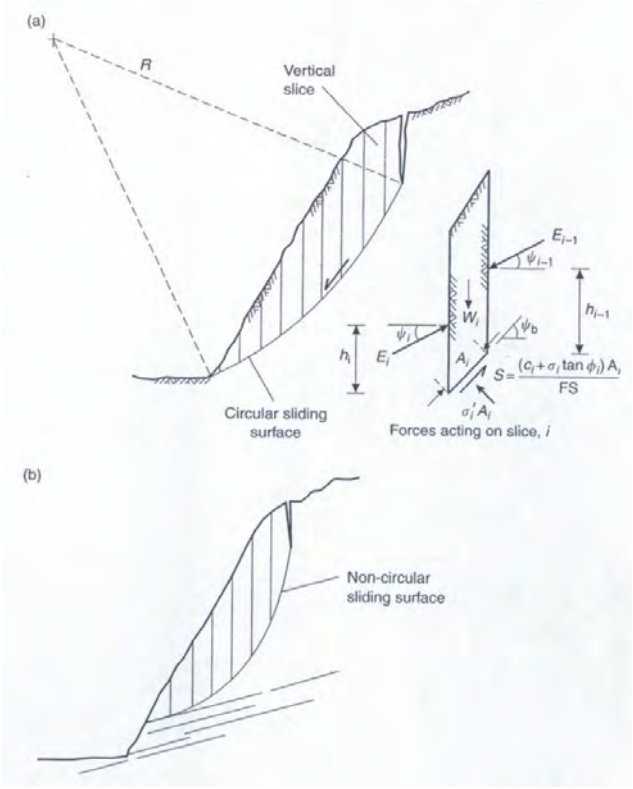

Figure 2-5 - Break down of circular failure component. Noted for detailed failure analysis the slip is broken into slices where respective forces can be examined (Wyllie and Mah, 2006).

Toppling Failure

Unlike the previous three failure mechanisms toppling failures are not dependant on existing or induced sliding surfaces. Instead they occur as a column or block of rock rotates out from a slope about a fixed base. The potential for toppling failure is fundamentally brought about by a steeply dipping rockmass orientated away from a cut slope. As the bedding is effectively overhanging the slope the rock begins to bend before toppling occurs as the name suggests.

There are a number of different types of toppling failures that can be catagorised by the way in which failure occurs. These include Block, Flexure, Block-flexure and secondary toppling modes. The type of toppling that is likely to occur is dependent on the material characteristics of the rock such as defect spacing, bedding thickness and material hardness. Common triggers for such failures include sliding, excavation or erosion of a slope which acts in a retrogressive nature forming deep tension cracks where the rockmass flexes forward from the

slope and failure occurs. Figure 2-6 illustrates the various models of toppling failure, of particular interest is the difference in block to flexure toppling (Wyllie and Mah, 2006).

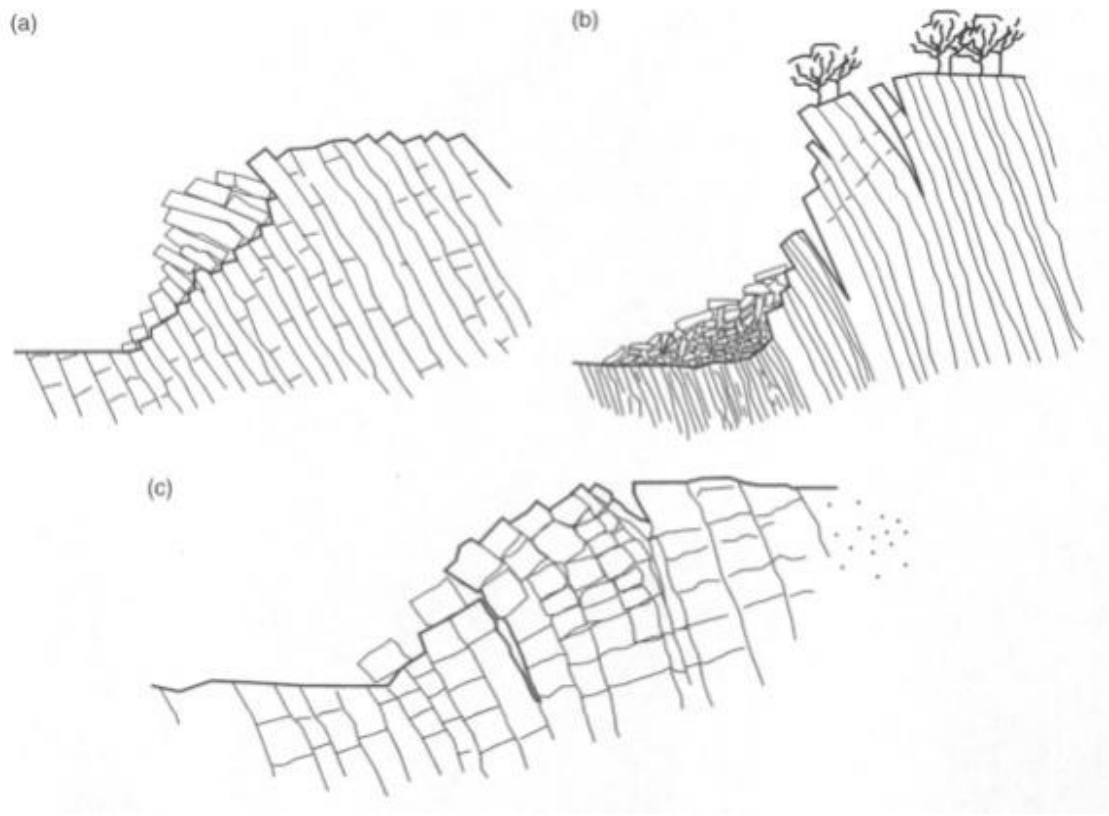

Figure 2-6 - Variations of Toppling failure a) Block toppling, b) Flexure toppling and c) Flexure block toppling failure mechanisms (Wyllie and Mah, 2006).

2.4 Groundwater

Groundwater in simple terms is water beneath the surface of the earth which saturates the pores and fractures of sand, gravel, and rock formations. Freshwater is distributed approximately as follows: 75 percent is locked in polar ice caps; nearly 25 percent exists as groundwater, and less than one percent in lakes, rivers and the atmosphere.

The supply of water on the earth although very large is none the less finite. The hydrologic cycle (Figure 2-7) is the circulation of water between the continents, the oceans, and the atmosphere (Deming, 2002). Water condenses in the atmosphere and falls on earth as precipitation. In temperate zones when precipitation falls, a portion runs off directly forming streams which flow towards the sea. Another portion is absorbed into the ground. Of this infiltration some never gets deeper than the soil horizon, this is known as the “vadose zone”. Of all the water absorbed into the ground some is evaporated back into the atmosphere, some

is used by vegetation, and is then returned to the atmosphere through evapotranspiration. Of the remaining water, a portion will stay in the upper soil horizon while the rest percolates downward and becomes groundwater. There is also a small (relative to other sources) percentage of water held within magmas deep in the earth's crust. This is known as magmatic water. If the magma rises up and reaches surface of the earth or the ocean floor water can be added to the hydrologic cycle. It is important to note however that the majority of steam associated with a volcanic event is not magmatic water but simply groundwater that has come in contact with the rising magma (Deming, 2002, Wyllie and Mah, 2006, Powers et al., 2007, Fetter, 1994).

This large proportion of groundwater effects construction as both growth and concentration of population has contributed to soaring land values and the demand to develop sites previously considered to be unsuitable (Powers et al., 2007, Deming, 2002).

This growth and development has not simply been constrained to the construction sector, the increasing demands for primary construction materials has forced the minerals industry to push for deepening open pit and underground mines. Increasingly mining operations are now working below the groundwater table which has presented numerous challenges for mine development.

Patterns of groundwater movement change from time to time with changes in climate and with natural changes in topography due to erosion and deposition. Mankind's activities have been modifying the groundwater situation for millennia. Land drainage projects lower the water table, while dams and surface reservoirs encourage infiltration, and when a river is confined within levee's infiltration is reduced (Powers et al., 2007).

Groundwater is defined as the water located below the water table and where by the material from this point below is primarily saturated. It is often referred to in other fields as the zone of saturation for this very reason. "The boundary between the saturated and unsaturated soil or rock where the pressure in pores is zero (p=0) relative to atmospheric pressure is the phreatic surface or otherwise known as the groundwater table" (Atkinson, 2001).The materials below the surface have an effect; sandy, free draining soils permit fairly rapid downward percolation of water. Conversely clays and silts (which have low hydraulic conductivity) tend to hold water near the surface. This may often be characterised by a marshy area, whereby more water is returned to the atmosphere (Powers et al., 2007).

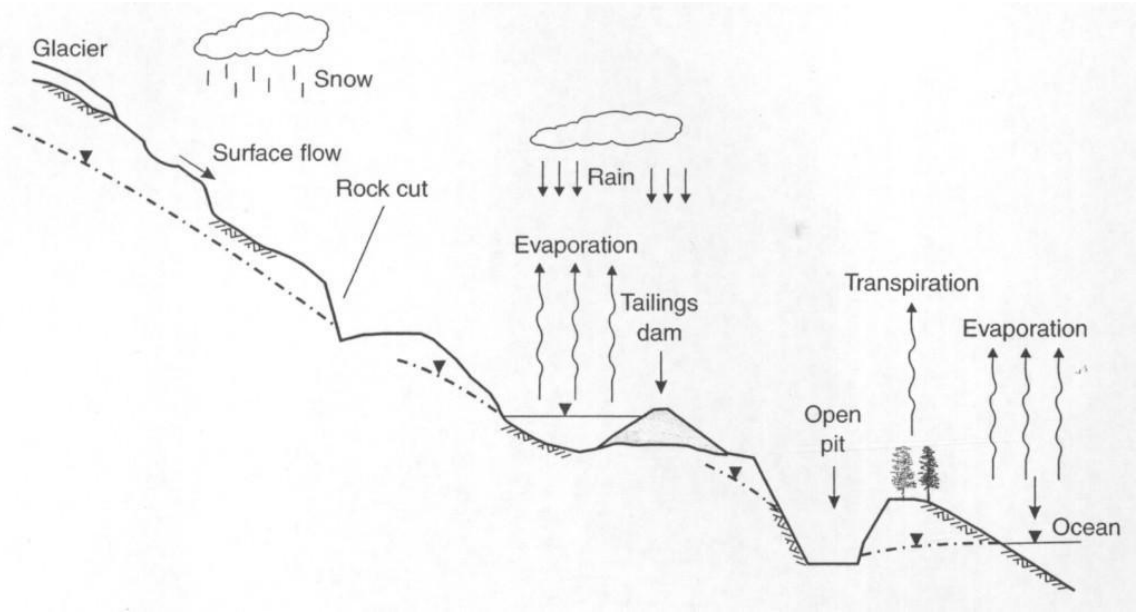

Figure 2-7 - Overview of the hydrogeological cycle (Wyllie and Mah, 2006).

There are a number of factors that influence the flow/movement of groundwater through various mediums; these are summarised by Fetter, (2004) , defining flow in terms of forces.

The most obvious force is gravity which acts to pull water downwards toward the centre of the earth. Secondly; external (atmospheric) pressures come from above the zone of saturation, the culmination of atmospheric pressures and the weight of the water itself creates pressures in the zone of saturation. The final force identified by Fetter (1994) is that of molecular attraction which causes the water to adhere or bond to solid surfaces creating surface tension in the water when exposed to air. These are the fundamental contributing factors in the phenomenon known as capillarity.

Although the earth's lithosphere is made up of numerous materials very few, if any are absolutely impermeable. Weathering processes, fracturing and faulting as well as solution affects all rocks to some degree. As a result of this, groundwater is present to some degree in the majority of rocks. Variations in hydraulic conductivity cause some units to have very slow groundwater movement while others can maintain high levels of flow (high hydraulic conductivity). An aquifer is defined as a geologic unit that can store and transmit water at rates fast enough to supply reasonable amounts to wells. The intrinsic permeability of aquifers ranges from 10^{-14} m^2/day upwards. Typical lithologies that are known to be common aquifers include unconsolidated sands and gravels, sandstones, limestones and dolomites. In

addition basaltic flows, fractured plutonic and metamorphic rock units make up aquifers throughout the world (Fetter, 1994).

2.4.1 Aquifer structure

As groundwater infiltrates soil in uplands area it begins to move downwards following the natural topography on the area. Depending on the hydraulic conductivity of the soil/rock and the height of the water source a considerable amount of pressure can build up in the confined aquifer. If the pressure head reaches a height greater than that of the overlying ground artesian flow can develop in the form of a spring (Fetter, 1994, Powers et al., 2007, Cornforth, 2005). The pressure within the aquifer will vary depending on the amount of replenishment into the system and the rate of discharge.

Water table aquifers are characterised by a lack of upper confining beds, the quantity of water in storage is highly dependent on movements/changes in the height of the phreatic surface. A variation to this type of aquifer is known as a perched water table; these occur as a result of an impermeable layer of clay or silt inhibiting the downward seepage/transfer of water to the underlying aquifer. The product of this is a layer of saturated material close to the surface. The layer below the clay or silt is not saturated and therefore is disconnected from the main aquifer and therefore is termed to be “perched”. Replenishment of a perched water table is often limited as is discharge, quantities of water are usually relatively small and can therefore be drained with relative ease if encountered in construction (Fetter, 1994, Powers et al., 2007).

Aquifers can develop in a range of different lithologies. Sandstones and gravels are a common water bearing strata (especially where river systems have previously occupied) however, limestone, dolomite and other karstic terrain can hold water as a result of dissolution pH on different geology in aquifers Possibly develop ideas mentioned in above paragraph dealing with aquifer structure; sandstones and gravels, limestone and dolomite based carbonate aquifers that develop through solution. The ongoing dissolution of can create large voids and cavities that allow for high flow rates. If dissolution is allowed to continue overlying strata can collapse due to a lack of structural integrity (Bell, 1990).

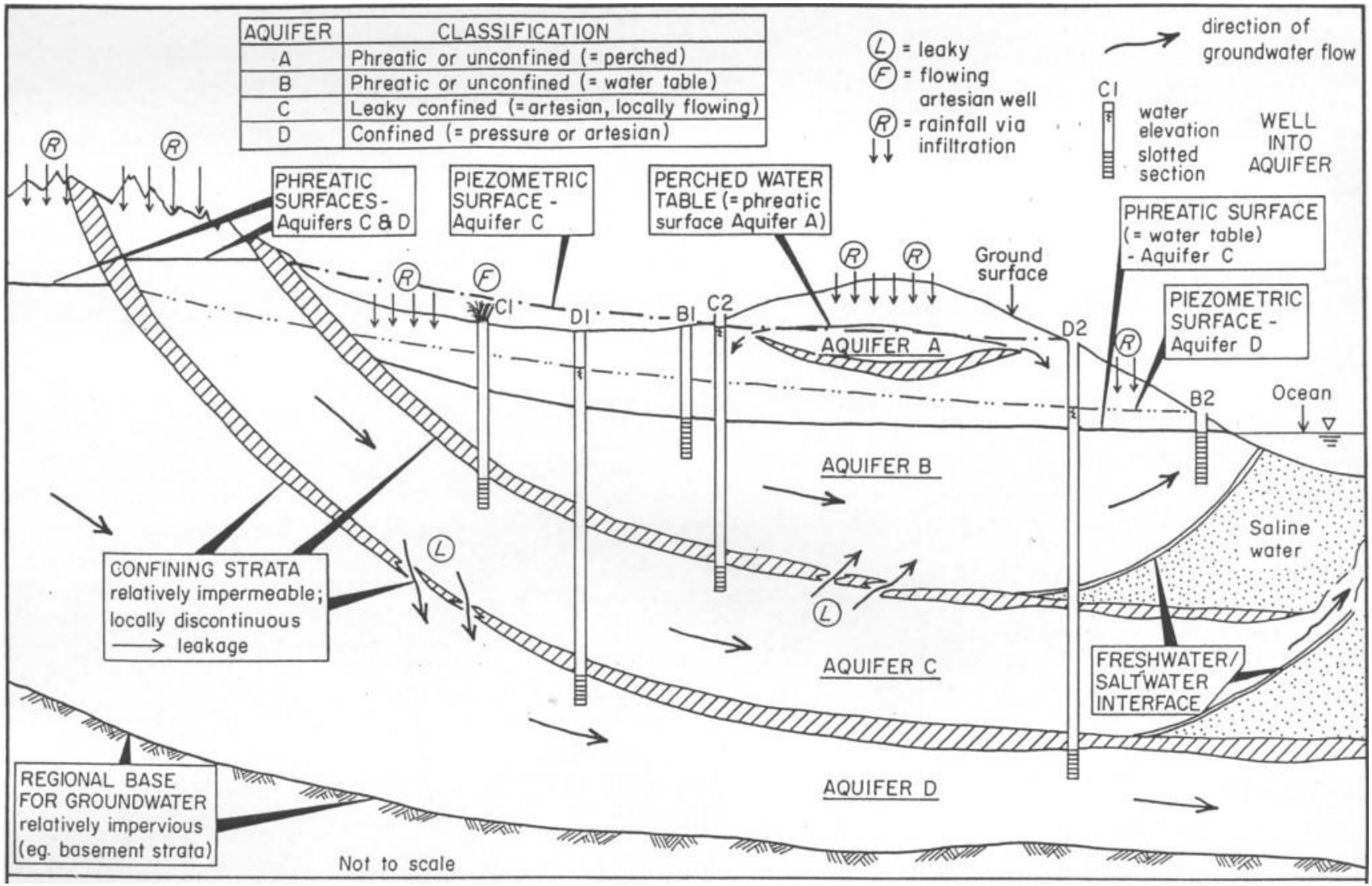

Figure 2-8 – Generalised aquifer structure and interaction of groundwater flow with the landscape (Bell, 1990).

Aquifer types

An aquifer has traditionally been defined in the context of groundwater utilisation as "a saturated permeable geologic unit that can transmit significant quantities of water under ordinary hydraulic gradients" (Freeze and Cherry, 1979). It can be described as a zone of rock or soil through which groundwater moves (Powers et al., 2007). Aquifers can either be confined or unconfined. A confined aquifer is one that is bounded by less permeable layers (aquitards). For example a sandstone layer underlain and overlain by shales may be a confined aquifer. Recharge to a confined aquifer usually relies on a recharge area, or a leaky confining bed. Leakage from above usually provides a small flow/trickle of water that has infiltrated from above. In this case the aquifer is more commonly known as a leaky confined aquifer. An unconfined aquifer is not completely bounded by less permeable strata. The typical unconfined aquifer consists of near surface unconsolidated sediments such as sands and gravels (Deming, 2002, Fetter, 1994).

Confining layers

A confining layer is a term used to describe a geologic unit that has no or little intrinsic permeability. Groundwater can still move through a confining layer; however the rate of movement will be very slow. The highest order of confining layer that permits no water transfer is known as an aquiclude although they are not common geologic features (Powers et al., 2007, Deming, 2002, Fetter, 1994). Structural complexities within landforms can also act as aquiclude; fault gauge for example can form a tight bond within itself and act as a barrier to flow. Such features can cause additional technicalities through compartmentalisation for engineers when designing dewatering systems (Freeze and Cherry, 1979, Wyllie and Mah, 2006).

2.4.2 Heterogeneous and Anisotropic flow

In simplified aquifers (high hydraulic conductivity sandstone bounded above and below by a low permeability shale) heterogeneous or isotropic flow conditions are likely to be present. This is due to the hydraulic conductivity of the material is not having variation as a function of the flow direction. More commonly rock materials are anisotropic. An anisotropic material is one whose properties work as a function of the flow direction. Most rocks will have a maximum and minimum hydraulic conductivity in two directions with 180 degrees symmetry, as shown in Figure 2-9. Sedimentary rocks for example have two principal directions of anisotropy, both parallel and perpendicular to bedding. The preferential or direction of highest conductivity is usually parallel to bedding (Deming, 2002).

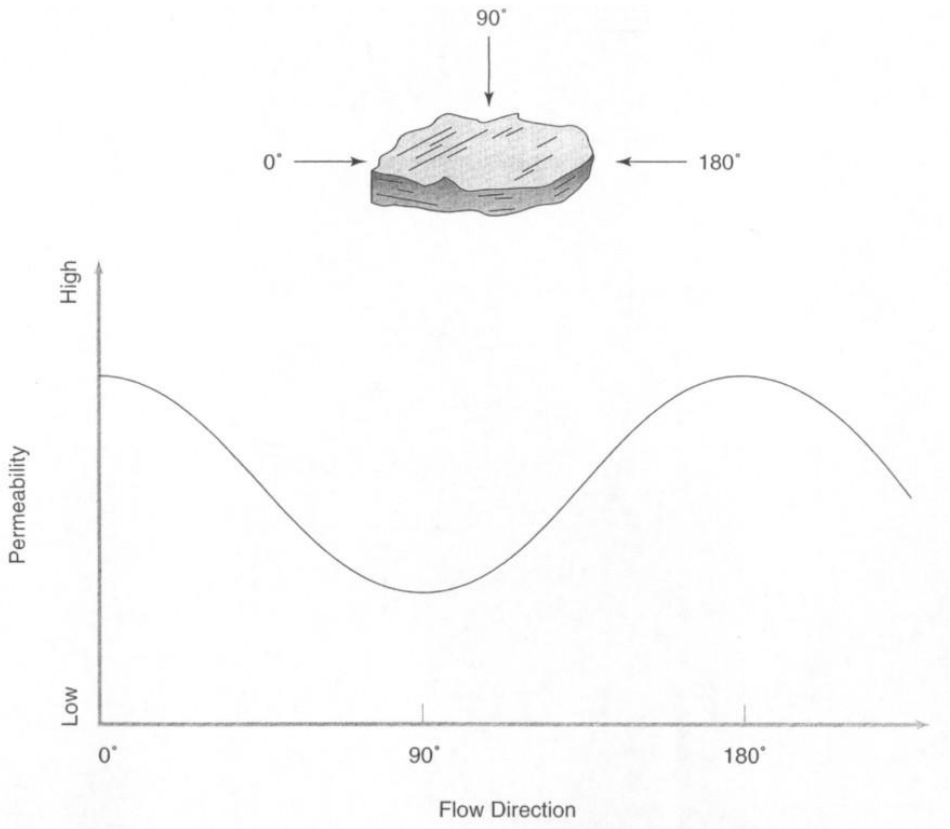

Figure 2-9 - Anisotropic flow; variable rates of permeability as a function of flow direction (Deming, 2002).

The concept of heterogeneity in rock masses in a mine area is easily understood because it can affect ore grades as well as hydrogeologic and geotechnical projects. For hydrogeologic considerations, heterogeneity in rock masses is one of the most significant features to deal with in terms of hydraulic conductivity for both primary and secondary flow. In hard rock mines secondary fracture flow is usually predominant and therefore heterogeneous hydraulic conductivity (k) value. These variations can happen both within a single lithology and across different units. Structural discontinuities such shear zones (mentioned above) are most likely to result in anisotropic hydraulic conductivity values with different directions of flow (Atkinson, 2001).

The concept of hydraulic conductivity within a single fracture plan (modelled by two smooth parallel plates) can be described using the following equation:

Equation 2-2

$$K = \frac{\rho g a^2}{12\mu}$$

Where:

a= aperture or width of fracture
μ= viscosity of water

2.4.3 Aquifer Characteristics

Hydraulic Conductivity – (K, ms^{-1})

Is defined as the ease at which water moves through rock or soil, more accurately using Darcy's Law in Equation 2-3 below (Powers et al., 2007, Deming, 2002, Atkinson, 2001, Fetter, 1994).

Equation 2-3

$$Q = KA\frac{h}{L}$$

Where: Q = quantity of water
K = hydraulic conductivity of soil
A = cross sectional area
H = head loss due to friction in distance L
h/L = also known as the hydraulic gradient (i)

The hydraulic conductivity can also be calculated using a rate of flow over a unit area, otherwise expressed by Equation 2-4 below (Powers et al., 2007, Deming, 2002, Atkinson, 2001, Fetter, 1994).

Equation 2-4

$$K = \frac{Q}{A}$$

As mentioned above geological materials have a wide range of hydraulic conductivities which can extend over 13 orders of magnitude. It is not unusual to have adjacent lithologies with 4 orders of magnitude difference in K across their boundary. Figure 2-10 shows the range of common materials and their respective K values.

Transmissivity - (T, m^2s^{-1})

Is defined as the product of saturated aquifer thickness (Δz, *m*) and hydraulic conductivity (K, ms^{-1}) which can be defined by Equation 2-5 as "the volumetric flux or flow rate per unit head gradient per unit aquifer width":

Equation 2-5

$$T = \Delta zK$$

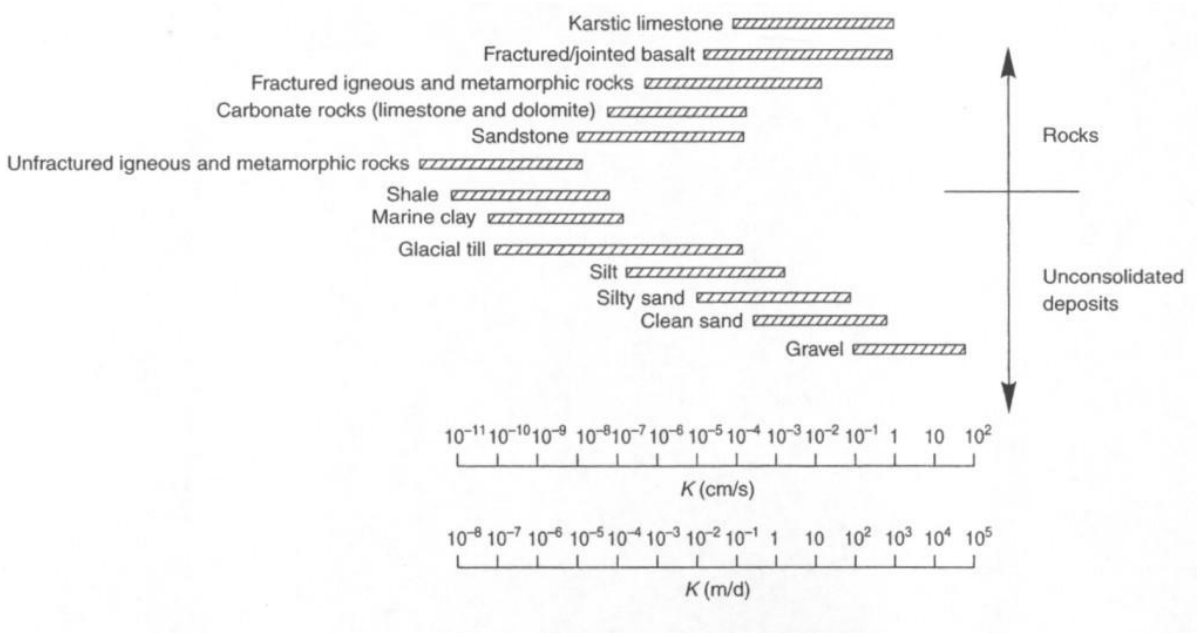

Figure 2-10- Diagram of hydraulic conductivities for a wide range of rock types/materials (Wyllie and Mah, 2006).

Specific Storage - (S_s)

Specific storage can be defined as the amount of water released per unit volume of a saturated portion of soil or rock mass that is stored (or expelled from storage) as a function of both the porosity and compressibility of the rock mass and the compressibility of water per unit change in head (Atkinson, 2001, Fetter, 1994) This can be more accurately described using Equation 2-6 below:

Equation 2-6

$$S_s = \rho g(\alpha + n\beta)$$

Where: α = compressibility of material
n = porosity
β = compressibility of water in pores

As a representation for the typical ranges of Specific Storage, compressibility of soil and rock from (Freeze and Cherry, 1979) are used to give values between $1x10^{-4}$ m^{-1} for very compressible rock which is highly fractured and altered through to $5x10^{-7}$ m^{-1} for very rigid, intact rock. It has been noted that the SI units for these values are in m^{-1} which is determined through dimensionless analysis (Atkinson, 2001).

Specific Yield - (Sy, %)

Specific Yield is defined as the volume of water that is released from pore spaces when the phreatic surface is lowered. It is important to note that not all water held within a materials pore space will be released through drainage, a significant portion will be retained in the pore space, adhering to the soil grains and rock particles by surface tension. This is known as specific retention. The percentage of released water will vary from material to material. For example a soil with a coarse grain size may have a porosity of 30% however draining this material may only yield two thirds of this water. In this case the specific yield is said to be 20%. The sum of the specific yield and specific retention equals the materials overall porosity (Powers et al., 2007).

Storativity - (S, dimensionless)

Is defined as the volume of water released from (or taken into) storage per unit head drop (or increase) per unit surface area of a confined aquifer. Storativity (S) is defined by Equation 2-7 to be the product of thickness and specific storage (S_s).

Equation 2-7

$$S = \Delta z \, S_s$$

2.4.4 Potentiometric Surface

The potentiometric surface (Figure 2-8 - Aquifer C) represents the hydrostatic head in a confined (or partially confined) aquifer, where the pore space of the aquifer is saturated and the aquifer is under additional pressure. The water in a standpipe will rise above the level of the saturated aquifer until it reaches the equivalent pressure of the hydrostatic head or potentiometric surface. In cases where the potentiometric surface is above the surface level groundwater will "flow" which is known as artesian flow as mentioned earlier (Hall, 2003).

2.5 Dewatering and Depressurisation

Evidence of land drainage (through large aqueducts and even water tunnels) to convert fetid marshes into arable land can be found amid the ruins of the great civilizations of Babylon, Rome and Egypt. This shows humans have tried to control water since records began (Powers et al., 2007).

"Explanations for the sluggish progress in understanding hydrology come readily to mind. In the simplest aquifer situations the mathematics of groundwater flow are complex and most natural aquifers are far from simple. Observation of groundwater levels is difficult, expensive and often confusing. In the 1950's, impelled by the growing economic significance of

groundwater for water supply and irrigation, hydrologists like Muskat, Theis, Jacob, Hantush, and others were developing practical techniques for aquifer testing and analysis. These methods were later adapted to the solution of dewatering problems. Some dewatering problems defied solution by analytic techniques until powerful personal computers and software appeared in the 1980's" (Powers et al., 2007: pg 7).

In recent years the effects of water pressures on pit slope stability have increasingly concerned open pit designers and geotechnical engineers (Harmen et al., 2007). As mines become deeper, steeping of pit walls and optimisation of mine design become increasingly important. Having a robust and effective dewatering operation is now more important than ever.

It is important to have a sound understanding of the different processes that are utilised in the management of controlling groundwater for mining. A key misconceptions from parties not directly associated with hydrogeological operations is that "dewatering" is a simply process that can be undertaken with relative ease at any site where water related problems are present. There is much more to lowering of a phreatic surface than simply installing a pumping well. In the following sections, details of dewatering and depressurisation are explained including site investigation, system/method selection and design will be covered. Measuring the effectiveness of a system and example case studies from varying sites around the world where different geological and hydrogeological conditions have been intercepted. Reword sentence as this doesn't make sense.

Dewatering as stated by (Hall, 2003) involves the removal of sufficient water from the rock mass or soil profile such that water levels are lowered to allow for safe and economic mining. It can be defined as "the physical draining of the pore space within the rock mass or soil, and results in the lowering of the water table (or phreatic surface)". The volume of water that is removed, per unit decline in the water table is defined by the unconfined storativity, known as the specific yield (or drainage porosity). This is a dimensionless term usually in the range of one per cent for fine sediments and fractured rock, to thirty percent for coarse gravels and karstic terrain" (Hall, 2003: pg 167).

"Benefits of dewatering include improvements and cost savings for blasting, trafficability and ore quality/handling. In particular for this study are the increases in pit wall stability as over pressuring in weak wall rocks and/or lubrication of slip planes" (Hall, 2003: Pg 167).

"Depressurisation refers to the lowering of the hydrostatic head (or potentiometric surface) of the rock mass or soil without actually draining the pore space of the rock. The volume of

water removed per unit decline in the potentiometric surface is defined by the confined storativity, known as the storage coefficient. This will be a much smaller number than the specific yield quoted for dewatering. Usually it is in the range of 10^{-5} to 10^{-3}" (Hall, 2003: Pg 165).

"Depressurisation is commonly a problem in deeper mining pits. The main object is to reduce the potential of "over pressure" related problems within the pit walls. These can include pit wall and floor heave in softer interbedded aquifer /aquaclude sequences. Slip failure driven by excess hydrostatic heads and possibly also facilitated by lubrication and finally burst inflows were confined aquifers burst through thin/weak aquitard layers in the footwall zones" (Hall, 2003: Pg 167).

The role of groundwater in slope stability has been researched and studied throughout the world for a number of decades. As construction projects have increased in scale and site locations have become more complex an in depth understanding of groundwater processes has become fundamental in the investigation and planning for geotechnical designs (Powers et al., 2007).

The inflow from the surrounding strata towards an operating pit requires installation of dewatering facilities to ensure workings are kept dry and to create an extensive and prolonged cone of depression (Doulati Ardejani et al., 2003).

Pore water pressures acting within discontinuities in the rock masses reduce effective normal stress with a consequent reduction in the effective shear strength (Harmen et al., 2007, Tsao et al., 2005). Hard rocks that have a low primary permeability, groundwater flow and depressurisation are essentially controlled by the geometry and nature of the discontinuities and structural geological characteristics. These factors influence the hydraulic conductivity/permeability of the rock mass and each is typically subject to a large degree of uncertainty due to the heterogeneous and anisotropic nature of the rock masses (Harmen et al., 2007). The authors note that primary concern is often groundwater flow however the pore water pressures built up in the rock mass that can exist even if groundwater flows are minimal. "Depressurisation of a system occurs as a result of groundwater flow or its removal, however small that may be" (Harmen et al., 2007). Although pore water pressure fluctuation is an important factor contributing to landslide activity it is often very difficult to understand the true interactions pore water pressure is having on a slip surface at varying depths due to the often complex nature of the hydrogeological conditions (Tsao et al., 2005). Tsao et al., (2005) investigated the variability of pore water pressures with depth in a slope using an

array piezometers to measure the pressure head both before and after drainage was installed. Two key characteristic results were noticed at the conclusion of the study. Firstly "the pressure corresponds to drilling depth and seepage water in a horizontal drain". Secondly "the decreasing effect of pore water pressure is evident as the drilling direction of a horizontal hole is near the vertical observation borehole".

In all cases in open pit mining practise more than 40% of slope instability risks depend on groundwater conditions within the slope. To prevent slope failure, effective drainage systems can be installed, and other factors can remain unchanged. The importance of controlling water surface in open pit slope is emphasised. In general, increasing the open pit slope angle and decreasing the failure risks, is directly proportional to effective drainage system (Mandzic, 1992).

In all open pit slope stability problems it is important to determine the pore water pressure from a prescribed phreatic surface. Phreatic surfaces in an open pit slope area are not constant and it depends on different factors. In order to include the effects of pore pressure in a stability analysis we use the pore pressure ratio r_u. The pore pressure ratio in a material is defined as a ratio between the total upward force due to water pressure and the total downward force due to the weight or overburden pressure. According to the Archimedes' principle, the upward force is equal to the weight of water displaced or the volume of sliding mass under water multiplied by the unit weight of water. The downward force is equal to the weight of sliding mass. Equation 2-8 shows the components necessary to calculate the pore pressure ratio for a soil after (Mandzic, 1992):

Equation 2-8

$$r_u = \frac{Volume\ of\ sliding\ mass\ under\ water\ \times Unit\ Weight\ of\ water}{Volume\ of\ sliding\ mass\ \times Unit\ weight\ of\ soil}$$

The overlying influence that water pressures has on a slope is the angle at which a slope can be safely excavated. Water pressure acting on discontinuities (joints, fractures and bedding planes) in a rock mass reduces the effect stress on discontinuities which leads to an overall lose in shear strength. These problems are worsened if the above discontinuities are orientated so to dip into the high wall (Atkinson, 2001).

Fully depressurised slopes have been shown to remain stable at an additional 10 degrees of steepness than those that remain wet. In some cases flattening a wet slope is possible but for mine related projects and those that are working within tight footprints draining and

depressurizing the slope is a much more effective solution both economically and in terms of required site (Powers et al., 2007, Brown, 1981, Atkinson, 2001).

Additional benefits of advanced dewatering in open pit other than creating an extensive cone of depression include; reduced blasting costs as dry holes require less emulsion explosive, dry ore is lighter and therefore reducing haulage costs both in terms of required fuel but more importantly wear and tear on machinery. Finally the overall working conditions of the pit/site will be improved creating better trafficability and increased diggability (Doulati Ardejani et al., 2003, Rowe and Beale, 2007).

2.5.1 Site feasibility and primary investigations

Initial dewatering investigations for a site should be completed in the pre feasibility stages of the development program and aim to generate a sound characterisation of the hydrogeological conditions. Collection of hydrogeological data should begin at this time and continue throughout development to the end of mining. Key features to look for include the likely magnitude of required dewatering, the time scale required and the possible environmental impacts (as well as any mitigation works to minimize/eliminate these). Finally an overall costing analysis for both capital and running costs related to the project (Cornforth, 2005, Atkinson, 2001, Cividini and Gioda, 2007, Bell and Pettinga, 1983, Hall, 2003)

During the projects' feasibility study more specific investigations may be required; this could involve drilling, trial bore installation, test pumping and detailed groundwater flow and depressurisation modelling. A key point to note at this stage of the system design is that considerations need to be made to changes to the plan/mine layout as well as unforeseen circumstances (Hall, 2003)

Atkinson (2001) outlines what is thought to be the minimum data requirements for analysis when considering the commission of a dewatering scheme. This includes geological maps and cross section depicting the general geological framework. Hydraulic heads within the major geologic units; this should show any significant differences both vertically and laterally within the geology. The hydraulic conductivity of all lithologies that will be intercepted during operations, this should also include anisotropy. Testing for these characteristics should ideally be carried out during the exploration program to maximise efficiency of the available personal and equipment where possible. A simple way to establish water levels and estimates of hydraulic conductivity in holes drilled with air is to measure and record the airlift production while drilling (Kauffman and Van Dell, 1983) in (Atkinson, 2001).

"The significant unknowns for any dewatering system are the total quantity of water (Q) that must be pumped to accomplish the states purpose, and the quantity of water (Q_w) that can be expected from an individual well or well points in the system under the dewatered condition". Q and Q_w are factors that influence spacing, design and construction of wells or well points, and on pumps and piping systems are based" (Powers et al, 2007; Ch 6). Understanding groundwater conditions to select appropriate action is the most important aspect to be considered when planning any hydrogeological based operations (Hall, 2003, Rowe and Beale, 2007, Cornforth, 2005).

"Key components required to ensure effective management of groundwater related issues include allowing sufficient time to investigate and install the required dewatering plans. The requirement for dewatering needs to be understood, these will likely involved assessment of hydrogeological and geotechnical conditions and lead times required to achieve said targets". The results from feasibility studies may also require changes to mining processes and overall pit plans if potential problems have been identified in early analysis (Hall, 2003).

Packer tests provide a major advantage for hydrogeological investigations as they can be conducted in holes that have been specifically oriented to intersect discontinuities which allows for anisotropy of the rock units and discontinuities to be established. In addition, analysis of rock core from drilling allows for discontinuity sets to be examined providing rock-quality designation (RQD), fracture orientation and density as well as any other applicable factors such as staining (from water/oxidation) or clay alterations (Atkinson, 2001).

2.5.2 **Dewatering system design**

At the conclusion of pre feasibility a rough idea of the required works should be known. Choosing an appropriate method of dewatering is the next critical step in developing an effective, economically viable system that will, most importantly provide the desired outputs within the time frame available.

To achieve the above goals, a number of factors need to be considered when choosing a method of dewatering (Hall, 2003, Powers et al., 2007).

- The hydrogeological (and geotechnical) conditions and should be confirmed to determine magnitude of dewatering required (as mentioned above).
- The optimal extraction/drainage method needs to be confirmed as does the time period available.

- The pumping design and discharge reticulation system to removed water from the site should be investigated.
- The available time frame.
- Finally the overall cost of the project and any necessary environmental implications need to be planned for with management strategies developed with approval for the appropriate regulatory bodies.

In some cases the rock mass that makes up a pit slope may not have adequate permeability to support the use of pumping wells. Elevated pore pressure can develop in the slope because the rock is unable to adequately drain as mining advances. Depressurisation may then become necessary. Common approaches involve horizontal or vertical drains installed directly into the sections of slope that are of concern. In some larger pits throughout the world, cost benefit analysis may justify the creation of a depressurisation tunnel or adit driven in behind the major push-backs and expansions. The installation of drainage galleries within an adit will then promote focussed drainage deep within the slope. Detailed interaction with larger slope scale structural and geotechnical programs is required to ensure that measures are planned and focused in areas where depressurisation will provide the greatest value to a given region (Rowe and Beale, 2007).

Lithologies that are predominantly made up of clay and other finer grained soils are not ideally suited for installation of horizontal drain hole as they are often ineffective both in terms of yielding water and ongoing blockages in uncased holes (Cornforth, 2005). Materials that have intrinsically low permeability's (approximately $\leq$ 0.01m/d), the level of drawdown from any reasonable number of pumping wells is going to develop slowly; therefore a significant amount of lead time is required. A comparison between material grainsize and most applicable dewatering system is shown in Figure 2-11 as a guideline to system design.

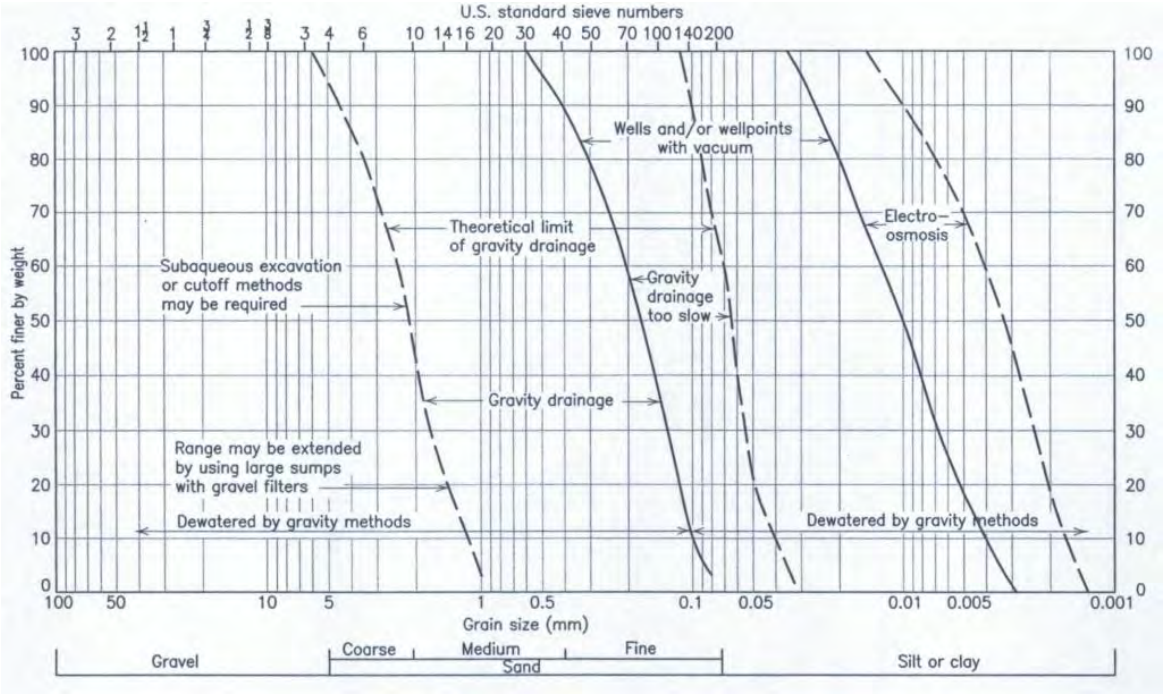

Figure 2-11 – Chart to aid in the selection of appropriated dewatering system based material grain size (Atkinson, 2001).

The most suitable data for the confirmation of site conditions, dewatering performance, and validation of dewatering models is long-term operational data. In the absence of any monitoring data it become very difficult to establish the effects the planned drainage initiative is having on the slope, both specific pore water pressures and background groundwater levels (Hall, 2003). The following points have been outlined by (Atkinson, 2001) as a list of basic considerations to look at when designing a dewatering system:

- If recharge sources are present in the system is it preferable to cut them off where ever possible, especially if they have low hydraulic conductivity as mentioned above. It is more straight forward to drain/depressurise a unit that is not being feed from a large recharge source.
- Ensure that drain holes are drilled to sufficient depths to achieve maximum drawdown with distance. Some materials tend to have reductions in their hydraulic conductivity with depth and therefore there become a limit to the effective drainhole depth.
- Almost all rocks that are fractured have some degree of anisotropy. Let this aid in the dewatering system design. Orientate drains so that the maximum numbers of fractures (or water bearing features) are intersected orthogonally to promote the greatest level of drainage yields.

It is not uncommon for aquifer systems to "tighten" with depth due to changes in the coefficient of consolidation. A study undertaken by Ahlbom et al., (1991) in (Forth, 2004) confirmed the assumption that permeability decreases as a function of depth where an order of 10^{-10} m/s was measured in crystalline rock (Figure 2-12). Brown (1981) also identifies that a limiting factor in horizontal drain holes is their effectiveness at depths greater than approximately 150 m. This is said to make them inadequate as a total pressure control method if used exclusively in deep mines.

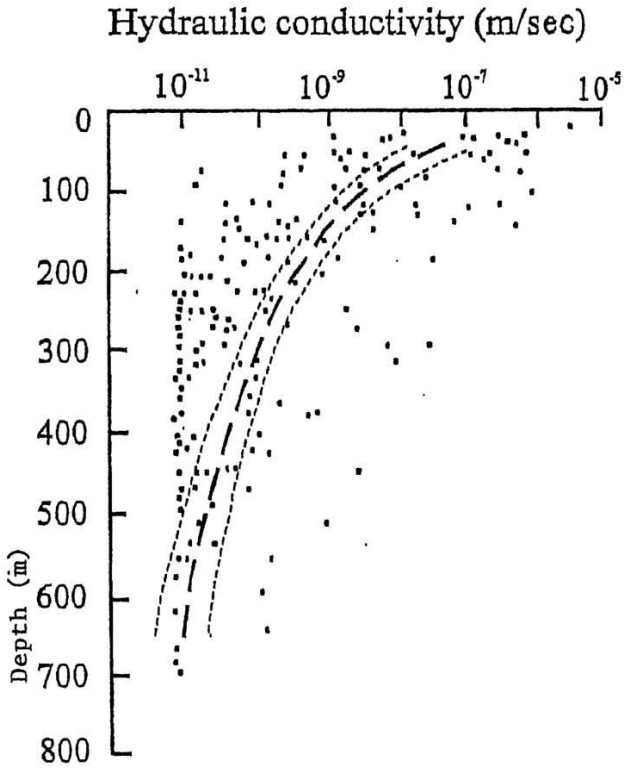

Figure 2-12 - Graph showing Hydraulic conductivity as a function of depth from a swedest case study looking at dewatering of fractured crystalline rockmass (Ahlbom et al., 1991).

2.5.3 **Dewatering methods**

The actions of drains reduces overlying pore pressures in surrounding rock/soil, subsequently increasing the effective stresses and shear strength of the rock or soil in question. Although drains are used widely in geotechnical design, the effect they have on slope stability is not always fully understood or modelled. The role of drains in slope stability is to minimise the effects of peaks/spikes in the pore water pressures that result from episodes of high recharge/infiltration rates which ultimately contribute to land instability (D'Acunto and Urciuoli, 2006, Tsao et al., 2005).

There are numerous methods of dealing with excess water related issues in mining and construction projects. These can be grouped into two primary categories of active or advanced dewatering and passive or real time dewatering. Although there are a multitude of possible methods for dewatering only those that are applicable to the chosen case study within this research will be discuss in this review. The use of drainage adits for example allows for high concentrations of drain holes to be installed deep behind a slope however they require pre development design and are not best suited to scenarios where operations are well underway such as a working mine where access is often restricted (Brown, 1981, Hall, 2003). Larger civil projects such as the Brewery Creek landslide, upstream of the Clyde dam in Central Otago New Zealand are prime examples of successful drainage adits (pers. comms. Bell, 2007).

2.5.4 **Active dewatering:**

Pumping wells – installation of bores can be located both inside and outside the pit wall perimeters. Primary advanced dewatering will be set up around the perimeter of the pit. In situations where there is a clear hydraulic gradient it is often beneficial to locate these up gradient from the developing pit as this acts to both lower the potentiometric surface and cut off the continuing recharge source for the pit (Cividini and Gioda, 2007, Rowe and Beale, 2007). In pit dewatering pumping wells act to remove the water occupying the pore space and fracture zones within the rock mass and within the surrounding mine shell. Dewatering wells are primarily installed to achieve the lowering of groundwater levels ahead of active benches. There are risks involved with the operation of wells within the active pit shell, due to heavy machinery and blasting wells can be lost or damaged. Replacement wells need to be planned for as a result of such scenarios to ensure that dewatering can continue without production being affected (Rowe and Beale, 2007).

Wells are typically installed with slotted or screened sections to allow inflow from the water bearing strata or aquifer, in some cases this can extend entire length of the well depending on the ground conditions. If wells are installed in areas of poor cementation the outer perimeter of the well is packed with gravels so that to prevent collapse. Is collapse of the well was to occur the effectiveness and potential of pumping is significantly limited (Powers et al., 2007).

The most common types of pumps installed in dewatering wells are electric submersible or shaft driven turbines. The main difference between dewatering wells and water supply wells is the level at which they are pumped to; dewatering wells are typically pumped to the lowest extent possible to maximise the cone of depression and subsequent pressure reduction effects

as opposed to a level with sustainable supply for consumption (human or industry). Water from pumping wells is usually pumped directly to a zone of discharge without the opportunity of contamination. If contamination occurs a treatment process of required before the water can be discharge which increases the overall costs of the respective program (Brown, 1981).

2.5.5 **Passive dewatering:**

Unaided drainage – utilisation of the cut face of excavation as a collector drain. This method relies on the coefficient of consolidation of the rock/soil being excavated. The major disadvantage of this method is that water is released uncontrollably into the base of the pit. Water is therefore required to be redirected to a sump of other similar location to be pumped out of the pit. Ongoing seepage from the walls also lowers operational efficiency of the pit as the wet working environment reduces trafficability and increase weigh of material being excavated (Brown, 1981).

In rock, significant amounts of groundwater flow occurs as a result of secondary permeability through open joints, faults and other discontinuities as opposed to through the intact rock. Horizontal drainholes are small-diameter holes (Dimension 150-300 mm) drilled into slopes at an orientation approximately 5 degrees above horizontal. This incline allows the holes to be free draining and be predominantly gravity driven as well as self clearing. Spacing of drain holes is commonly between 25 and 100 m horizontally with vertical spacing dependant on floor advances (Brown, 1981). The installation of such drains is best suited to achieve one of two primary objectives; a) to lower the groundwater levels (phreatic surface) generally within a slope, b) to tap into and relieve the aquifers that are feeding the slope from behind. They are especially effective as reducing “spikes” in groundwater levels through periods of heavy precipitation and/or snow melt which are known for causing large influxes in groundwater within slopes (Cornforth, 2005).

Depending on the project and design life of the drains, the holes can be cased with slotted PVC pipes. This ensures the holes are kept clear of obstructions wherever possible. Casing of horizontal drain holes is more commonly utilized in civil and landslide applications where the drains are to remain in place for a long duration to give ongoing relief from the build up of water pressures within the slope (Powers et al., 2007, Cornforth, 2005).

Studies (both field and parametric) conducted by (Rahardjo et al., 2003) suggest that to ensure the maximum effectiveness and long levity of drain holes they need to be installed at the lowest point possible in a slope to achieve maximum drawdown through greatest

attraction of groundwater. (Rahardjo et al., 2003: pg 296) suggest that "a small number of drains installed at appropriate locations in accordance with a well conceived conceptual groundwater model may be more effective than a large number of drains installed at uniform spacing over a slope"

Experience has shown that flow rates and yields from horizontal drains should be expected to be variable from drain to drain in certain geological conditions. Often compartmentalisation causes analogous flow across an array of install drains (Tsao et al., 2005). Landslide sites also show variable flow where soils and rock are intermixed and cracked (Tsao et al., 2005, Cornforth, 2005).

Finally, it is important to ensure drain outlets are directed towards a centralised sump area where the water can be pumped/routed out of the pit. During slope push backs horizontal drain holes are prone to being lost as well as being damaged during operational blasts (Brown, 1981).

2.5.6 **Effects of Horizontal Drain Hole Spacing**

Design methods for horizontal drain installations appear to vary across the literature, (Cornforth, 2005, Brown, 1981) suggest to be effective a large number of drains should be installed (preferably in array's to minimize cost of installation). Post installation a program of monitoring, inspection and clearing should be initiated to ensure the long levity of the drains. Depending on the project and site, drains may not be cased in a effort to reduce economic pressures on the project. Where soils or rocks have a percentage of fines, blockage of drains is possible especially if not cased.

The practical advantage of horizontal drain holes is that the can be orientated to penetrate structures deep within the wall rock and relief pressure (depressurisation) that would otherwise be unable to be released. As many large mines exhibit steeply dipping strata that is made up of or filled with low permeability material, horizontal drain holes have been proven to be extremely effective at reducing pressure build ups within the wall rock (Brown, 1981).

In areas of limited data availability an observatory approach can be adopted, whereby the initial array of holes is drilled and depending on the yield of these holes the program can be either abandoned or concentrated in significant or all areas of the slope(Cornforth, 2005).

2.5.7 **Monitoring effectiveness of installed dewatering/depressurisation systems.**

To assess the impacts of any installed drainage systems a range of monitoring instrumentation should be utilised. Depending on the site, the monitoring requirements will

range significantly in scale. A small site may only have a limited number of observation wells that can be monitored manually on a daily basis. In comparison a large road cutting adjacent to a highway or deep open pit mine wall could quite feasibly have an exhaustive and intricate installation of observation wells, standpipe piezometers, vibrating wire piezometers and tensiometers that are linked to a central hub where automatic, round the clock monitoring is undertaken. Such extensive monitoring systems allow the operators to analyse the conditions to a much greater detail and fine tune mitigation and remediation measures to the greatest of efficiency. These systems are most commonly found in locations where the potential costs of slope instability are extremely high in both an economic and public safety viewpoint (Powers et al., 2007, Tsao et al., 2005, Mandzic, 1992).

Hydraulic piezometers are usually employed in soil, but in rock, where flow is often along discrete discontinuities, the groundwater pressure is more accurately measured using pneumatic piezometers (Forth, 2004).

Misinterpretation of piezometric data has resulted in a number of serious difficulties with performance of dewatering systems in the past. To interrupt piezometric data correctly it is essential to have an accurate picture of the subsurface conditions in which the piezometer is located. The planned location, depth, design and construction details cannot be properly selected until adequate geological and geotechnical information has been obtained through analysis of drilling samples such as core (diamond rigs, or chips from a reverse circulation operation) (Wyllie and Mah, 2006, Powers et al., 2007, Fetter, 1994). This emphasises the importance of thorough and accurate drill hole logging whenever an investigation is being undertaken.

2.5.8 **Flow Nets**

Flow nets provide a simple solution to practical seepage problems where complex numerical analysis (using the Laplacian equation) is not required. Common situations where flow nets are effective include the modelling of flow around a sheet pile wall, through a homogeneous earth dam or dewatering of deep excavations such as open pit mining .

Flow and Equipotential lines

The flow function $\varphi(x,z)$ of a seepage problem is dependent on the boundary conditions that are present. This function is often shown using curves known as flow lines. Flow lines can be imaged as lines that trace the direction and path of groundwater through an aquifer in areas where there is a head difference. In situations where the aquifer is isotropic, flow lines will cross equipotential lines at right angles. An infinite number of flow lines can be represented

in a cross section, however to ensure the model is non-cluttered four or five flow lines are recommended for construction (Fetter, 1994, Das, 2002, Craig, 1997).

Constant flow channels are represented by the interval between adjacent flow lines. Partial flow channels can be used to show seepage paths against an impermeable boundary. The proportion of visible channel width indicates the percentage of flow that will pass through that "channel".

The potential function $\psi(x,z)$ of a seepage problem is indicated using curves known as "Equipotential Lines". These represent equal energy levels or equal total head. As water flows through the pore spaces of a material energy is lost due to friction. The equipotential lines form "contours" to show the drop in energy from level to level. As with flow lines, the intervals between adjacent equipotential lines indicate a constant difference in total head loss (Craig, 1997, Fetter, 1994, Das, 2002)

Having a completed flow net allows a number of parameters such as flow rate, total head and pore water pressure to be calculated, thus generating outputs for use in geotechnical design. A generic illustration of a flow net has been included in Figure 2-13 below.

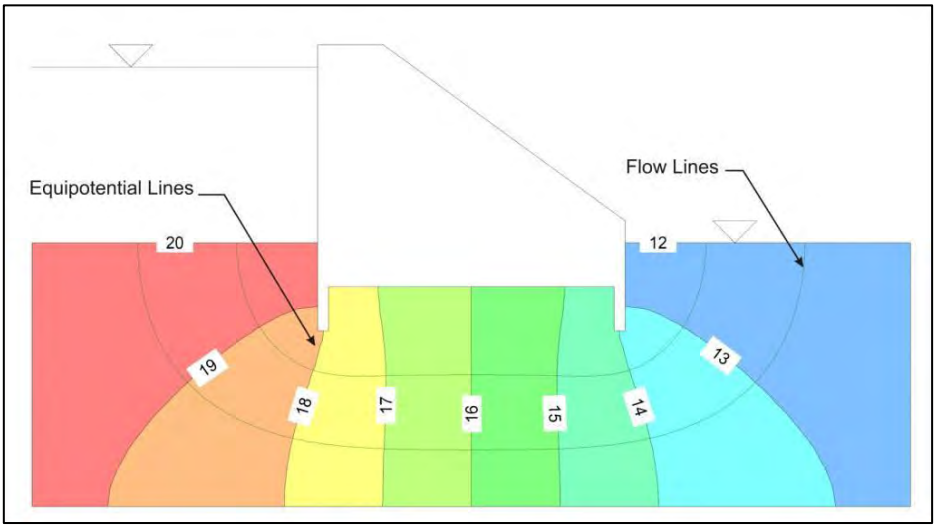

Figure 2-13 - Example flow net plot of total head contours or equipotential lines (GeoSlope International, 2009).

2.6 Hydromechanical Coupling

The theory of hydromechanical coupling in soils was developed initially to explain the consolidation of soils over time and the dissipation of pore fluid pressures by flow. The vertical effective stress (σ') can be calculated using Equation 2-9:

Equation 2-9

$$\sigma = \sigma - \mu_n'$$

Where: σ_n = total stress, or the applied load

μ = pressure in the pores or joints

This is the fundamental equation for describing hydromechanical coupling. The concept of effective stress lies at the core of the understanding of hydromechanical coupling. In describing the consolidation response the two key parameters are Specific Storage (S_s), which is the volume of water released per unit drop in head, and hydraulic conductivity (K). In soil mechanics it is usual to describe consolidation in terms of the Coefficient of Consolidation, C_v (Sullivan, 2007).

Mohr diagrams are useful for considering the relationship between stresses, pore pressures and slip on geological structures or failure of the rock mass. Figure 2-14 shows this relationship. Shear failure of the rock or slip along pre-existing discontinuity, can occur due to either an increase in the major principal stress (σ_1) or a decrease in the minimum principal stress (σ_3), which in open pit mining could equate to either continued deepening of the pit or an increase in the pore fluid pressure, respectively.

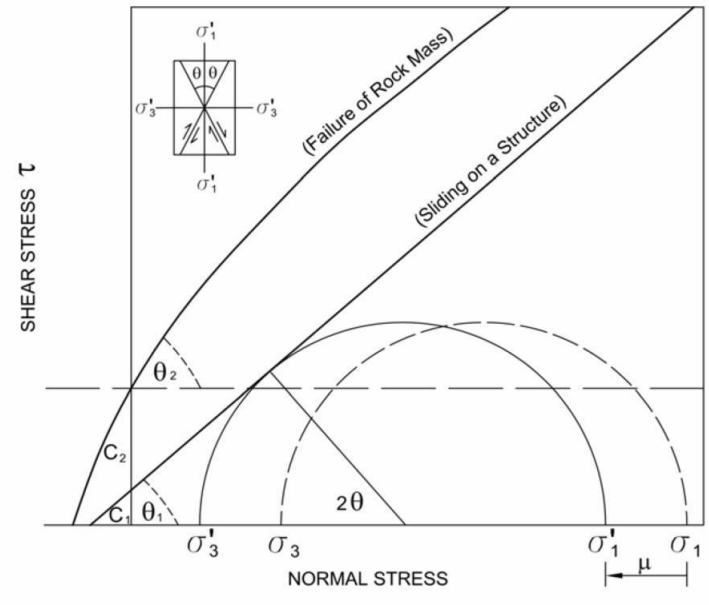

Figure 2-14 - Mohr circle diagram illustrating the typical failure envelope for shear failures in a rock mass and sliding along structures with the inclusion of total and effective stresses (σ_1, σ_3) (σ'_1, σ'_3). In the presence of excess pore water pressures (μ) the failure envelope can be seen to shift to the left indicating failure along a structure is likely. This mechanism is highly applicable to deep hard rock excavations operating below the groundwater table (Sullivan, 2007).

Typically in open pits shear displacement occurs on structures. This can be continuous over time or more typically for large failures, cyclic with "stick-slip" behaviour often related to periodic rainfall and groundwater pressure build-up (Pells Sullivan Meynink Pty Ltd, 2005, Sullivan, 2007, Rutqvist and Stephansson, 2003, Stephansson, 2003).

2.7 Numerical Analysis

A groundwater model is "a physical or mathematical approximation of a real world groundwater system, usually created either to understand the behaviour of an existing groundwater system or to predict its response to a subsequent change" (Powers et al, 2007: pg 84). The power and versatility of numerical models to solve complex hydrogeological problems was first discovered in the late 1960's. However, at the time computing power was limited and therefore a widespread lack of modelling application ensued. As technology developed, especially in the last two decades the ability to compute complex multidimensional problems quickly has meant that numerical based models are now commonly used throughout the world (Powers et al., 2007).

It has been noted that there is an increasing dependency being placed on sophisticated numerical techniques both for hydrogeological and geotechnical analysis. The concern appears to be that this reliance on software generated outputs is taking away from basic conceptual understanding and theoretical based analysis through solid engineering and geological precedent (Harmen et al., 2007, Pariseau, 2007).

The majority of experts in this field have stressed the importance of having quality data to use for the allocation of initial conditions. As Powers et al.(2007) and Harman et al. (2007) state that using high powered graphic adaptors and powerful computer software will never make up for inadequate primary data or an insufficient understanding of primary groundwater flow dynamics.

In contrast to this, Starfield and Cundall (1988) view numerical models as a simplification of reality rather than an imitation of reality. It is an intellectual tool that has to be designed or chosen for a specific task. The purpose of modelling in situations where only limited data is available is to gain understanding and to investigate potential trade-offs and alternatives, rather than to establish a set of "definite" results.

The design of the model should be driven by the questions that the model is supposed to answer rather than the details of the system that is being modelled. It can often be beneficial to develop a number of very simple models rather than a single complex one. Simple models

can be specified to relate to different aspects of a problem, or alternatively address the same questions from a variety of different perspectives.

In the early stages of a project it can be highly valuable to develop a conceptual model to as soon as possible. A good conceptual model can lead to savings in time and money as specific field testing programs can be designed. People commonly say “the results are only as good as the data” however modelling in a cautious and considered way leads to new knowledge or, at the least, fresh understanding (Starfield and Cundall, 1988).

Numerical models are used throughout the civil and mining industries as a tool for analysis and not to generate stand alone solutions. To increase the credibility of solutions generated through the use of numerical modelling methods it is important to incorporate a parallel field study. A comprehensive field based monitoring program is often the best means of calibrating such a model (Rahardjo et al., 2003). Standpipe piezometers or observation wells are especially useful as mentioned in Section 2.5.7.

There are also a number of advantages gained through numerical modelling compared with creation of physical lab based models. They can be set up in relatively short time periods and without the monetary outlay. A physical model is usually limited to a narrow set of initial conditions. A numerical model can be used to investigate sensitivities within a wide variety of different scenarios at a range of scales providing information and results for any given location within a designated cross section. In addition, difficulties while attempting to account for gravity in laboratory models are nonexistent with a numerical alternative (Geo-slope_International, 2007).

There are two categories of models, analytical and numerical. Analytical models are best applied to situations that are based around simple aquifer systems. They are not ideal for use where complex aquifers exist, for this type of work a numerical based groundwater model is much more applicable. It should be noted that analytical models are assumed to be in equilibrium (Aryafar et al., 2007, Doulati Ardejani et al., 2003, Powers et al., 2007).

Table 2-2 - Comparison between Numerical and Analytical Models (Powers et al, 2007)

Numerical Model (2D or 3D)	**Analytical Model**
Can account for both vertical and horizontal flow through aquifer	Simplified- assume groundwater flow through aquifer is horizontal
Where proximate or irregular boundaries exist	Aquifer boundaries are or inferred as regular and are fairly distant from site
Multiple pumping wells or variations in aquifer properties are involved	Will calculate the non-steady state drawdown around a single , fully penetrating pumping well
Useful when- significant spatial changes in hydraulic conductivity or aquifer thickness, spatial variations in transmissvities or where flow cannot be assumed to flow horizontally	Simplifying assumptions based on homogenous and isotropic aquifer- using a single vertically averaged tranmissivity

Numerical models are able to represent complex hydrogeological situations including aquifer structure and flow dynamics. These models describe the groundwater flow system in detail, with both spatial and temporal variations in aquifer properties, boundaries, and applied stresses defined for each point. These models can accommodate aquifer heterogeneity, anisotropy, complex and irregular boundary conditions and transient and steady state flow simulations in two or three dimensions (Powers et al., 2007, Kihm et al., 2007).

The most important step when embarking on any form of numerical modelling is to design a robust conceptual model to develop some estimates of the perceived results. This requires the assembly and understanding of all the available geologic, soil and groundwater information for the site and surrounding areas. From this an approximate plan and cross section can be prepared to visualise and understand the data which will ultimately assist in the model construction. Identification of any information gaps can at this point be investigated further or level of uncertainties within the future model can be predicted.(Powers et al., 2007)

Finite element and finite difference are the most commonly used numerical models throughout industry. Finite element allows more versatile meshing constraints, providing a more realistic representation of complex structures, whereas finite difference employs simple uniform meshing geometries.

Geotechnical sensitivity analysis of slopes can be achieved using numerical methods. Limit equilibrium analysis allows geotechnical engineers to evaluate the relationships between material strengths and groundwater in a variety of structural settings. A multitude of potential failure mechanisms (outlined in section 2.3.1) can be simulated where the distribution of forces acting on a point in the slope are calculated using a method of slices. This allows for a slope to be broken down into smaller manageable sections where force equilibrium calculations are undertaken as illustrated in Figure 2-5.

D'Acunto and Urciuoli (2006) note that many models attempting to quantify the stability of slope (with installed drainage) can often fail to accommodate the effects of transient aspects within the groundwater regime that relate to atmospheric changes. Instead a simple steady state or equilibrium groundwater condition is often utilised.

Accurate knowledge of precipitation, infiltration and/or other recharge sources is therefore paramount when undertaking an analysis where the results will be used in geotechnical sensitivity modelling. Pore pressures are ideally suited for analysis of slope stability in hard rock environments as they create an accurate representation of site based groundwater conditions. Computer models often use a "phreatic surface" as a starting point for any analysis although this has been seen as potentially incorrect due to the nature of secondary fracture flow and compartmentalisation (Harmen et al., 2007).

Limitations in modeling

It would be incorrect to assume that numerical models can be developed without limitations. The response of hydrogeological models to environmental changes in temperature, volume and even chemical balances (eg: karstic terrain) can alter a systems seepage flow characteristics. It is possible to accommodate some of these factors however to include all these processes in the same formulation is not possible. It would require even more sophisticated mathematics that could easily become over complicated and complex. Some of these difficulties can be mitigated with the ongoing advances in both computing power and software development however the output results are still dependant on the quality of the input data used. The more variables that are incorporated into a simulation the higher the potential for a result to become erroneous. This emphasises the need to calibrate and confirm any numerical solutions with relevant field data and have a sound level of practical experience to qualify the output results (Jeremic et al., 2008, Geo-slope_International, 2007, Aryafar et al., 2007).

Chapter 3: Geology of the Hamersley Basin, WA.

3.1 Introduction

The Hamersley Basin (Figure 3-1) is situated approximately 1200 km north of Perth, Western Australia with an area of approximately 80,000 km^2. The primary stratigraphic succession in the area is known as the Mount Bruce Supergroup, containing the ~2.5 km thick stratified assemblage known as the Hamersley Group which is the focus of this study. Banded Iron Formations (BIF) represent the largest volumes of iron on the Earth's surface. Formed during the late Archean and Paleoproterozoic BIF are characterised by well developed, thin laminations of iron rich material interbedded with iron poor material (Robb, 2005, Simonson, 2003).

BIF of the Hamersley Province are a classic example of "Superior BIF". These formations were generally deposited on stable continental platforms away from the wave base. At times these deposits interacted with the wave base, and cross beds are seen within some of the Hamersley units (Robb, 2005, Simonson, 2003).

BIF is formed in unique atmospheric, hydrospheric, lithospheric and biospheric conditions. These conditions were particularly sensitive to the acidity and redox state of the depositional environment. The typical mineral assemblages of BIF are iron oxides (haematite or magnetite), carbonates, silicates and sulphides. Cherts and carbonaceous shales often occur together with iron minerals (Robb, 2005, Simonson, 2003).

This region is of high economic significance due to the presence of several large high-grade iron ore deposits. The two largest deposits are located at Mount Whaleback near Newman and Mount Tom Price where reserves have been estimated at 1400 Mt and 900 Mt respectively. These ore bodies have been quantified as being high grade resources at approximately 64% Fe, with a high lump to fines ratio, and low impurities (MacLeod et al., 1963, MacLeod, 1966, Taylor et al., 2001, Morris, 1980)

Numerous hypotheses have been developed to explain the likely series of events responsible for the iron enrichment within the Hamersley basin. The work of Taylor et al., (2001) has been used for the ore genesis model to explain the staged hypergene and supergene enrichment within the area. In addition to this, a detailed overview of the Hamersley Group stratigraphy has been included as these lithologies are shown to outcrop extensively at the Mount Tom Price deposit which is the focal point of this research.

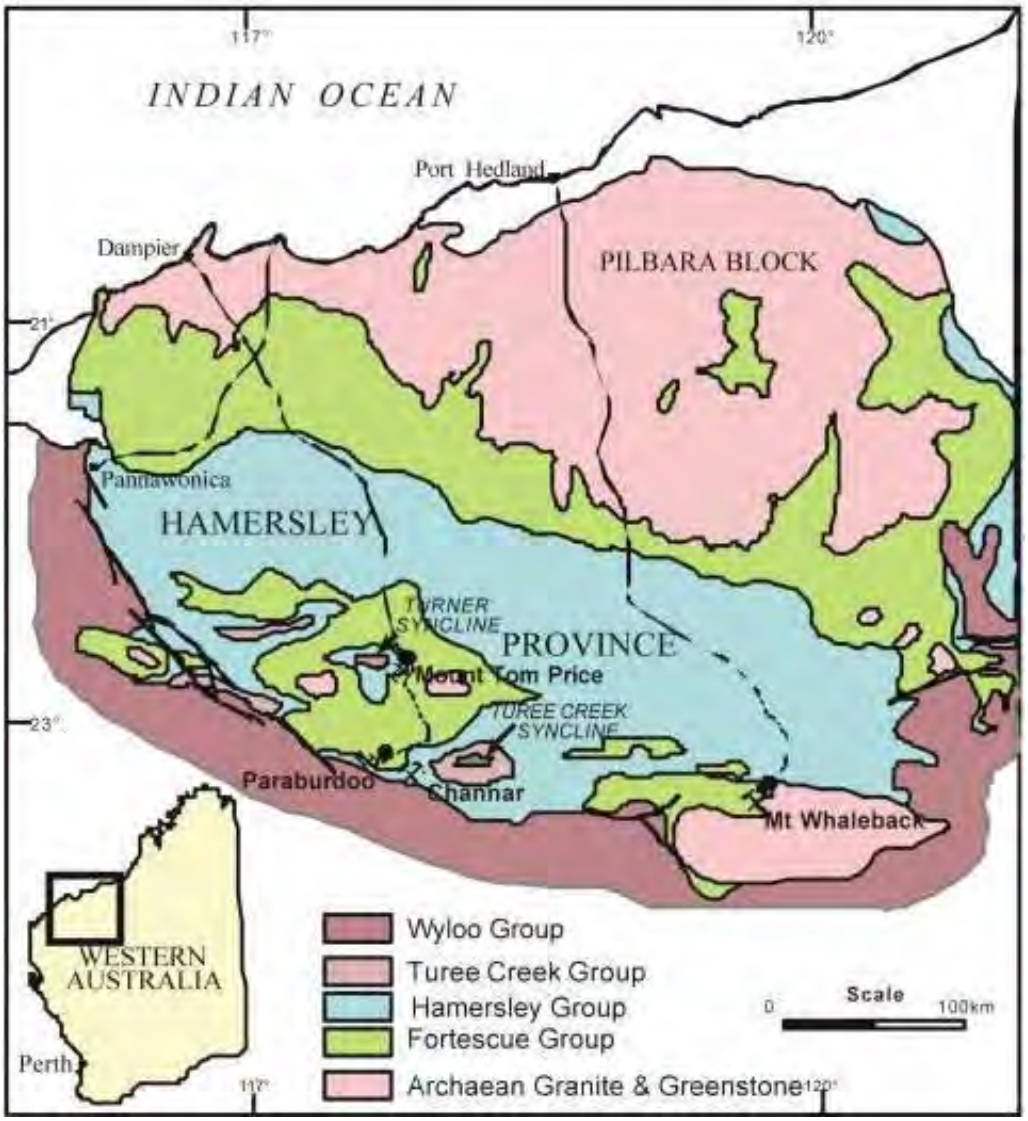

Figure 3-1 - Plan of the greater Pilbara region showing the Hamersley Province and the Mount Tom Price (Taylor et al., 2001)

3.2 Ore Genesis and Characterisation

Studies of iron ore genesis involve supergene vs syngenetic (otherwise known as hypergene) enrichment (Morris, 1985, Powell et al., 1999, Taylor et al., 2001) in three contrasting tectonic environments.

1) Compression during the Ophthalmian orogeny (Powell et al., 1999),
2) Post-Ophthalmian orogeny extensional collapse (Webb et al., 2003) and,
3) Aanorogenic Ashburton aged rifting (Li et al., 2008, Barley et al., 1999, Taylor et al., 2001)

It has been accepted by the above authors that ore formations within the Hamersley Basin occurred during the Paleoproterozoic, neither its age relative to known tectonic events nor the absolute age of those events is well established.

The Marra Mamba to Brockman Iron Formations of the Hamersley Group are exclusively deep-water sediments: they contain thin, laterally persistent tuff bands and spherulite horizons, evidence of distant volcanism and meteorite impacts (Simonson et al., 1993). The tectonic setting for this sedimentation up to and including the Brockman Iron Formation, was probably a slowly subsiding passive continental margin (Taylor et al., 2001).

It has been considered by (Morris, 1980, Harmsworth et al., 1990) that the martite-goethite ores are a product of Cretaceous supergene enrichment, while the hematite ores are all Proterozoic in age.

High grade hematite often occurs with martite and microplaty hematite but with little to no goethite. This characteristic high grade ore forms a small number of large deposits within the Hamersley Basin such as Mount Tom Price and Mount Whaleback. These major ore bodies extend to great depths (>400 m) which is significantly more than martite-goethite ore bodies. These high grade ores are predominantly confined to the Brockman Iron Formation where the greatest enrichment has occurred within lower Dales Gorge Member (DG). As a result of the extensive enrichment and associated high ore grades, the DG (~64% Fe) is the target lithology for the majority of mining operations within the Pilbara region (Taylor et al., 2001).

Martite-goethite ores from the parent Marra Mamba and Brockman Iron Formations formed by deep supergene enrichment through the precursor banded iron formations (BIF). The original magnetite is oxidised to hematite (martite), while iron silicates and carbonates are oxidised and hydrated to goethite. Other carbonates and quartz are leached out and replaced by goethite (Taylor et al., 2001).

The martite-goethite ore bodies are extensive and generally flat-lying, although in places they extend to depths >100 m, all are related to the present land surface. The ore bodies are predominantly soft with the exception of the upper hematite-rich hard cap. The abundance of goethite, yields a lump product (31.5 - 6.3mm) of lower grade ore than the high-grade hematite ore bodies (Harmsworth et al., 1990)

Mineralisation of ore bodies has been strongly linked to the influence of structural features within the Hamersley Basin as they promote the transportation of fluids to significant depths. Mount Tom Price (Figure 3-2) has a steeply dipping normal fault known as the Southern Batter Fault (SBF) which runs parallel to strike through the Southern Ridge (SR) and SEP

which has been credited in aiding the development of high grade hematite ores in the area (Harmsworth et al., 1990, Taylor et al., 2001)

Primarily the enrichment of BIF to ore is a subtractive process, where precursor components are removed from BIF allowing for residual concentrations of insoluble components; iron, aluminium and titanium.

Enrichment is undertaken through four distinct phases (Figure 3-3) as identified by Taylor et al (2001) where basin fluids and shallow supergene waters provided an environment for the evolution of the ore body and surrounding strata. These phases of alteration are evident in the paragenesis from BIF to ore in the Hamersley Basin where each process is a necessary precursor to the next.

The initial stage of hypergene enrichment removes all free silica from the iron formation, while leaving emplaced iron and carbonate; from both BIF and shale bands. This has resulted in thinning of the stratigraphic sequence. Fluids involved in this stage of enrichment are said to have been highly saline. Mafic dykes present within the basin are converted to a hydrous chlorite and talc bearing suite (Taylor et al., 2001).

Mineralogical investigation into these dykes provides evidence to suggest that a relatively low temperature (150 – 250°C) enrichment process was present at the time. The overlying origin of these large quantities of water to achieve such outcomes is yet to be confined to an ultimate source. Isotope work in Taylor et al (2001) carried out by (Becker and Clayton, 1972, Becker and Clayton, 1976) suggests a high level of exchange with carbonates in the Wittenoom Formation (WF) which would constrain the waters to be from a basin source.

Deep meteoric water (oxidised, low-salinity fluid with elevated temperature) circulation signifies the initiation of the second stage of enrichment within the basin creating the signature microplaty hematite. Oxidation extended downward through the strata leaving only a few remnants of the initial enrichment along the edges and bottom of the ore body. Other alterations occurring during this time involved magnitite converting to martite and siderite-stilpnomelane to low iron ankerite-hematite assemblages. Overall there is no noticeable loss in volume during this stage. The addition of oxygen to the environment does however continue the ongoing leaching of silica (Taylor et al., 2001).

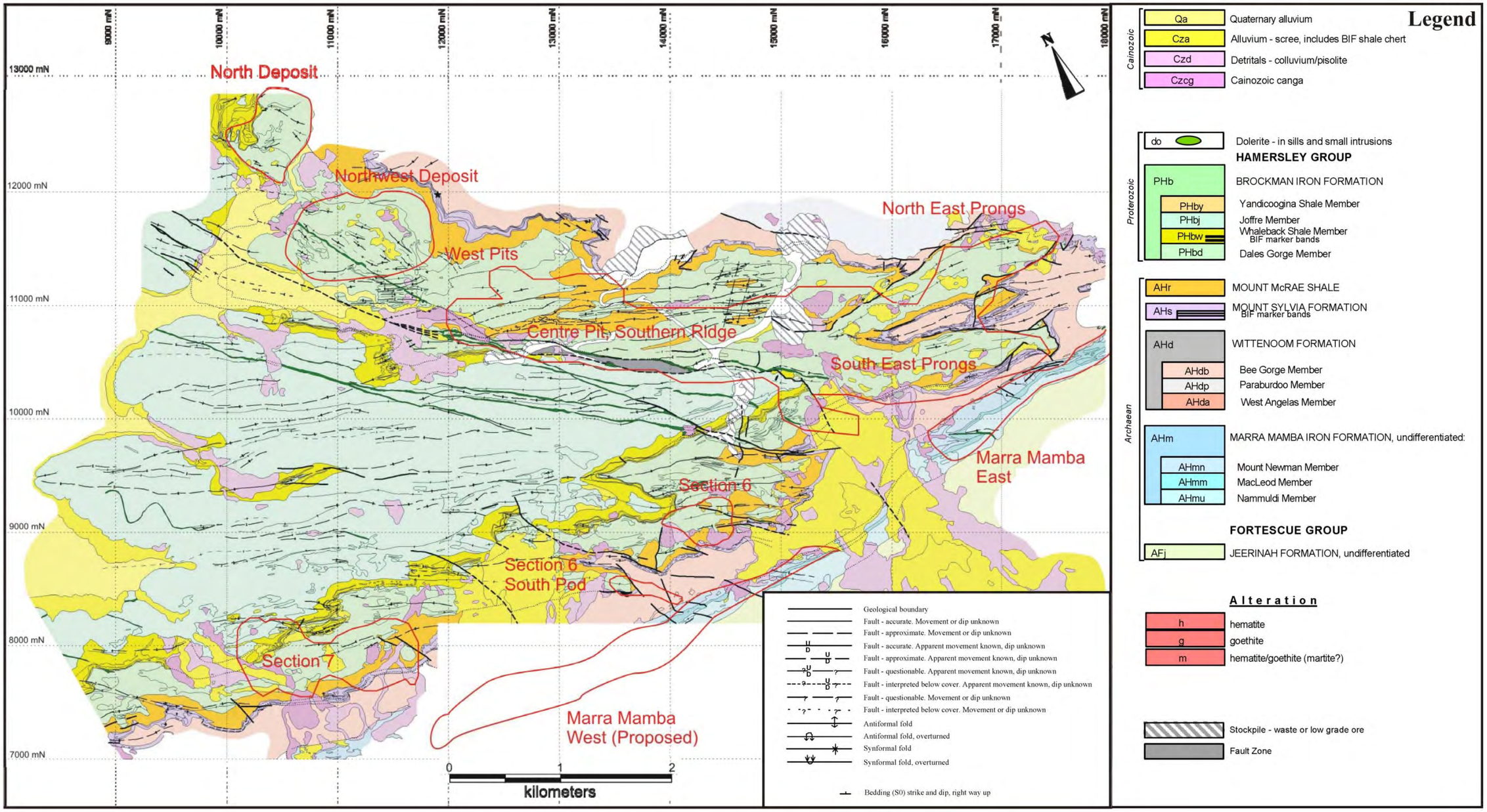

Figure 3-2 - Geological map of Mount Tom Price with associated pit locations (RTIO, 2009)

In the third stage of enrichment, leaching of the remaining carbonate gangue material occurs within the BIF sequence. This leaves a very porous magnetite-apatite or hematite-apatite assemblage. This process is evident at considerable depth at the eastern end of the Mount Tom Price deposit. This is responsible for dissolving most of the remaining dolomite from the Paraburdoo Member underlying the SEP (Taylor et al., 2001).

The final phase of supergene enrichment as modelled by Taylor et al, (2001) was underpinned by a final weathering sequence (consisting of oxidising fluids said to be cold shallow meteoric waters) where the shale bands underwent some major alterations. This is undistinguishable from other modern weathering surfaces however the level of penetration was a lot greater than modern weathering. All remaining magnesium and calcium was lost while the pyrite that was present was oxidised to limonite. The BIF experienced leaching of almost all its calcium and phosphorus which resulted in a final residiumm of highly porous high grade hematite ore. The shale bands had a significant volume reduction and were left consisting largely of clay with high aluminium and titanium values which now constitute the main impurities found within the ore body.

The final product can be characterised as being a highly porous hematite ore with a distinctive microplaty texture that is interbedded with kaolinitic shale. The major impurities are aluminium and titanium which retain their relative proportions throughout the upgraded process (Taylor et al., 2001).

High grade hematite enrichment models differ between the respective authors. Morris, (1980) and Powel et al., (1999) suggests this occurs through deep penetration of oxidising meteoric water. Taylor et al., (2001) however, raises the concept of surface weathering from adjacent BIF sequences where it migrates down to favourable locations and allows for the replacement of silica from BIF, with goethite. This process accounts more accurately for the original mesoaband textural preservation.

The genetic model by Taylor et al., (2001) proposed that the initial process of hypergene silica leaching and resultant compaction took place at substantial depths with elevated temperature during a phase of basin dewatering. Early normal faults in the area have allowed for the outflow of silica unsaturated waters from the underlying carbonate aquifers of the WF and up into the overlying Brockman Iron Formation.

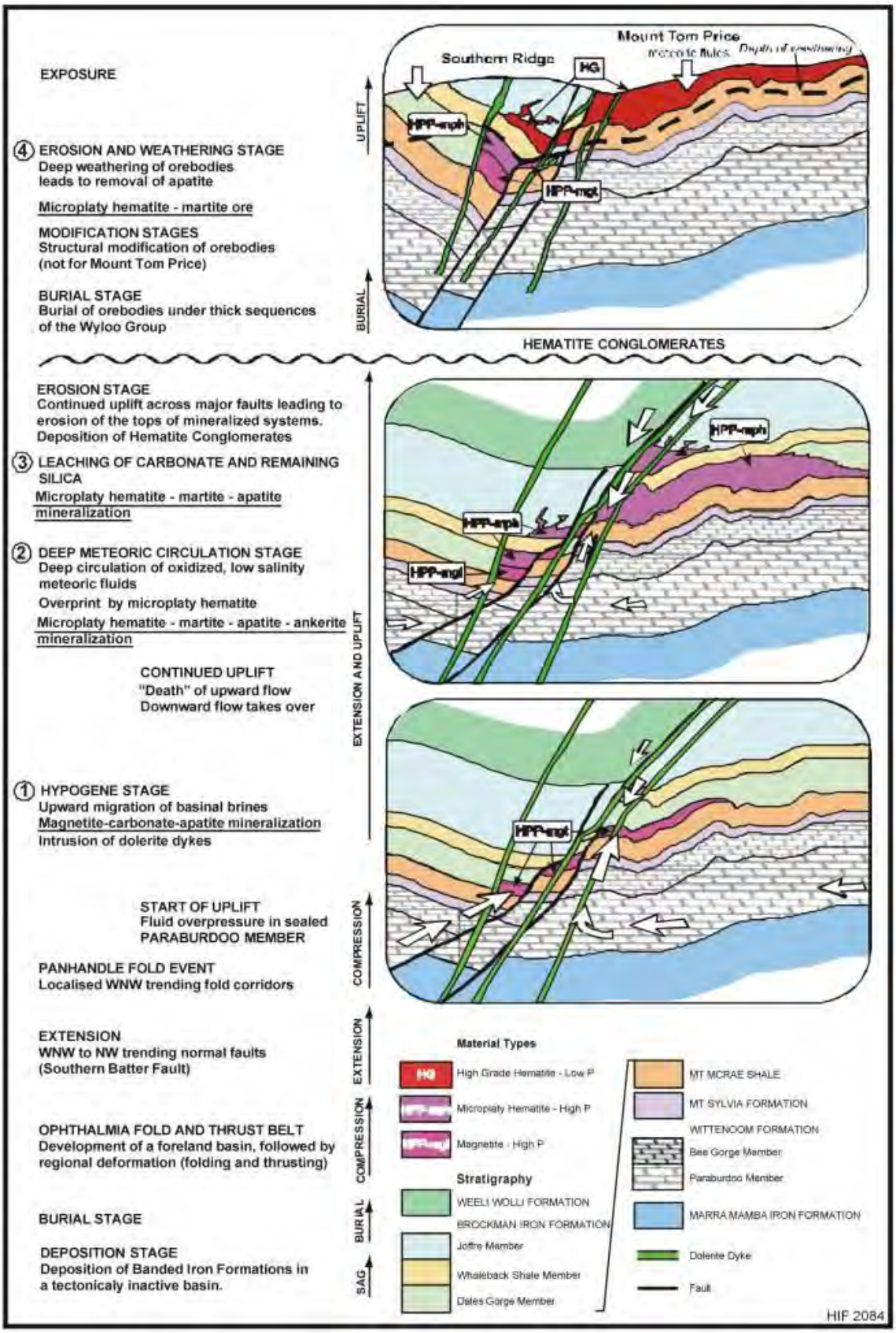

Figure 3-3 - Overview of enrichment process responsible for high grade hematite development in the Hamersley Province as suggested by Taylor et al, 2001.

3.3 Stratigraphy of the Hamersley Province

The Hamersley group outcrops over 800km^2 in the Pilbara Region (Figure 3-1) were it conformably overlies the volcanics and sediments of the Fortescue Group. It is in turn overlain by the Wyloo Group with broad regional conformity but with local discordance. The three groups together comprise the Mount Bruce Supergroup (Morris, 1980). An outline of each formation making up these respective groups has been included in stratigraphic order below.

3.3.1 Fortescue Group

Jeerinah Formation

The Jeerinah Formation, forming around 2750 Ma in a sub-aerial volcanic environment is the earliest observable formation in the Mount Tom Price mining area (Trendall et al., 1998). This formation consists of a sequence of dolerite, shale, dolomite, dolomitic mudstone, chert, and minor tuff. The formation measures approximately 1000 m thick with a conformable contact overlying the Marra Mamba Iron Formation at the majority of locations. However, the contact at the Turner Syncline, is unconformable which is most likely caused by localised slipping during the formation of the syncline during the late Archaean (Trendall and Blockley, 1970).

3.3.2 Hamersley Group

The Hamersley Group was first defined by MacLeod et al (1963) with subsequent studies carried out by (Gilhome, 1975, Harmsworth et al., 1990, Blake and Barley, 1992, Trendall et al., 1998). The following formation descriptions are based on a summary of the above author's works in addition to (Rivers, 1998).

Marra Mamba Formation

The Marra Mamba Iron Formation/Supersequence as defined by Blake and Barley (1992) has been dated near its base at c 2597±5 Ma utilising Ion Microprobe U-Pb zircon dating (Trendall et al., 1998). It has a stratigraphic thickness of ~230 m (Figure 3-4). The uppermost unit hosts major iron deposits in the region. This Supersequence/Formation is the basal unit of the Hamersley Group and is divided into three members which are outlined below.

The Nammuldi Member has a stratigraphic thickness of ~135 m. This unit contains cherty BIF (chert and magnetite bands) interbedded with thin shales. The Nammuldi Member is overlain by the MacLeod Member (35 m) which comprises BIF, chert and carbonate with interbedded shales. The Mount Newman Member is the uppermost member in the sequence with a thickness of ~60 m. It contains manganese-bearing BIF with interbedded carbonate

and shale. The interbedded shale bands of the Marra Mamba Formation are laterally continuous; these represent kaolinised volcanic tuff layers, which provide an excellent set of regional markers. Characterisation of "macrobands" can be achieved using unique radioactive log „signatures' within the formation (Trendall and Blockley, 1970, Gilhome, 1975, Harmsworth et al., 1990, Blake and Barley, 1992, Krapez, 1997).

Wittenoom Formation

Stratigraphic thickness of the WF varies throughout the Hamersley Province, it has been estimated that the thickness ranges from 300 - 600 m (Figure 3-4). It is difficult to accurately constrain the true thickness of the Wittenoom Dolomite due to dolomitic solutioning, geological structure, sparse nature of the outcrop, and high weathering rates (Trendall et al., 1998). The distribution of the outcrop directly corresponds to the broad valleys between the hog-back ridges of the Brockman and Marra Mamba Iron Formations. This formation represents a reversion to principally clastic sedimentation within the basin, with a gradual transition to chemically precipitated sedimentation as seen in the dolomites low in the formation. These units have a limited lateral persistence, with chert and dolomite lenses measuring less than 2 m long. Due to the weak nature of the shale, the formation has a greater degree of folding compared to the other units (Trendall and Blockley, 1970, Harmsworth, 1990).

The Wittenoom Formation is subdivided into three separate stratigraphic units; the lowermost West Angela Member, the Paraburdoo Member (often referred to as the Wittenoom Dolomite) and the uppermost Bee Gorge Member (Trendall and Blockley, 1970, Harmsworth et al., 1990, Simonson et al., 1993, Blockley et al., 1993).

With a thickness of ~40 m the West Angela Member consists of shale (often magniferous), chert, and massive, medium to thin-bedded dolomite (in unweathered sections) with minor BIF near its base. When observing a fresh sample, dolomite is finely crystalline with faintly banded brown, pink or grey colouration. Other diagnostic features include sedimentary structures such as cross-beds and slumps, with diagenetic features such as styolites, and chert nodules (Trendall and Blockley, 1970). The Paraburdoo Member has a stratigraphic thickness of up to 150 m. The crystalline dolomite has interspersed chert bands throughout. The upper most Bee Gorge Member has an age of ~2561 ± 8 Ma (Trendall et al., 1998) made up of alternating shale bands and dolomite with minor cherts, volcaniclastics and BIF (Trendall and Blockley, 1970, Harmsworth et al., 1990).

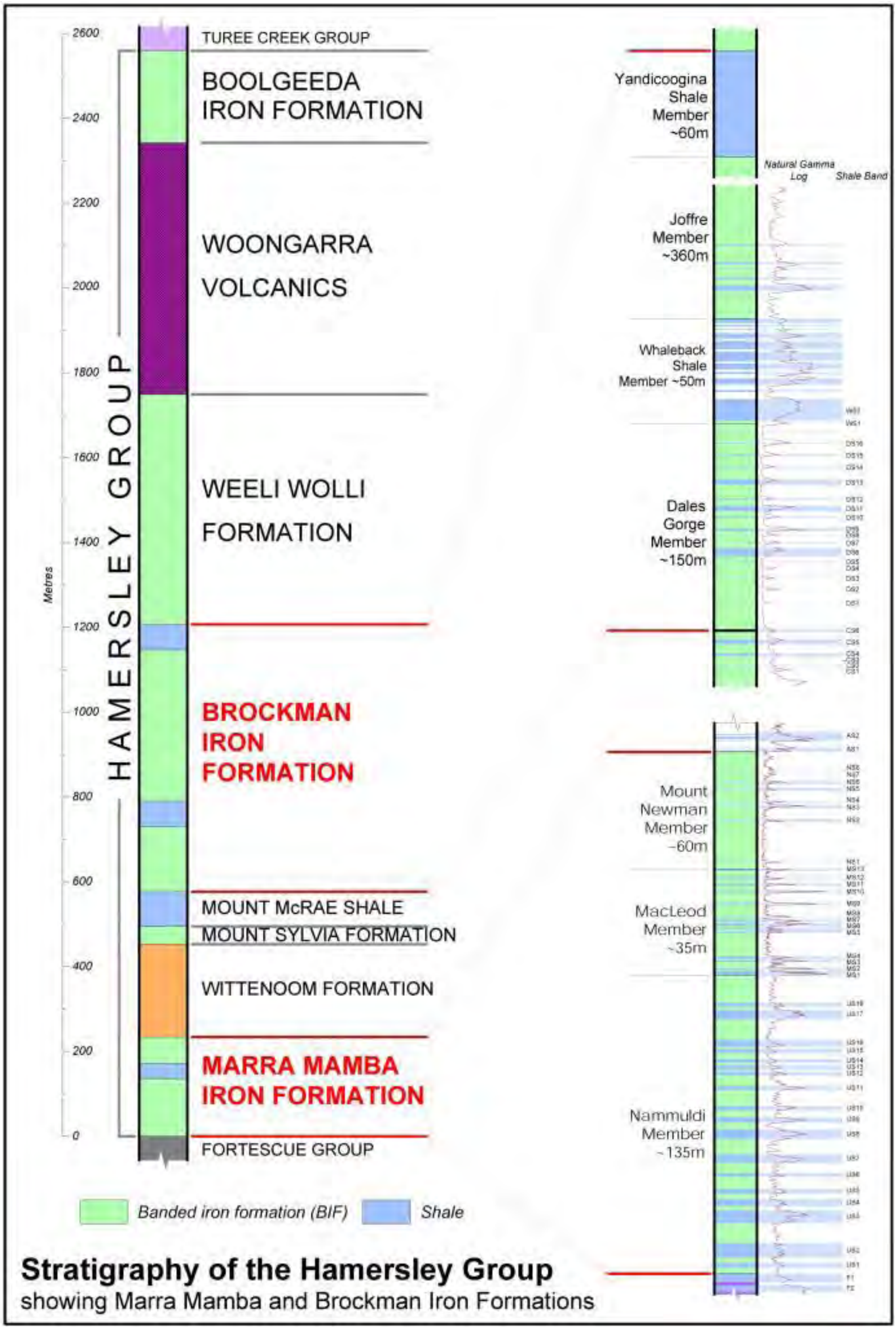

Figure 3-4 - Stratigraphic Column of the Hamersley Group showing detailed section of the mineralised Brockman Iron Formation and Marra Mamba Iron Formation (RTIO, 2000).

Mount Sylvia Shale

The Mount Sylvia Shale (MTS) is approximately 30 m thick (Figure 3-4) and has a conformable contact with the underlying Wittenoom Formation. The formation is defined by three prominent BIF-chert units separated by interbedded chert, shale and dolomite. The uppermost BIF (8m) has been informally named „Brunos Band' and is one of the most continuously outcropping units in the basin which makes it an excellent lateral stratigraphic marker. A siltstone, with tuffaceous zones and intermittent cross-bedding, characteristically occurs below Brunos Band. The Mount Sylvia Formation is spatially restricted to the eastern part of the Hamersley Province, providing a rare example of terrigenous elastics in the Hamersley Group (Harmsworth et al., 1990, Trendall and Blockley, 1970, Gilhome, 1975, Taylor et al., 2001).

Mount McRae Shale

The Mount McRae Shale (MCS) is a 50 m thick formation (Figure 3-4) which conformably overlies the Mt. Sylvia Formation and is subdivided into four members, based on lithology and pyrite content. Where outcrops are visible they are often veiled by Brockman Iron Formation debris as a result of high weathering rates.

This predominantly shale formation is made up of argillaceous materials of varying structure and colour according to the presence of free carbon. Pyrite nodules and zones of ferruginous concretions are abundant. These zones are not confined to individual beds, suggesting that they derived through chemical precipitation during diagenesis. There are also thin bands of volcanic shards in beds of volcanic breccias (Trendall and Blockley, 1970, Harmsworth, 1990).

The MCS has characteristic black carbonaceous shale within the lowermost 15 m of its stratigraphic thickness. Towards the top of this section the chert becomes increasingly pyritic where a triple chert band (< 3m thick) is a useful marker. Overlying these beds is a 10 to 15m thick zone of alternating chert, black shale and minor dolornitic shale (this can contain up to 7% pyrite), above the pyritic zone is a 10 m zone of non-pyritic black shale. The top 12 m of the MCS is formally known as the "Colonial Chert Member", comprising of thin BIF with interbedded shales (Trendall and Blockley, 1970, Harmsworth, 1990).

Brockman Iron Formation Supersequence

The Brockman Iron Formation (Figure 3-4) or supersequence (Blake and Barley, 1992) is the most economically viable, minable ore resource in the Hamersley Province. The stratigraphic thickness varies extensively as it ranges from 500 m at Paraburdoo and Newman to 620 m at

Mount Tom Price. It is characterised by alternating sequences of BIF, shale and chert, subdivided into four principal members; the Dales Gorge Member, the Whaleback Shale Member, the Joffre Member and the Yandicoogina Shale Member (Harmsworth et al., 1990, Blake and Barley, 1992, Krapez, 1997).

Dales Gorge Member

The Dales Gorge Member (DG) ranges in thickness from ~150-180 m. Its assemblage is comprised of 17 alternating BIF macrobands (DB0-16) and 16 shale macrobands (DS1-16) (Figure 3-4). The shale macrobands are laterally persistent throughout the province, they are divided into three units DG1-DG3: *DG1* (to the base of shale band DS6); *DG2* (base of DS6 to the top of DS11); and *DG3* (top of DS11 to the upper contact of the Member). The composition of BIF is made up of banded iron, chert, jaspilte, hematite and magnetite. The shale macrobands are usually unaltered, however these can contain ferruginous zones of which iron percentages can reach up to 60% (Hamersley Iron Pty Ltd, 2000, Trendall and Blockley, 1970, Gilhome, 1975, Harmsworth et al., 1990). The DG1-DG3 units within this member make up the primary mineralised ore material sourced in the province.

Whaleback Shale Member

The Whaleback Shale Member (Figure 3-4) has a thickness of ~50 m. This member is divided into two zones: a lower zone consisting of four alternating macrobands of shale and BIF (WS1, WB1, WS2, WB2); and an upper zone (WS3) consisting of numerous mesobands of chert and shale. WB2 can be differentiated as it contains a 4 m thick cherty BIF which is typically crenulated (Gilhome, 1975, Harmsworth et al., 1990).

Joffre Member

The Joffre Member (Figure 3-4) has a stratigraphic thickness of ~360 m and is predominantly BIF with minor stilpnomelane-rich shale interbands and tuffaceous material. These shale interbands are thinner and do not exhibit the same lateral persistence as those belonging to the DG. This member has been separated informally to reflect their age and is known by the name J1 - J6. Strands J1, J3 and J5 contain more shale than J2, J4 and J6. BIF is typically more abundant than shale in this lithology, especially where unaltered. It is made up of alternating bands of magnetite, hematite and chert. This typically alters to hematite, goethite, limonite and ferruginous shale. Localised enrichment can be found where the Joffre and DG members are interconnected by a fault system allowing the transfer of fluid (Taylor et al., 2001, Trendall and Blockley, 1970, Harmsworth et al., 1990).

Yandicooginga Shale Member

The Yandicoogina Shale Member is a 60 m thick alternating sequence of interbedded chert and shale. The western extent of this member shows intrusions of dolerite sills while being locally enriched to form high grade hematite ore (Trendall and Blockley, 1970, Harmsworth et al., 1990).

Weeli Wolli Formation

This formation is ~450 m in thickness (Figure 3-4) and can be defined by an alternating sequence of BIF, shaly BIF, shale and dolerite (individual units show variations in thickness from 1 to 70 m). In locations of outcropping BIF is characteristically red in colour, and may be enriched to high grade ore on a local scale. This ore is of only minimal economic importance, and generally occurs adjacent to the enriched Brockman Iron Formation (Trendall and Blockley, 1970, Harmsworth et al., 1990).

3.4 Mount Tom Price Ore Bodies

Several discrete ore bodies occur near the keel of the large Turner Syncline. Surface outcrop of the ore body was originally noted to occur north of the WNW trending Southern Batter Fault. The main ore body extends for a total of seven kilometres at a width of up to 1.6 km (600 m average) from North Deposit to the SEP, “deep resources” can be found up to 500 m below the pre-mining surface. An overview of the Mount Tom Price pit network has been included in Figure 3-2. Attractive attributes of the deposit include a high lump to fines ratio and low impurities, especially Phosphorus <0.05%) (Taylor et al., 2001, Gilhome, 1975, Harmsworth et al., 1990, Thorne et al., 2004, Hamersley Iron Pty Ltd, 2000).

Iron ore in the Mount Tom Price deposit is primarily derived from BIF with a dominance of haematite, which is classified as Low P (Phosphorus) Brockman ore. This ore can be identified in hand specimen through its metallic lustre and dark red-brown and grey bandings as illustrated in Figure 3-5a. The SEP deposit is the largest of these ore bodies extending 1.0 x 0.3 km where high grade mineralisation of the DG is present to depths of 250 m. Mining areas to the south of the main Mount Tom Price deposit are examples of High P Brockman ore (haematite-goethite rich), that are typically capped with thick detrital and hydrated goethite deposits. A sample of High P Brockman ore is shown in Figure 3-5b where it can be characterised by the metallic grey lustre of haematite and zones of yellow brown goethite. Section 7 measures 1.5 km long and 0.8 km wide, where mineralised DG extends to depths of 120 m.

Further mineralisation of economic significance occurs with Marra Mamba Iron formation at a number of locations south of the Mount Tom Price deposit. The Marra Mamba East pit is now operational while the Marra Mamba West pit has been designated for future mining operations. Mineralisation of Marra Mamba ore within these pits extends to depths of 200 m and 4 km in length. Characteristic features of this ore in hand specimen include bands of haematite and goethite as shown in figure Figure 3-5c.

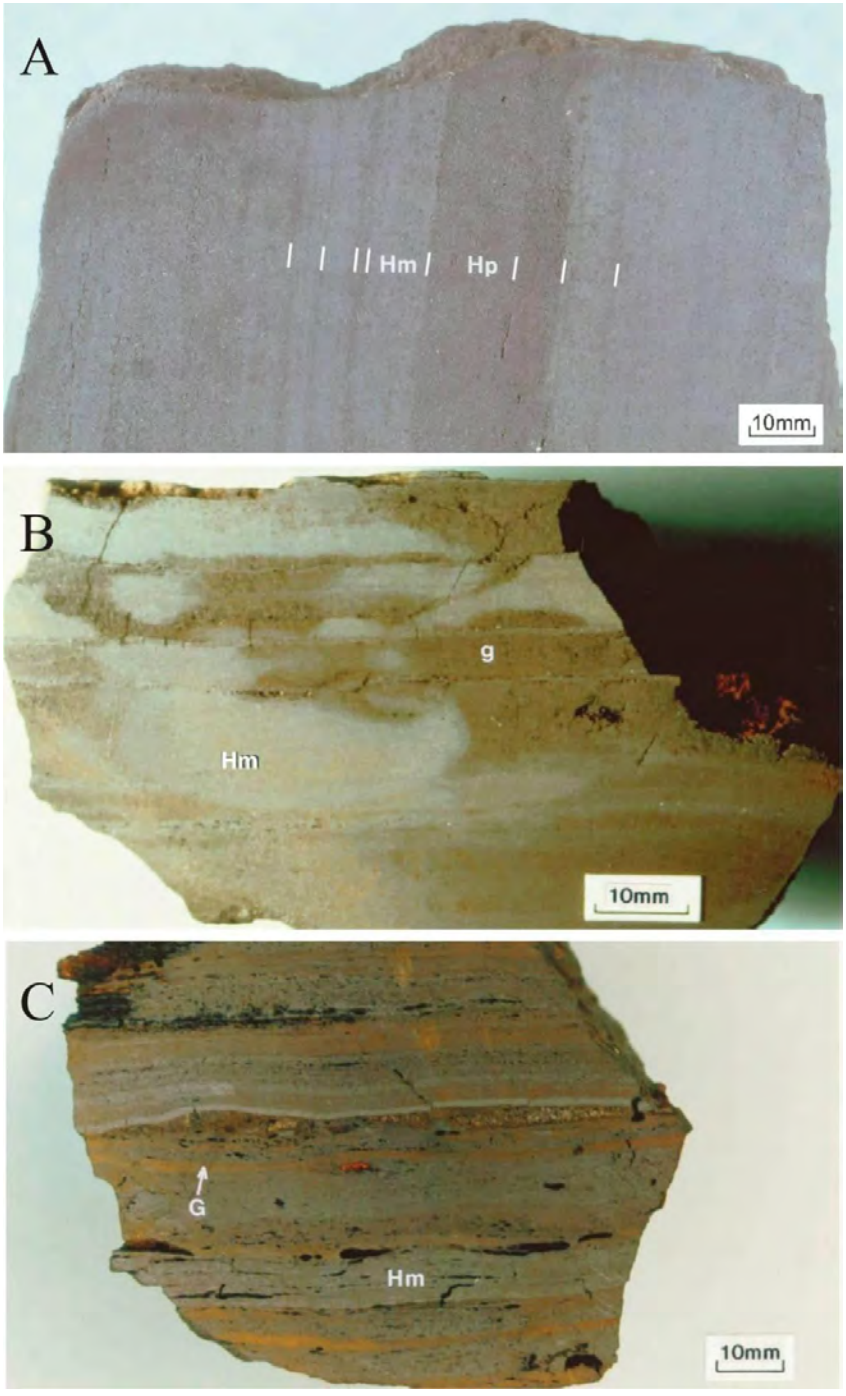

Figure 3-5 - Generic ore types found at Mount Tom Price. A) Low P Brockman, B) High P Brockman and C) Marra Mamba. Hm – Haematite (microplaty) Hp – Haematite (martite) G – Goethite.

3.5 Conclusion

Enrichment mechanisms of the original BIF material have been the subject of extensive debate for the last 30 years. A four stage enrichment process, suggested by Taylor et al., (2001) has been adopted for use in this study. Initial hypergene enriched was initiated by an upward migration of highly saline basin fluids. These acted to remove all free silica from the BIF sequences leaving emplaced iron and carbonate assemblages. This was followed by deep circulation of low salinity meteoric fluids creating the signature microplaty hematite ore material. The meteoric circulation effectively halted up previous upward fluid flow. Ongoing uplift and extension of the basin resulted in leaching of carbonate and silica gangue material leaving a suite of very porous magnetite-apatite or hematite-apatite assemblages. An episode of erosion and weathering took place through circulation of shallow cold meteoric waters. This signifies the final stage of supergene enrichment, BIF material experienced leaching of almost all its calcium and phosphorus. This resulted in a final residiumm of highly porous high grade hematite ore.

This enrichment process has resulted in the Hamersley Province containing two highly enriched iron ore sequences that are laterally persistent and can extend to great depths (~400 m). These include the Brockman and Marra Mamba Iron Formations. The Brockman Iron Formation (DG1-3) holds the majority of high grade deposits with iron grades in excess of 64% comprised of enriched hematite, goethite and limonite with minor amounts of magnetite. These are most extensively deposited within the Mount Tom Price and Mount Newman regions. The Marra Mamba Iron Formation is a slightly lower grade ore body at ~61% Fe. The ore has a higher ratio of fines product (<6.3 mm) compared to the Brockman derived ore which yields a higher ratio of lump product (31.5 - 6.3 mm).

Chapter 4: Local Hydrogeology

4.1 Introduction

Mining at the Mount Tom Price commenced in 1966, where ore recovery was primarily carried out above the groundwater table requiring relatively little hydrogeological related investigation. Initial hydrogeological work was carried out to develop and deliver a sustainable water supply to the mining towns of Tom Price, Paraburdoo and Panawonica (Hedley and Domahidy, 2007)

In addition to supplying water to these towns, hydrogeological requirements within the Mount Tom Price operation have developed significantly in the last forty years. Mine operations extending below the groundwater table now require in depth analysis to achieve the most efficient and effective groundwater management scheme possible. Priorities now include pumping from the rockmass, to lower the groundwater level for pit cutbacks and drop cuts. In addition a quantity is required to supply both for consumption and mine operations (e.g: dust suppression). Finally, depressurisation of pit walls within the SEP is required to achieve geotechnical stabilisation of the wall rock.

Groundwater within the Pilbara region is primarily derived from three main aquifer types. Shallow unconfined aquifers are present in recent alluvial deposits which can include calcrete. Semi confined aquifers can be found in palaeovalley fill deposits throughout the region. Finally, confined aquifers are located in the fractured and cavernous bedrock that makes up the majority of the region. For the purposes of this study the primary focus will be on the confined aquifers within the region as these best relate to the hydrogeological conditions present within the SEP pit.

Confined aquifers within the Tom Price region typically develop within generally low permeability bedrock strata of the DG member. Groundwater flow increases along fracture developments within these lithologies rock; this can be attributed to structural lineations and zones of mineralisation. Local fracturing and cavity development can also occur in areas where bedrock is exposed to high levels of weathering; developing an enhanced secondary permeability.

Recharge to the main aquifer (fractured, confined rock mass) is attributed to direct infiltration from seasonal rainfall. Water is known to percolate into bedrock aquifers where creek and

stream beds intersect with free lying outcrops. If shallow sediment bound aquifers are present in the overlying strata leakage can occur which can act as a recharge source.

4.2 Regional rainfall statistics and catchment details

The Pilbara region covers more than 500,000 square kilometres where the climate is classified as arid-tropical. Two distinctive seasons (wet and dry) can include hydrological extremes which can range from droughts to large scale flooding events. The wet season, from late November to early April, can bring high rainfall and possible cyclones. Rainfall records for Mount Tom Price 1972 - 1998 (Bureau of Meteorology, intermittent records) and 1998 - 2008 (RTIO, 2009a) show an annual average rainfall for Mount Tom Price is just over 400 mm. The rainfall is episodic and highly variable between years. The majority of rainfall occurs during the hottest months, between December and April, resulting from cyclonic lows. Winters are dry and mild in comparison with lighter, winter rainfall expected in June/July each year. Due to the low rainfall and brief wet season, watercourses flow, if at all, for only brief periods (Beckett, 2007).

Regional drainage is typically directed towards the Indian Ocean, this is made up of a combined inland and fringing coastal drainage systems. Of particular relevance to the hydrology of the Mount Tom Price region are the Hardey River, Seven Mile Creek and Turee Creek catchments (Hedley and Domahidy, 2007).

The elongated Hardey River catchment extends from Mount Tom Price in the northeast, southwest towards a confluence point with the Beasley River, while the Seven Mile Creek catchment extends from Mount Tom Price in the north and drains south into the Ashburton River (Hedley and Domahidy, 2007).

4.3 Aquifer Characteristics

Lithologies that make up the primary aquifers within the Hamersley Group rocks include the DG (DG1- DG3) as well as the mineralised segment of the FWZ. The DG in particular is more permeable than its parent host BIF. A lower aquifer system is present within the Marra Mamba Formation and includes the overlying WF. This can be visualised in Table 4-1 where the stratigraphic column for the area has been adapted to show the respective hydrogeological attributes of the strata. To accompany the stratigraphic column a table of the respective hydrogeological characteristics for the Hamersley Group lithologies has been included in Table 4-2. Other units of high permeability include the Brunos Band, located in the MTS. This unit is typically composed of impermeable shales, with a 10 m chert band that can act as

an aquifer, transmitting water at 1–5 m/day where the unit is faulted and folded (Rathbone, 2008).

Table 4-1 - Hamersley Iron stratigraphy with respective hydrogeological aquifer characteristics. (Preston, 1995).

Formations	Members	Features	
Tertiary & Quaternary Formations major unconformity		Detritals, Colluvium & restricted strips of Alluvium	permeable deposits
Brockman Iron Formation	Yandicoogina Shale Member	Chert - Shale Sequence	confining beds
	Joffre Member (J1 - J6)	Haematite BIF	poorly permeable
	Whaleback Shale Member	Chert - Shale Sequence (50% Haematite/50% Shale)	confining beds
	Dales Gorge Member (DG1 - DG3)	Haematite +7% Shale, when mineralised	AQUIFER
		Haematite +30% Shale, when mineralised	AQUIFER
		Haematite +6% Shale, when mineralised	AQUIFER
MCS (32m)	Foot Wall Zone	Haematite + Shale, when mineralised	AQUIFER
		Colonial Chert - interbedded shale and chert	confining beds
	'Pure Shale'	Massive Black Shale *Pyritic Black Shale Basal Shale Chert	confining beds
Mt Sylvia Formation		Shale with Dolomite and three distinctive iron formation bands - Bruno's band at top	confining beds
	Angelas Shale	Shale	
Wittenoom Dolomite		Dolomite	AQUIFER
Marra Mamba Iron Formation		Haematite + some Shale, when mineralised	AQUIFER
		Haematite BIF	poorly permeable

Note: Wittenoom Dolomite is now formally recognised as the Wittenoom Formation

Table 4-2 - Hydrogeological Characteristics for significant aquifer related lithologies within the Hamersley Group. (RTIO, 2009a).

Unit	Hydraulic Conductivity (m/day)	Specific Yield	Storativity
Ore	3	0.05	$2.0x10^{-4}$
Mount McRae Shale	0.01	N/A	$2.0x10^{-4}$
Brunos Band	17	0.01	$2.0x10^{-4}$
Mount Silva Shale	0.01	0.001	$1.8 x10^{-5}$
Wittenoom Formation	7	0.003	$3.1 x10^{-4}$
Fault Zones	0.5	N/A	N/A

Note: N/A infers Not Available

A series of intrusive dolerite dykes have penetrated the various formations throughout the province. When these dykes are exposed and highly weathered they break down into a low permeability clay rich material, which then can act as an aquitard or barrier to flow within the aquifers. In combination with fault gauge material a significant level of aquifer compartmentalisation has occurred in some aquifers throughout the regions, e.g. Paraburdoo (Preston, 1995).

Historically within the greater Mount Tom Price region, the hydraulic gradient has been defined as having an overall south west flow direction. A notable groundwater "mound" is evident in the centre of these radial flow paths beneath the Southern Ridge (and formerly Synclines) deposits. The overlying flow is represented in the contoured map in (Figure 4-1) which shows the evolution (or development) of the groundwater levels over the past 15 years.

This development could be viewed as being an aquifer response resulting from ~8 years of dewatering (as pumping at Mount Tom Price first began in 1994). The observed groundwater mound would appear to simply be a perched water table that has been segregated from the outer lying flow systems by an impermeable anticlinal structure, as it does not show a significant response to the ongoing pumping within mine. This could indicate that there is poor hydraulic conductivity throughout the mine. In addition, structural controls such as faults can act as barriers to flow in areas where gauge material has developed, which is likely to be responsible for creating compartmentalisation within the aquifers.

From the centrally located groundwater mound the hydraulic gradient tapers off and is visually lower to the North West in ND and to the east in SEP as the groundwater drainage appears to closely follow that of topographic drainage for surface water.

Recharge is primarily sourced via structural pathways which connect it to the underlying confined aquifer units (MTS and WT). Recharge also occurs through rainfall infiltration over the pit catchment area (RTIO, 2008).

4.4 Dewatering History

A large scale dewatering program was first commissioned at Mount Tom Price at the beginning of 1994. This was in response to pit floor progression first encountering both regional and perched water tables within the area. The first pit to require groundwater lowering was ND where a single pump (DB4) extracting approximately 300 kL/day from 1994-2004. Since the initial installations a further four bores (WB03NTD1, WB05NTD1, WD06NTD1 and WD06NTD2) have been installed. This gives a total pumping capacity of between 300–2500 kL/day.

The SEP has also been a focus of extensive dewatering infrastructure installations. Currently the SEP is the deepest pit within the RTIO operations and ore is exclusively mined from below the initial groundwater table. There are currently a total of four production bores (Bullnose - WB05SEP01, Eastern - WB06SEP01, Central -WB07SEP01 and Western - WB08SEP01) located within the pit. At least three of these pumping bores are active at any one time, each pumping volumes between 420–5160 kL/day on average. These intersect permeable mineralised units of the Dales Gorge Member of the Brockman Iron Formation. The ore body aquifer is enclosed by the low permeability MCS which is orientated in a broad synclinal structure.

There are currently active dewatering operations in place at Section Seven (WB05SSEV01) and the North East Prongs pits (Northern - WB07NTD02 and Switchback - WB07NTD01). A complete record of pump locations is included in Figure 4-3 (results approximated from Rio Tinto Hydrogeological Database, 2009a).

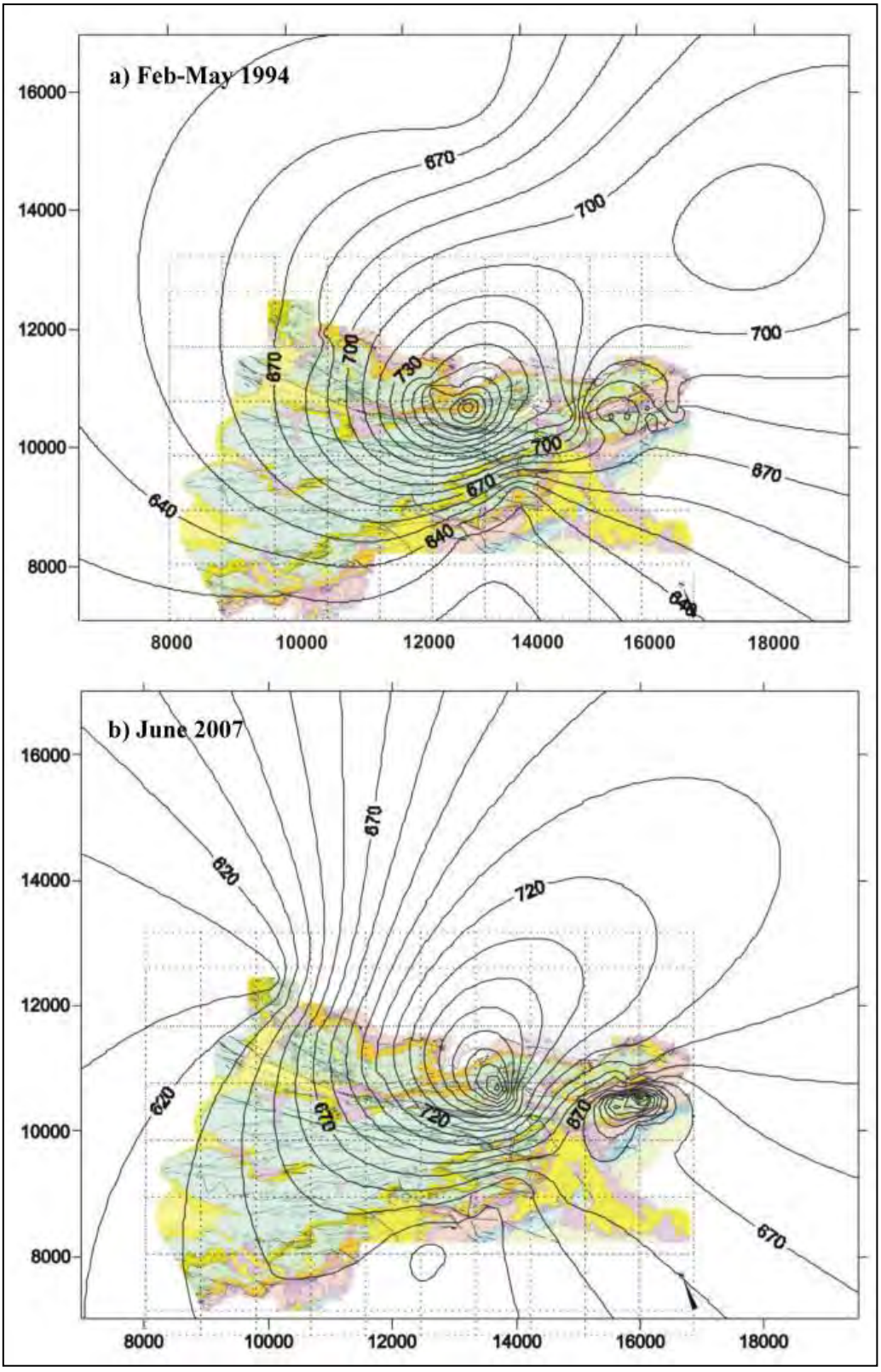

Figure 4-1 - Groundwater contours for great Mount Tom Price Mine area. A) Shows the pre pumping flow conditions while B) shows the effects of thirteen years of active dewatering. Of particular note is the groundwater "mound" that remains throughout the duration pumping, this is located within the Synclines/Southern Ridge area (Source: Manewell, 2008)

4.5 Aquifer Performance

Water levels in the SEP aquifer continue to draw down in response to pumping, with significant draw downs observed close to the new dewatering bores. The current water level (at the time of writing) in the centre of the pit floor (WB06SEP01) of the SEP is ~ 597mAHD. Water levels in the pit walls remain much higher than in the ore body aquifer as a result of the much lower permeability in the footwall sequence, although some enhanced drainage is occurring via the horizontal drainage depressurisation bores. A more in depth analysis of the SEP dewatering progress will be provided in Chapter 5 as a specific case study is developed. Since pumping commenced in 1994 there has been little to no effect on the perched groundwater mound either from the SEP or ND dewatering bores as shown by monitoring data and the respective contours (Figure 4-1). This would suggest that not all zones are hydraulically connected and that the major Southern Batter Fault that runs parallel to strike along the centre and SEP pits acts as a conduit to flow in these areas.

Utilising site based piezometric data and relating this to the relative groundwater levels throughout the Mount Tom Price mine, a certain level of localised hydraulic connectivity appears to be present. In locations such as the SEP there does appear to be a level of compartmentalisation present as a result of intersecting low permeability shales such as MCS and MTS that bound the ore. These are fault controlled zones where the folded nature of the lithologies form a double plunging synclinal structure within the pit. This effectively encapsulates the higher conductivity DG 1-3 and FWZ inside the MCS. Further structural discussion has been included in Chapter 5.

Areas that have been exposed to prolonged blasting will undoubtedly have an increased secondary permeability due to induced small scale fracturing. This is evident when analysing time vs drawdown hydrograph plots within the SEP. As a blast is executed there is a notable drop in the surrounding groundwater levels due to the increase secondary permeability (Figure 4-2). Another likely cause for increased secondary permeability will be the rock materials response to unloading of the overlying material. As ore is excavated from the pit the relative level of compression acting on the underlying strata will be reduced (Domahidy, 2008).

A study of the flow dynamics within the SEP by Rozlapa, (2008) has shown that some faults provide a hydraulic connection between the eastern and the western parts of the ore body aquifer in the SEP pit area. Outside the ore body aquifer, faults allow flow or drainage from the MCS, MTS and WT toward the pit that would not normally occur, as these units are

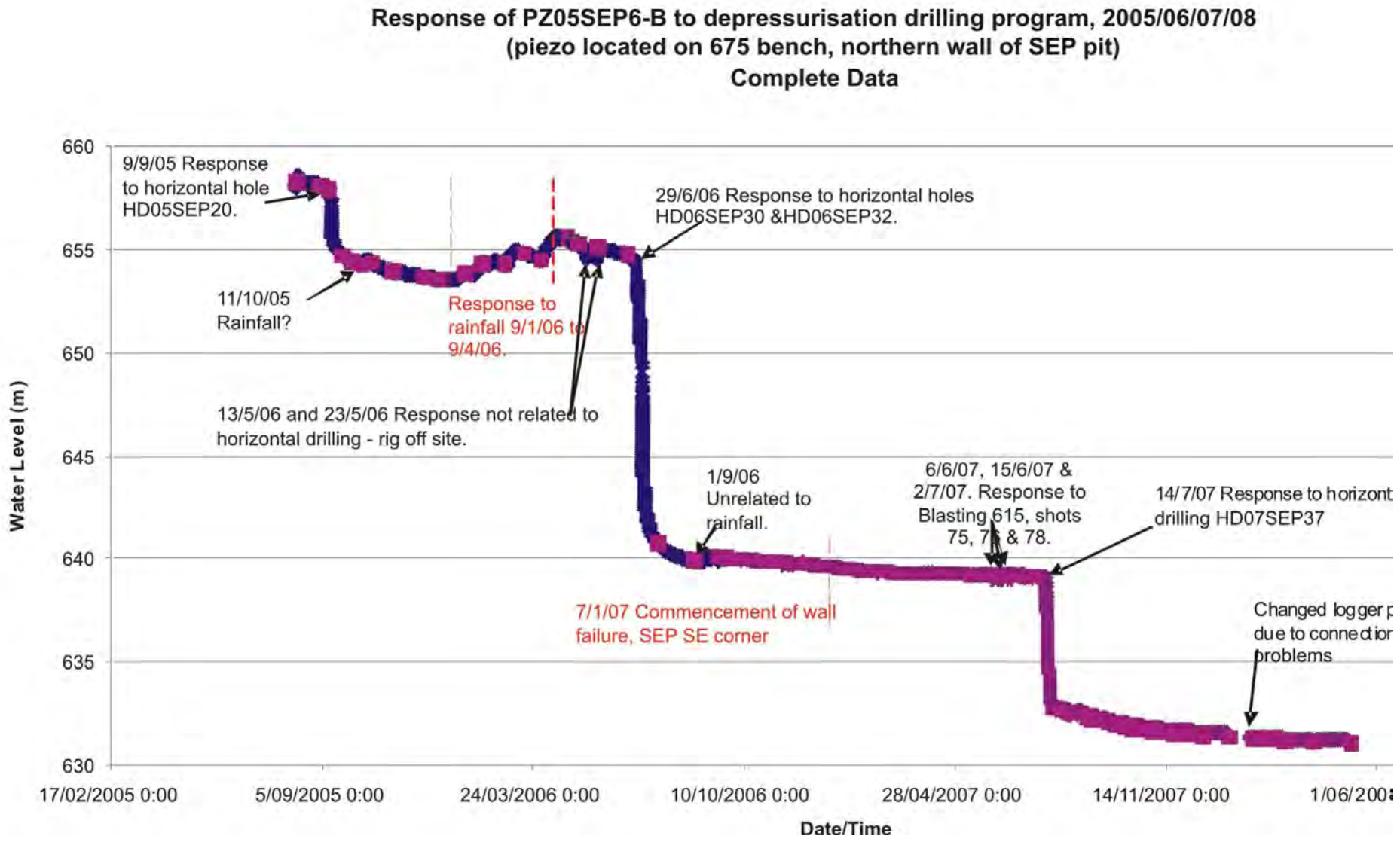

Figure 4-2 - Hydrograph showing response of north wall piezometer to drainhole installations (RTIO, 2008).

mostly aquitards with low hydraulic conductivity. Previous modelling of the SEP pit had assumed that the ore body aquifer was enclosed by aquitards and that dewatering requirements were controlled by aquifer storage in the ore and direct rainfall recharge. However, monitoring data over the last two years indicates that some groundwater is flowing into the pit from outside the ore body aquifer. Investigative drilling has indicated that fault structures (two faults with the SEPFZ in particular) were acting as flow conduits for groundwater from the underlying WF (Rozlapa, 2008).

4.6 Monitoring Network

As a result of pit developments approaching or targeted to go below the water table there became a need to understand the complex hydrogeological conditions present within the Mount Tom Price operation. The installation of an extensive piezometric monitoring network (Figure 4-3) throughout the site began in 1993. This was designed to facilitate sound groundwater management within the area and allow piezometric head levels within the rockmass to be monitored throughout pumping and dewatering operations.

Piezometers typically range in depth from 12 -180 m; the network does not simply target the mineralised DG despite it being the one of the highest yielding units within the mine. Groundwater levels within the pit walls and surrounding country rock are also monitored, these include the MCS, MTS and the WT (Preston, 1995). The influence of the current dewatering and depressurisation systems within the deeper pits of the Mount Tom Price operations can now be more accurately understood. This applies for both for application in water management and geotechnical stability assessments. The applications of groundwater monitoring within the mine will be discussed in the following chapter in extensive detail as this is of fundamental importance to the study.

Measurements and data collection from monitoring bores and piezometers is carried out both manually using electric water level probes and automatically with transducers and data loggers. It is important to note however that manual readings are necessary to ensure accuracy and calibration of the automated system.

Frequency of monitoring is dependent on bore location and priority to operations within the mine. A monthly monitoring run is carried out to manually dip all non automated bore holes throughout the mine while automated piezometers are programmed to collect data at daily intervals (Campbell, 2008).

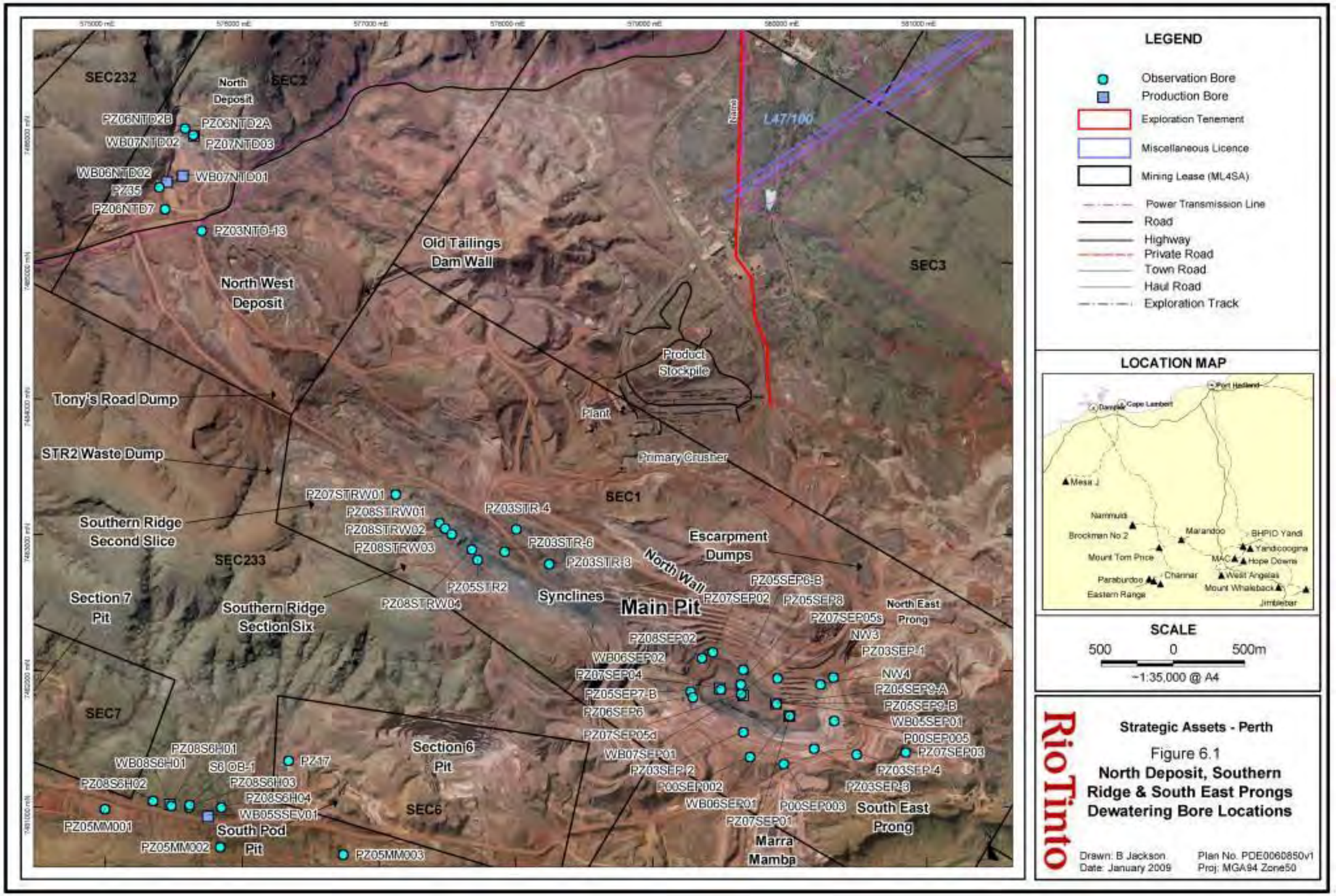

Figure 4-3 – Current dewatering bores and piezometric monitoring network installed at Tom Price as of December 2008 (RTIO, 2008)

4.7 Groundwater Management

Groundwater extracted from pumping bores is collected and transmitted in a pipe network that leads to storage tanks, processing plants, or as environmental discharge. Alternatively, groundwater is pumped away from active dewatering areas into worked out mine sites, such as Section Six, where approximately 1000 kL are deposited daily on average (December 2008).

Water abstracted from WB05SEP1 is used for dust suppression within the mining lease. All other water abstracted from the SEP, including storm water runoff, is acidic (pH <3) and is discharged into the disused Section Six Pit. An acid water treatment plant was commissioned during 2008 and is used intermittently to treat the contaminated water (RTIO, 2008).

4.8 Surface Water Management

Precipitation from normal seasonal rainfall events in general has little effect on long term water level fluctuations. Due to the high evaporation rates in the region, only around 1% of rainfall over Mount Tom Price reaches the groundwater (Beckett, 2007). Surface ponding and runoff however, are likely to contribute to water table variances. This occurs typically through broken rock in the pit floors, as well as along faulted and fractured rock zones throughout the area.

Intense, irregular (extreme) storm events are also likely to have an influence on water table fluctuations. During these events, a probable maximum precipitation (PMP) of 440 mm (Department of Environment, 2004) can fall over the period of 24 hours. All rainfall on slopes can be considered runoff, due to the rocky slopes and lack of vegetation (Preston, 1995).

The large open pits in the Mount Tom Price mining area are situated near topographic divides, effectively acting as their own micro-catchments. Extreme rainfall events, as well as above average periods of rainfall, can lead to significant ponding on berms on the pit walls and surface erosion of pit slopes and haul roads. Local creeks will also flow during these events, and it is therefore necessary that creek flow into the pits is diverted to limit flooding. Ponding within pits can eventually infiltrate through the pit floor, eventually creating perched water tables on previously dewatered rock units (Preston, 1995).

4.9 Conclusion

The local hydrogeology of the Mount Tom Price area has been developed around two main aquifer systems. The DG member of the Brockman Iron Formation with contributions from the upper mineralised section of FWZ make up to the main aquifer within the area. This can be described as being semi confined in nature due to the underlying low permeability MCS lithology. A secondary aquifer is located within the WT beneath the MTS member. This has shown recharge potential to the upper aquifer in areas on structural complexity where secondary permeability allows for vertical transport of groundwater.

An extensive dewatering program has been ongoing since installation in 1994. A primary focus has been placed on the ND and SEP pits as operations have moved below the regional groundwater table. Currently the groundwater table is located at 558 mAHD and 597 mAHD for the respective pits.

A perched groundwater mound has been observed through ongoing monitoring between the mentioned locations of intensive dewatering. This is an example of the compartmentalisation of the aquifers within the area resulting from structural complexities associated with faulting and folding. Weathered dolerite dykes form barriers to groundwater flow in a number of locations. Alternatively the SEP fault zone has shown to provide high levels of secondary permeability and acts as a conduit to flow.

Monitoring is achieved through an extensive monitoring network that extends across the mine area. As to be expected areas designated for productions and dewatering have a higher concentration of monitoring points.

Chapter 5: Case Study - South East Prongs, Mount Tom Price.

5.1 Introduction

The South East Prongs (SEP) pit, located within the Mount Tom Price mine, holds some of the most valued high grade hematite ore with low impurities of the entire eleven mine network based in the Pilbara. Maximum recovery of this resource through ongoing management of slope stability is therefore a fundamental component contributing towards the ongoing success of the Rio Tinto Iron Ore (RTIO) product.

The mining of this deposit relies on a comprehensive understanding of the complex geological structures, geotechnical and hydrogeological conditions within the pit. As progress continues towards the final stages of the long term mine plan, sensitivities within the rockmass will increase. Currently operations below the pre mining groundwater table and the pit walls are planned to be optimised in order to access the remaining resource.

The factors governing large scale slope stability are primarily: 1) the stress conditions in the pit slopes, including the effects of groundwater, 2) the geological structure, in particular the presence of large scale features, 3) the pit geometry, and 4) the rock mass strength (Sjoberg, 1996).

There have been ongoing small scale instabilities in addition to a number of large wall scale failures as noted by RTIO “Fall of Ground” reports. The majority of failures can be catagorised as being:

- Bench scale or less,
- Involve sliding along bedding planes that either daylight or near daylight within the MCS and,
- Occur during or within a close time frame after mining of final wall faces.

These highlight sensitivities within the rockmass and have been identified as potential risks to the success of future developments. Included in Figure 5-1 is a typical type of small scale failure than can occur within the SEP. Of particular note is the presence of seepage at the pit face.

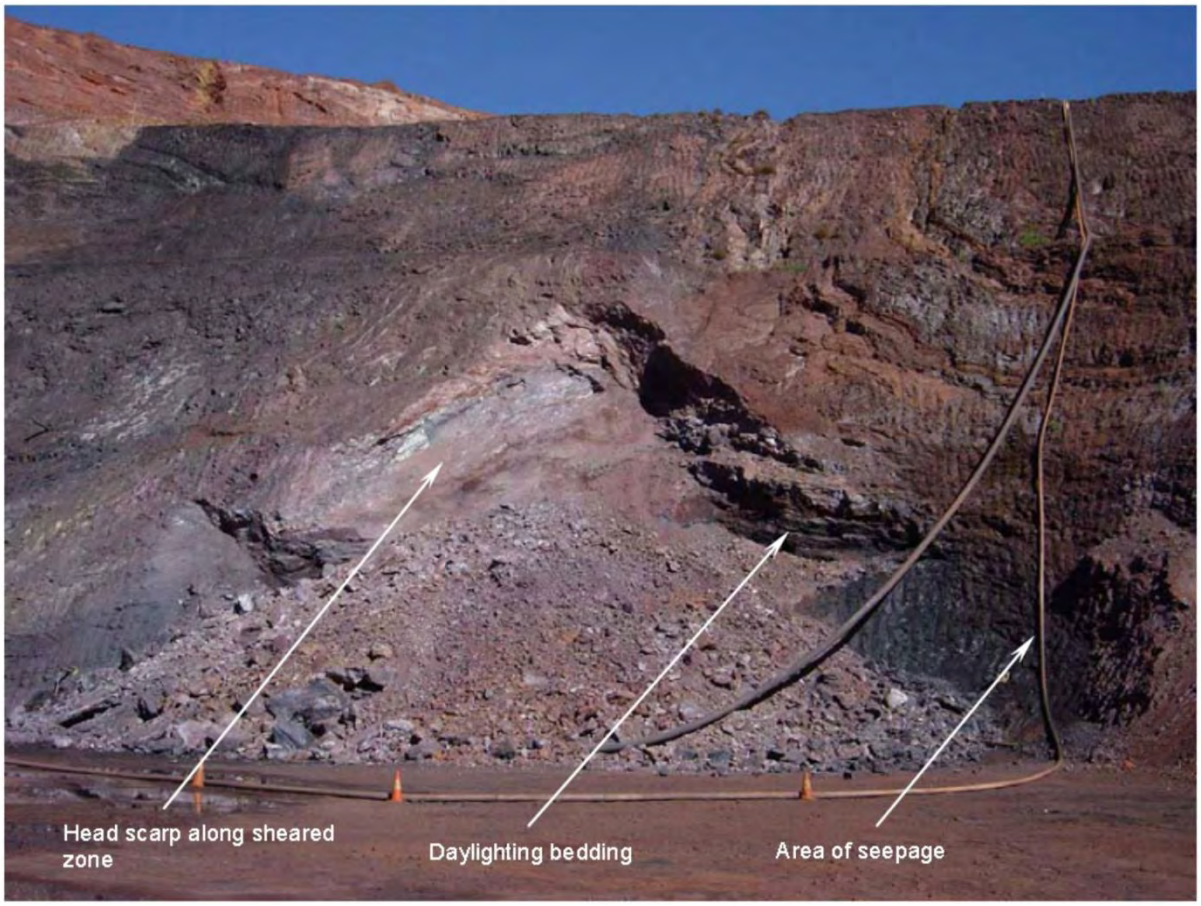

Figure 5-1 - Example of a bench scale failure within the south western corner of the SEP – June 2006. View towards the west south-west. Witch hats for scale (Pells Sullivan Meynink Pty Ltd, 2007).

5.2 Structural Geology

The Late Archean/Early Proterozoic rocks of the Hamersley Basin have experienced extensive amounts of structural alteration including folding, faulting and dolerite intrusions. MacLeod (1966) has subdivided the province into three structural zones; however Trendall (1975) has noted that these zones show gradational boundaries, with a gradual increase in structural complexity from north to south across the basin. The northern zone of gentle folding gives way to a central zone of broad well defined regional folds with dips up to 50°. These folds grade into the southern marginal zone of strong and occasional folding and block faulting. The Mount Tom Price mining operation is located within a large fold closure at the eastern end of the Turner Syncline which trends approximately east west (Solomon and Groves, 1994, Morris, 1980, MacLeod et al., 1963, Tyler and Thorne, 1990).

There is evidence to justify the occurrence of four folding events throughout the deformation history of Mount Tom Price, which is set within a graben extensional fault system. These folding events are summarised below (Brockman Solutions Pty Ltd, 2007):

- The initial folding “F1” occurred as a regional event with small scale recumbent isoclinals folds most likely related to basin compaction.

- Following this, the Capricorn Orogeny occurred during the early Proterozoic (2200-1600Ma) and shows evidence of origenic deformation within the Hamersley basin. This can be seen in the form of the Ophthalmian Fold Belt which has been divided into two groups:

    - In the South East region of the basin, intense deformation created small to medium scale overturned to recumbent north verging folds, with shallow to moderate dipping axial planes and associated thrust faulting

    - In the South West of the basin, the reduced intensity of the folding event is reflected in the east west trending dome and basin structures. Within the Mount Tom Price operation this variable regional deformation has been preserved as “F2” folds (Brockman Solutions Pty Ltd, 2007, Tyler and Thorne, 1990).

  Structural mapping within the SEP during 2008 has confirmed the presence of F2 folds throughout the pit with a predominant occurrence along the southern wall. These are particularly visible when fold closures occur within chert bands of the MCS. These folds occur throughout the pit, and are small to medium scale structures (amplitudes of < 10 m and wavelengths ranging from 5 – 30 m). There are a number of anticline/syncline pairs that can be traced the entire length of the southern wall of the SEP pit. These structures can be found on the north dipping, southern limb of an F3 syncline. Geotechnically the presence of these folds allows for an effective reduction in dip slope of the F3 folds, allowing for additional cohesion within the north dipping rockmass. F2 folds are present within the northern wall, however not as well exposed (Brockman Solutions Pty Ltd, 2007).

- “F3” folds can be attributed to the Ashburton Orogeny; this regional event is responsible for the outcrop pattern visible in most areas. Large scale open, upright east-west and northwest-southwest trending folds with amplitudes up to 20 km are present (Brockman Solutions Pty Ltd, 2007). It has been noted by Taylor et al, (2001) the well developed northwest-southeast trending folds within the Turner Syncline predate the northwest trending dolerite dykes which were formed as part of the Panhandle Orogeny.

The primary geological structure/morphology within the SEP can be attributed to an upright westerly trending F3 synclinal fold. The north dipping southern limb is persistent through the entire length of the deposit, while the length of the south dipping northern limb has been truncated as a result of the South East Prongs Fault Zone (SEPFZ). The F3 fold event has also caused rotation of the F2 folds axial surfaces to the north, as ongoing deformation of the area is noted (Brockman Solutions Pty Ltd, 2007).

- The final F4 folding event is described to be co-axial with the Panhandle Orogeny, however post dates the northwest trending dolerite dykes. F4 fold events have been deemed responsible for the reversal of bedding dips at both the eastern and western ends of the SEP pit. The eastern beds now dip to the west, while the western beds dip to the east. This effectively creates an encapsulated base as the bedding is primarily orientated to dip towards the centre of the pit (Brockman Solutions Pty Ltd, 2007).

The structural history within the Mount Tom Price mine is not limited to the multiple folding events that have been outlined above. Faulting throughout the area is extensive, with a number of large intersecting fault traces accompanied by smaller branching splays. Faults have been shown to cause a number of pit wall instabilities, with a recently revised geological model of the SEP more accurate pit design measures can be taken in the future.

The north wall of the SEP contains a number of south dipping normal faults as shown in Figure 5-2. These faults contribute to what is formally known as the "South East Prongs Fault Zone" that trends in a west - east direction. In addition to this, a north dipping normal fault was identified during surface mapping in 2001(Duncan, 2003) . This provides the southern fault pair for a graben feature within the north wall. The development of this graben structure is said to have occurred during a "robust extensional phase", immediately after the waning of the previously mentioned F3 folding events. This hypothesis can be supported by comparing the strike orientations of the dominant F3 syncline and the SEPFZ as illustrated in Figure 5-2 (Brockman Solutions Pty Ltd, 2007).

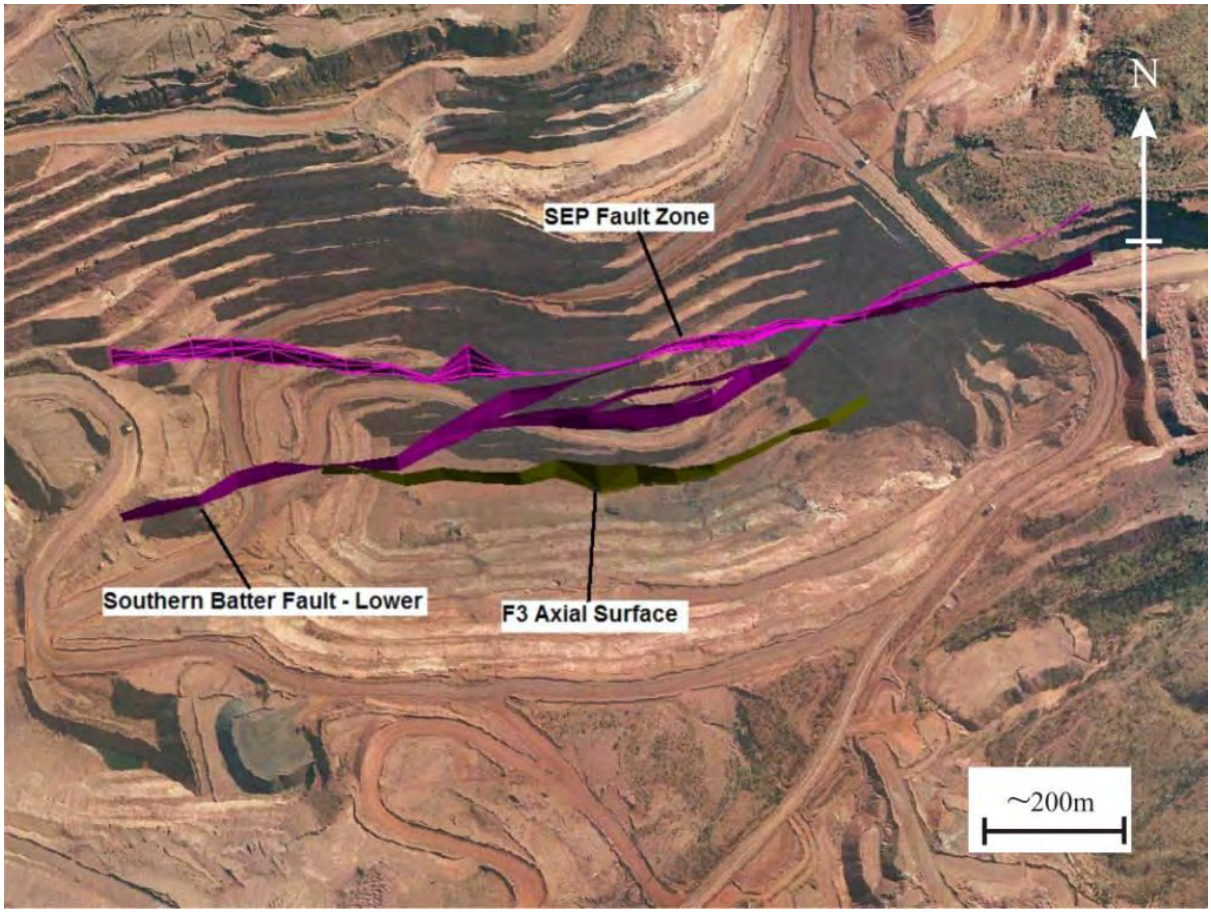

Figure 5-2 - Orientation of SEPFZ and F3 syncline axial plane (Brockman Solutions Pty Ltd, 2007).

5.2.1 South East Prongs Fault Zone

The SEPFZ is made up of vertical to south dipping normal faults that persist throughout the entire length of the pit. The maximum stratigraphic displacement of this fault zone has been measured to be ~140 m. This occurs in the northeast corner where the fault zone is at its narrowest (Figure 5-3). The Bee Gorge member of the WF can be seen to be faulted against the DG #1 member of the Brockman Iron Formation (Brockman Solutions Pty Ltd, 2007).

As the fault zone reaches the centre of the pit it has a much wider stratigraphic footprint, this results in displacement being taken up through a number of smaller faults within the network. The further west the fault zone is traced, the less displacement is present and thinning of the zone is noted. Combined with the northerly dip of the F3 syncline tracing of the fault zone becomes increasingly difficult at the western end of the pit (Brockman Solutions Pty Ltd, 2007).

In addition, the Lower Southern Batter Fault contributes to displacement within the pit as a key structural control. The Southern Batter Fault was first identified within the Southern Ridge East pit. It can be traced along the western wall of the SEP before merging with the

SEPFZ in the central section of the northern wall. Within the pit, the Southern Batter Fault dips towards the south while having a normal sense of displacement which has been stratigraphically constrained to between 5 - 15 m (Brockman Solutions Pty Ltd, 2007). The combined fault traces can have been shown with the use of triangulation in Figure 5-3 after the three dimensional digitisation work carried out by Brockman Solutions Pty Ltd, (2007).

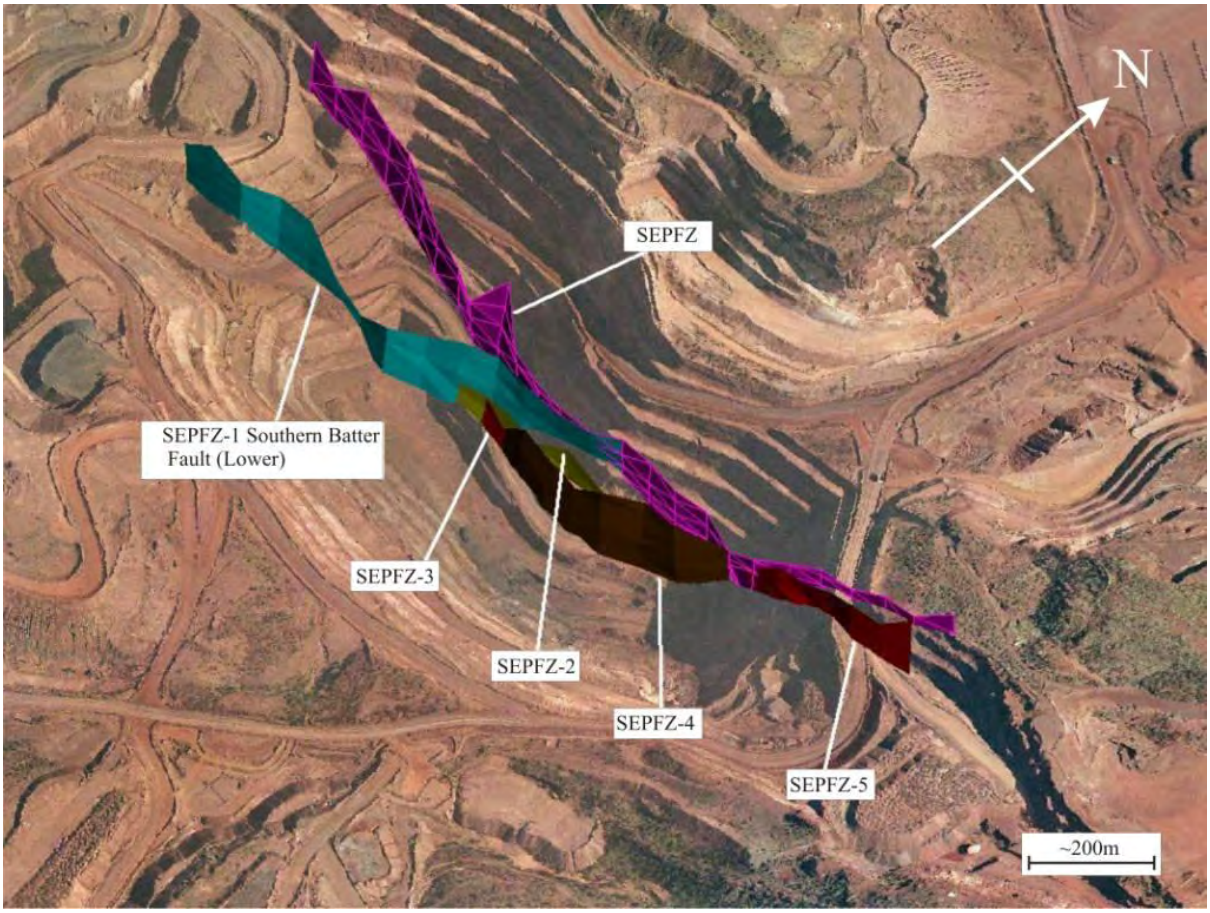

Figure 5-3 - Overview of South East Prongs Fault Zone and lower Southern Batter Fault.

A number of smaller faults daylighting in both the eastern and western walls of the pit make up the total fault network of the SEPFZ. Although the magnitude of displacement along these structures is much reduced (compared to the larger faults in the pit), they make a significant impact on geotechnical design and pit wall stability within the localised SEP area. A well documented pit slope failure (extended over six benches in height) occurred within the south east corner of the pit during January 2007 (Figure 5-7). After extensive investigations by RTIO personnel and specialist consultants, it was determined that the failure was fault controlled. Initially it was presumed the failure occurred as a result of high pore water pressure within the area, however for this instance these were not a contributing factor (RTIO, 2009b).

Drilling has confirmed a fault (F12) which shows Brunos Band separated from the FWZ by 6m of MCS which suggested a 40 m loss of stratigraphy. It is difficult to quantify the exact extent of this stratigraphic loss as until recently there had been a lack of drilling outside the pit shell. Such displacements and thinning of units can play an important role in the changing dynamics of both the geotechnical conditions and hydrogeological flow paths that occur within the wall rock of the pit. Brunos Band especially, has been noted to have a very high hydraulic conductivity in relation to its surrounding country rock. If a unit with such high recharge potential is known to be close to the pit face (with only a thin shale cap separating it), relative pore pressures could be significantly higher than adjacent blocks that have not experienced the same displacement.

The occurrence of multiple phase tectonics is a likely precursor to the currently interrupted structural model of the SEP. Compression, followed by extension can transform reverse faults (which are typically tight folding), into normal faults (which are more typical of extensional environments). Faults occurring later in a tectonic phase could simply tilt faults in opposite directions, which would reverse their sense of displacement. The overall series of inward dipping normal faults within the SEP is typical of a horst and graben system, or a fault system peripheral to a large scale karst feature or "doline".

There has been a considerable level of subsidence and dissolution within the base of the pit. This can be related to leaching and dissolution of the underlying WF which is predominantly dolerite. This can provide justification for the steeply dipping strata at both western and eastern ends of the SEP syncline, creating the aforementioned "bath tub" type structure (Xamine Consulting Services, 2008).

5.3 Hydrogeology

5.3.1 Flow Characteristics

The general hydrogeology of the Mount Tom Price area has been discussed in detail in Chapter Four. This section aims to give a greater understanding of the specific groundwater dynamics within the SEP, where geotechnical considerations relating to the hydrogeology may need to be addressed. Historically groundwater levels were simply lowered through pumping to access ore located below the water table. Geotechnical considerations were not included in such planning (pers. comm. L Campbell, 2008)

The primary aquifer acting within the SEP lies within the DG member and the mineralised section of the FWZ. This has been informally referenced as the "Ore Body Aquifer". This

aquifer is bounded above and below in the geological sequence by confining layers. The Mount Whaleback Shale located above the DG, has little effect on the aquifer within the pit due to the majority of it being mined out over the past 50 years. Of great importance to the nature of groundwater flow within the pit is the underlying MCS situated within the footwall. As shown in Table 4-2, the MCS has a hydraulic conductivity that is an order of magnitude lower than that of the ore body aquifer.

In addition to the bedded sequence of the Hamersley Group, there are a series of steeply dipping north-west trending dolerite dykes. A number of dykes are known to penetrate the geology within the pit. When weathered, these swarms of dykes typically form barriers to groundwater flow, as noted throughout a number of iron ore mines with the western Hamersley Basin. Although these dykes only form a relatively small component of the geology within the pit, they can have a major influence on groundwater flow dynamics as they can lead to localised compartmentalisation within the pit walls. This small scale compartmentalisation is one of the primary focuses of this hydrogeological investigation. The presence of elevated pore water pressures can have a large influence on pit wall stability as future developments commence.

5.3.2 **Pit Dewatering**

The present in pit dewatering infrastructure includes a total of four production bores (Bullnose - WB05SEP01, Eastern - WB06SEP01, Central -WB07SEP01 and Western - WB08SEP01) as shown in Figure 4-3. At least three of these pumping bores are active at any one time, with a combined extraction of ~ 25 L/s. The original bores were installed to intersect permeable mineralised units of the DG of the Brockman Iron Formation.

As operations have developed a need for high grade ore, abstraction from deep in the ore body is required. During July 2005 one of the four in pit dewatering bores (located in the northern bull nose area) was extended below the highly permeable mineralised DG and into the underlying shale layer (MCS) in an attempt to increase dewatering capacity. Piezometer readings at the time of installation showed the potentiometric head to be nearing the height of the of the upper pit walls. This resulted in the creation of an artesian spring at the base of the pit as illustrated in Figure 5-4. This provided clear evidence that the groundwater model of the time was not entirely accurate. The once considered confined “bath tub” aquifer within DG and FWZ required revision. After extensive investigation and installation of further observation bores it has been indicated that leakage from the underlying aquifer in the WF is acting to recharge the base of the ore body aquifer (pers. comms. L Campbell, 2008).

Figure 5-4 - Artesian flow at the base of the SEP in the Northern BullNose area resulting from the extension of a dewatering bore through the confined MCS member (RTIO, 2009).

As mentioned in the previous chapter, groundwater investigations were not initially directed towards working below the pre mining groundwater table. Hydrogeologists simply investigating the area for production wells to supply operations and the town consumption. As a consequence, the lead times that would be ideally utilised in a project such as this were not available. This can prove critical to the speed at which cutback and pit developments can commence. This emphasises the need to have a robust understanding of site conditions prior to designing a dewatering system (Hall, 2003).

At the time of writing, the groundwater level in the centre of the pit floor (WB06SEP01) is ~ 597 mAHD, a total of 77 m below the pre mining water table in the area. The current water table however is behind the targeted two benches dewatering buffer suggested by Xamine Consulting Services (2008) as the current pit floor is located at 600 mRL. Prior to the commencement of the dewatering program at the SEP the groundwater level was approximately 674 mRL, with no significant hydraulic gradient between the DG and the MCS (RTIO, 2009a).

Since dewatering in the pit commenced 15 years ago a steep hydraulic gradient has developed between the two pit walls (MCS) and the ore body aquifer (mineralised DG and FWZ). This is a direct response to the contrasting hydraulic conductivities between the two lithologies.

5.3.3 Slope Depressurisation

Seepage on pit walls within the SEP first identified the need for depressurisation ten years ago by site based personnel. Internal communications within RTIO note in January 2000, "The pit design at Mount Tom Price is constructed on the premise that all walls would not be subject to any water pressures. To maintain the current design we need to satisfy this requirement. In the event that advanced dewatering does not depressurise the wall as well as initially thought we will require depressurisation holes to be installed into walls below the water table" (RTIO, 2000).

To better understand the process of depressurisation, utilising passive horizontal drainage personnel visited the competing BHP Billiton Mount Whaleback iron ore mine in Newman. There are obvious differences within the two sites such as pit depth and slope angle. The final cut backs extending further into the MCS than at Mount Tom Price however the stratigraphy and aquifer locations are the same. Key lessons taken from this visit included the emphasis of maintaining depressurisation infrastructure (such as outflow reticulation systems) as well as an initial guide to drain hole spacing along the walls of the pit. BHP, at that time had chosen to utilise a 20 m horizontal spacing between drill collars. This was established purely through trial and error judgements. Hole depth was also considerable with the deepest extending a total of 240 m into the wall. The monitoring systems installed at Mount Whaleback consisted of a series of stacked vibrating wire piezometers (VWP) to accurately record changes in pit wall pressures.

In 2005 the first passive horizontal drainhole installations were undertaken in the SEP. This marked the beginning of an extensive horizontal drainage program within the pit. Over the past four years more than 131 holes have been drilled around the SEP pit walls. A comprehensive network of piezometers installed around the pit (Figure 4-3) have recorded notable reductions in pore water pressures within the wall rock, as illustrated in Figure 4-2.

Figure 5-5 and Figure 5-6 included below illustrate the installation of passive horizontal drainholes and the potential volumes released from the wall rock when intersection of a water bear structure is made.

Figure 5-5 - Typical installation of horizontal drainholes within the SEP. The horizontal drill rig can be seen at rear of the photo with support trucks in front. Operational drains previously installed drains are also included (RTIO, 2006).

Figure 5-6 - Aerial view looking along the southern wall of the SEP pit. High yielding horizontal drainholes have exceeded the capacity of sump and flooded the pit floor (RTIO, 2006).

5.4 Geotechnical

5.4.1 Pit slope design philosophy

A series of geotechnical reviews have been carried out over the past four years within the Mount Tom Price operation with a specific focus on the SEP pit. “The general pit slope design philosophy for RTIO open pits in the Pilbara is to accept a degree of bench failure, normally between 10 and 30% with sliding along bedding or shale bands being the typical controlling mechanism. A check of interramp structural, rock mass, combination and other mechanisms which may involve adjustments to the slope design if they are a control. Slope designs below water table assume drained conditions for bench scale sliding and for any controlling interramp mechanism, involves accepting a degree of depressurisation that is assessed as being achievable by natural and artificial drainage measures” (Pells Sullivan Meynink Pty Ltd, 2007). Of particular relevance to this study is the slope design below the water table where depressurisation works are required.

Maintaining such conditions within the rockmass throughout periods of rapid progression has the potential to cause problems within the dewatering network as the anisotropic rockmass has been shown to drain at differential rates. This is a product of both structure and lithological variability.

5.4.2 Rock Mass Characteristics

To quantify the mechanical characteristics of the rockmass within the SEP, a comprehensive investigative programme has been undertaken by a range of RTIO personnel and external consultants. This has included structural face mapping and drilling throughout the pit, followed by of series of laboratory based tests and statistical analysis of the data. This has enabled a comprehensive understanding of the rock mass to be developed for the SEP which is supported by the completion of a geomechanical model which includes the assignment of specific geotechnical domains for the pit. Such domains allow for anisotropy to be accommodated along with structural variations.

The complete suite of data encompasses intact rock strength parameters including: unit weight, unconfined compressive strength (UCS), estimated strength vs tested strength, elasticity and triaxial strength. Further to this rockmass strength was determined using the Rock Mass Rating system (RMR) and the Geological Strength Index (GSI) which includes respective disturbance factors and anisotropic strength. Finally the defect shear strength for the rockmass was analysed by way of direct shear strength testing, defect roughness and

infilling (logged core), large scale roughness and finally Barton Bandis Strength (for use in kinematic analysis).

A complete compilation of this geotechnical data has been included for reference in Appendix B. This data was obtained and arranged by MiningOne (2009) for use in the latest "SEP Stage 3 Geotechnical Design" which was completed to aid in development of the final drop cuts within the pit. Specific data relevant to the parametric geotechnical modelling carried out as part of this research has been included in Chapter 7.

5.4.3 **Failure Mechanisms**

Documented failures that have occurred within the last four to five years have shown that translational failures along structural defects are the fundamental mechanisms influencing slope performance the SEP. This incorporates both major structures, such as faults and shale bands in addition to minor structures like bedding planes that are distributed throughout the rock mass. These failures have been noted to occur as a result of day lighting or near day lighting structures at final cut faces or where intersection of defect sets causes block releases (otherwise known as wedge failures). Localised failures have also been known to occur where the F2 fold axis has caused daylighting of bedding structures.

Two examples include a 30 m high bench failure within the MSC within the north wall during December 2006. Secondly a 20 m high failure in the south-western corner of the pit where a block release occurred. It was noted that a prominent seepage face was present to the north of this failure which suggests that elevated pore water pressures may have played some part in the failure. The historically high water level in the south western corner of the pit could be due to the keel of the major SEP F3 syncline as it changes in relative height from a high position in the Synclines to a lower position in the SEP (Pells Sullivan Meynink Pty Ltd, 2005).

There is known low shear strength along the FWZ and MCS contact where translational failures have historically occurred. As a result of this, it has been recommended that the final cut faces are terminated within the MCS unit as pit floor developments occur in the latter stages of the SEP ore recovery (Eggers, 2008).

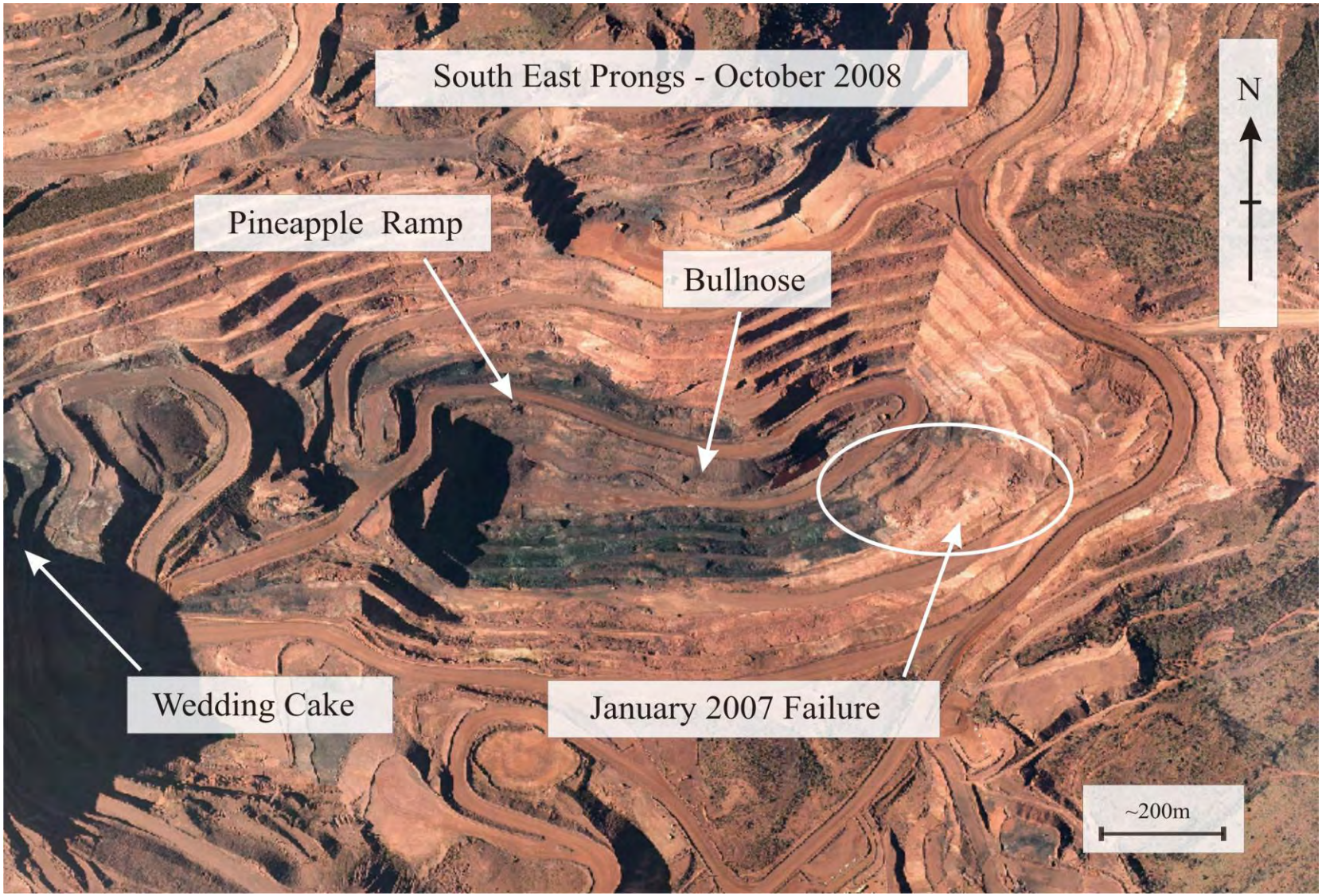

Figure 5-7 - Current overview of the SEP pit as of October 2008. Key features noted in discussion have been labelled accordingly (RTIO, 2009).

5.4.4 Future Pit Development

The current SEP pit floor (at the time of writing) is located at 600 mRL. The long term development plan for the western end of this pit encompasses a further 30 m of excavation to a final depth of 570 mRL. This currently poses a number of stability issues that require resolution before any development can be undertaken. Additional issues include the location of the access ramp to the base of the pit. The "Pineapple Ramp" is currently located on the north wall of the pit from the wedding cake and down past the Bullnose area, this can be seen in Figure 5-7 with the current pit lay out as at 600 mRL.

As identified by Xamine Consulting Services (2008) and MiningOne (2009) in respective geotechnical reviews and design work for the proposed three stage long term mine plan, effective management of pore water pressures within the wall rock (especially the north wall) through ongoing depressurisation is essential. It has been noted however that due to a lack of advanced dewatering within the SEP, passive horizontal drainage systems may not be able to provide a sufficient level of depressurisation in the available time frame. To achieve this it has been suggested that a detailed hydrogeological investigation into the efficiency of the current depressurisation system be undertaken.

Chapter 6: Hydrogeological Drainage Modelling

6.1 Introduction

The aim of the seepage modelling within the SEP was to determine the controlling mechanisms of flow acting within the highwall of the SEP pit and their interactions with a passive horizontal drainage system. Current monitoring of the site has indicated a lowering of the potentiometric surface in response to these drains. There has been very little scientific investigation into their effectiveness, however, with concerns being raised as to the suitability of such a system in a time-limited scenario of pit cutbacks.

Recommendations from two recent geotechnical reviews within the SEP have stated that a specific hydrogeological investigation needs to be undertaken in an attempt to understand the flow mechanisms acting within the wall rock of the pit. A target of 15m vertically and 25m horizontally has been indicated in a geotechnical review carried out by Xamine Consulting Services, (2008). An approximation of the time required to achieve this level of dewatering will determine the likelihood of achieving the mining targets set for future production.

The numerical modelling carried out in this research has aimed to provide a conceptual view of the local aquifer response to the installation of a passive horizontal gravity drainage system, and to verify these findings in comparison to data collected through field observations. A software package developed by GeoSlope International known as "Seep/W" was utilised to carry out the finite element numerical modelling within this research. Finite element models allow for complex geometries to be represented using a computer-aided design interface where meshing properties to define computational locations are not confined to simple, tetrahedral shapes. An advantage offered by Seep/W includes the ability to represent the hydrogeological conditions in both saturated and unsaturated states. In addition to this, time dependant (transient) simulations are able to be carried out which complement steady-state equilibrium solutions. This allows for a much greater level of understanding and forward prediction in each scenario.

6.2 Spatial Analysis

Understanding of the flow dynamics and spatial distribution of water-bearing structures within a pit is a fundamental requirement in creating an effective and efficient drainage system. Since 2005 there has been in excess of 130 horizontal drainholes installed over four bench levels within the SEP pit. These drains surround the inner circumference of the pit,

extending up to and excess of 100 m in length with a horizontal spacing of approximately 30 m. Discussions with sited based personnel revealed that no formal drill hole logging had taken place throughout the horizontal drain hole installation program. The only available data was recorded in driller's notebooks consisting of only the most basic lithological descriptions.

In light of this, a spatial analysis was carried out to determine if any links could be made in relation to common water bearing structures or lithologies within the wall rock. Data from a total of 131 horizontal drainhole logs was collated over a three year period and analysed to determine if there were any visible trends in water intersections within the pit walls. Data was sorted first chronologically and then by bench and location. The depth to respective water intersections were recorded followed by lithological contacts, flow rates and yield estimates. This information was then combined with the recently revised structural geology model provided by Brockman Solutions in an attempt to make spatial connections between observed water intersections and known geological contacts.

A number of significant trends relating to wall rock flow dynamics were identified as a result of this analysis. Brunos Band (defined as a 10 m chert band at the top of the MTS) has been previously acknowledged by personnel at BHP Billiton's Mount Whaleback mine to be a known conduit for groundwater flow. In areas of considerable structural deformation (such as F2 fold hinges or faulted zones) within the Mount Whaleback pit transmission rates between 1– 5 m/day have been recorded.

Basic flow rate estimates for the SEP horizontal drainhole installations have shown a large variability across the pit with a range from 0.5 – 30L/s. The complex structural nature of the pit (discussed in section 5.2) has a notable asymmetry between the northern and southern walls.

This current knowledge would confirm the findings made in from the spatial analysis in this study and provide a basis for further investigations to be carried out into flow dynamics within the wall rock. A full list of the spatial plots and data from the horizontal drilling has been included for reference in Appendix C.

The lack of water yielding intersections within the northern wall raises the issues of anisotropic groundwater flow and potential compartmentalisation within the wall rock. A greater understanding of water levels and the related effects of fault structures will allow for more accurate planning and design of future drainage system to improve the efficiency of the

dewatering and depressurisations programs within both Mount Tom Price and the wider RTIO operations.

6.3 Finite Element Numerical Modelling

Finite element numerical modelling using software developed by Geo-slope International has been undertaken as part of this research to simulate drawdown characteristics within the SEP pit. Geo-slope's Seep/W package allows for the simulation of both saturated and unsaturated flow through any number of material types. The ability to assume unsaturated flow conditions allows the software to solve a wider range of groundwater related scenarios and to simulate realistic flow dynamics. This is possible due to the programs alibility to calculate drainage potential for a material through the use of volumetric water content functions. In addition, the model is able to simulate seepage faces on slopes be it a hill side, embankment dam or high wall excavation in an open cast mining operation. This allows for the prediction of and configurations of both the phreatic surface and the height of the seepage face on a slope, thus providing the information needed for slope stability analysis.

As briefly alluded to above, one of the great features and capabilities of the model is providing the user with the ability to define the hydraulic conductivity and volumetric water content as a function of pore-water pressure in saturated/unsaturated flow systems. The model simulates heterogeneous hydraulic properties such as hydraulic conductivity and its storage in an isotropic and heterogeneous flow system. A conductivity function, which defines the relationship between hydraulic conductivity and pore-water pressure, can be defined for each unit. This allows for the simulation of ground conditions resulting from slope drainage or pumping with multiple materials where some rock/soil may be insitu where as adjacent units could have been deformed through faulting creating either higher permeability (secondary) or the development of flow barriers where gouge material is present. The ability of the software to carry out transient analysis enables simulations to be carried out over extended time periods. Boundary conditions are also able to be modified in response to model outputs to ensure that the desired flow concepts and behaviours are accurately captured.

The governing partial differential equation for two dimensional saturated/unsaturated flow of ground water can be obtain by coupling the continuity equation and Darcy's Law (Freeze and Cherry, 1979) in (Aryafar et al., 2007, Jeremic et al., 2008, Kihm et al., 2007).

Equation 6-1

$$\frac{\partial}{\partial x}\left(K_x \frac{\partial h}{\partial x}\right) + \frac{\partial}{\partial y}\left(K_y \frac{\partial h}{\partial y}\right) = C \frac{\partial}{\partial t}(h) + Q$$

Where: K_x & K_y = Hydraulic conductivities in the *x* and *y* directions respectively
Q = Recharge or discharge per unit volume
h = Hydraulic head
t = Time
θ = Volumetric water content or moisture content. A change in moisture content (θ) may be related to a change in the total hydraulic head using Equation 6-2 below: (Freeze and Cherry, 1979).

Equation 6-2

$$\frac{\partial \theta}{\partial t} = C_{xy} \frac{\partial h}{\partial t}$$

Where: C_{xy} = slope of the water storage curve.

To solve Equation 6-2, using finite element analysis, Seep/W utilises the Galerkin approach to determine an approximate solution (Aryafar et al., 2007, Geo-slope_International, 2007, Doulati Ardejani et al., 2003).

6.3.1 Model Setup

Current hydrogeological understanding within the SEP pit (outlined in section 5.3.1) has highlighted the significance of structural features such as the SEPFZ and SBF to flow dynamics, especially aquifer compartmentalisation. In light of this, unique structural domains within the Northern wall of the pit have been identified as the primary concern of this two dimensional drawdown analysis. To provide an accurate and detailed representation of groundwater flow within the pit walls one of the more structurally complex sections was selected for analysis along easting coordinate 15790E. An overview of this section has been included in Figure 6-1 to provide some spatial context within the SEP pit.

6.3.2 Geometry

As stated by Starfield and Cundall, (1988) the geometry used in a numerical model ia designed to represent a simplification of reality rather than to be an imitation of reality. In light of this, the level of complexity incorporated into the geological cross section for this model has only depicted features deemed necessary to fulfil the requirements of the proposed drawdown analysis.

Key features within Section 15790E (Figure 6-2) include the intersection of four fault traces of the FSEP throughout the height of the pit wall; two of which daylight within the current haul road accessing the base of the pit. Brunos Band is located in close proximity to the pit wall between 620 mRL and 660 mRL. As mentioned in section 6.2, Brunos Band has a high hydraulic conductivity (17 m/day) in relation to its surrounding lithologies (MCS/MTS K= 0.01 m/day). This allows for a potentially increased risk of elevated pore water pressures within close proximity to the pit wall.

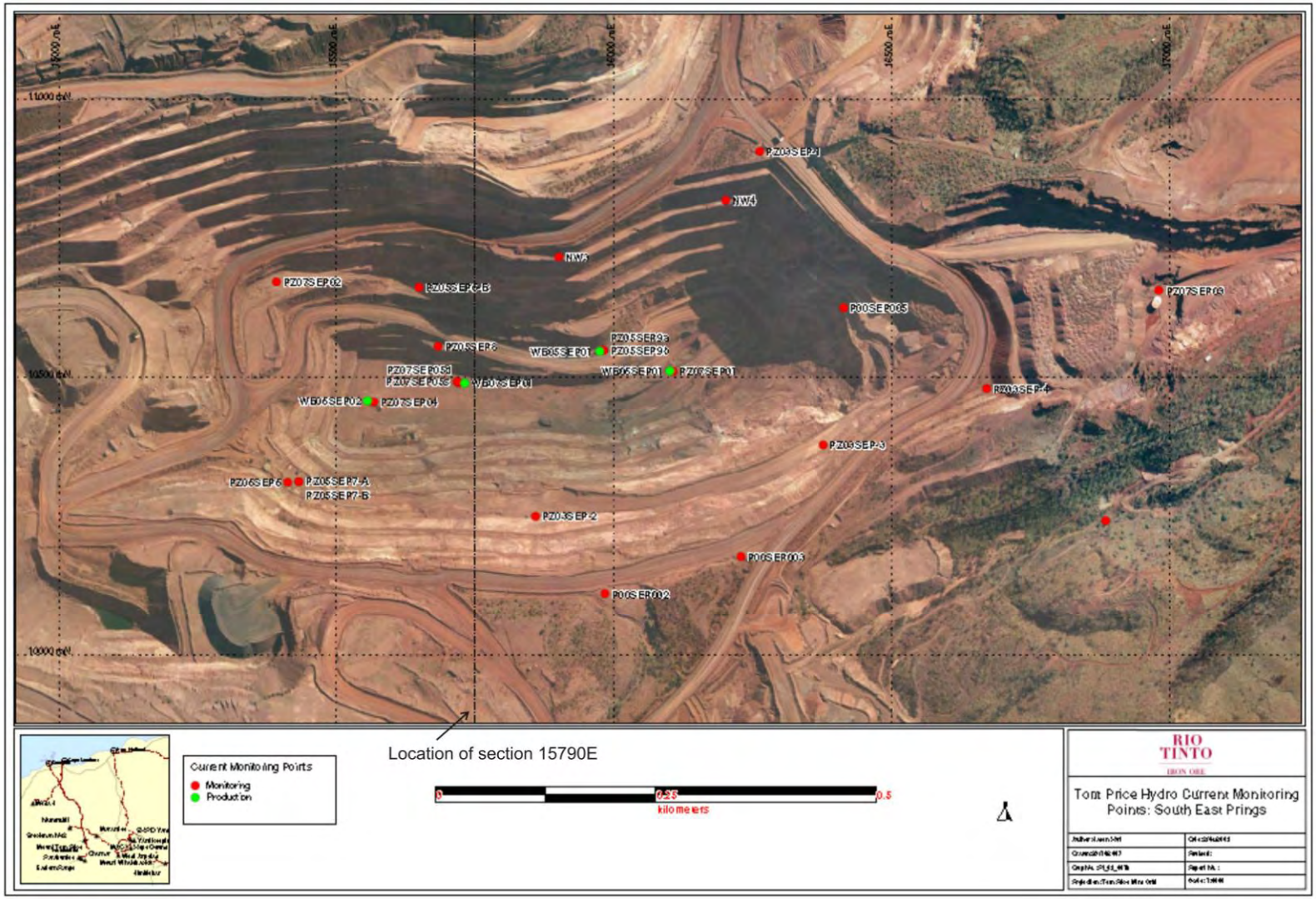

Figure 6-1 - Overview of SEP pit with location of Section 15790.

The geological section was initially exported from the digitised 2008 structural geology created by Brockman Solutions using Maptek's Vulcan software. In Seep/w the section was scaled to fit respective spatial coordinates ensuring no distortion occurred during the transfer between software packages.

The position of outer boundary extents can play an influential role on the response of finite element seepage models. If outer extents (boundary conditions) are set too close to the predefined seepage faces on inner pit walls, any adjustments made to the initial input parameters (eg total head) will have a biased effect on the resulting pressure head contours for the model (Geo-slope_International, 2007). For this reason the far field cross section boundaries in this model have been located at a minimum distance of 200 m (horizontally) from drainholes outlets on the inner pit walls (Figure 6-2).

The geological units represented in the model were somewhat streamlined for use in the analysis. The major lithologies located within the pit shell were all incorporated (DG, MCS, MTS and WT) however specific shale bands were omitted with the exception of Brunos Band in the MTS for reasons previously mentioned at the beginning of this section. The DG member was also amalgamated with the FWZ as they both possess similar hydraulic conductivity for use in a hydrogeological analysis (outlined in section 6.3.4). Faults have been represented as their own unique lithology without making any differentiation to what country rock they had intersected. This was preferred as fault structures have shown through previous investigation to have alternative hydraulic behaviours to the adjacent units.

To allow for the evolution of the pit geometry as slope optimisation and cutbacks are made, the model geometry has been developed to follow progressive step downs (Figure 6-3). This has been created to be in sequence with the provisional timeline provided by the Mount Tom Price Mine Operations Manager. These steps have been integrated into the transient seepage analysis; more detail relating to this type of analysis is given below in section 6.4.2.

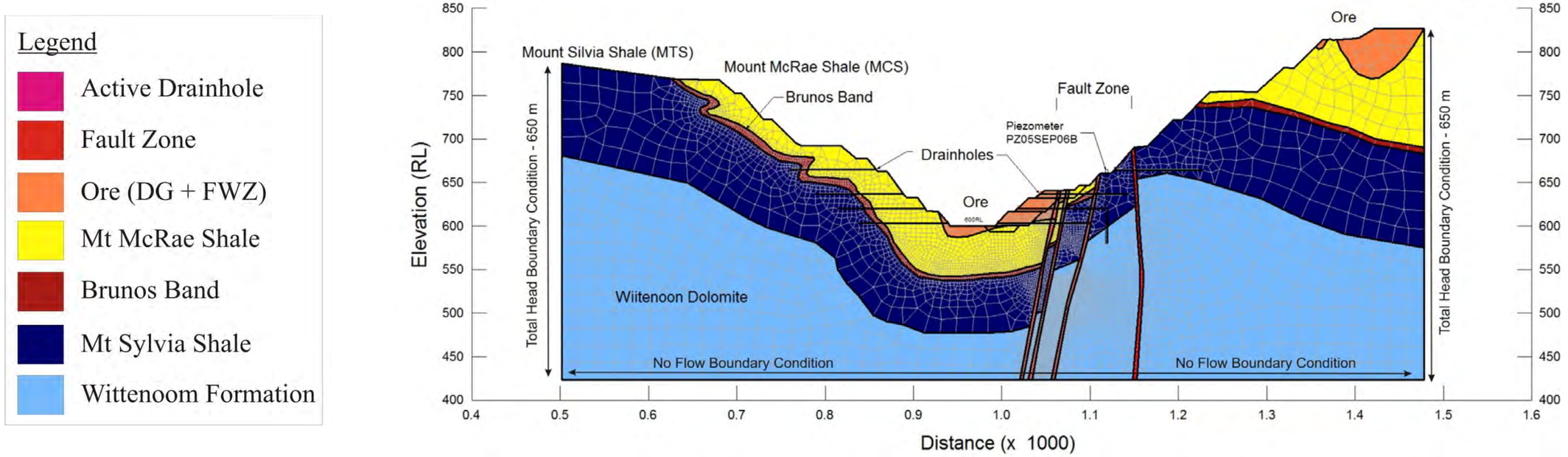

Figure 6-2 - Seep/W model domain showing geological representation, meshing and external boundary conditions within the SEP.

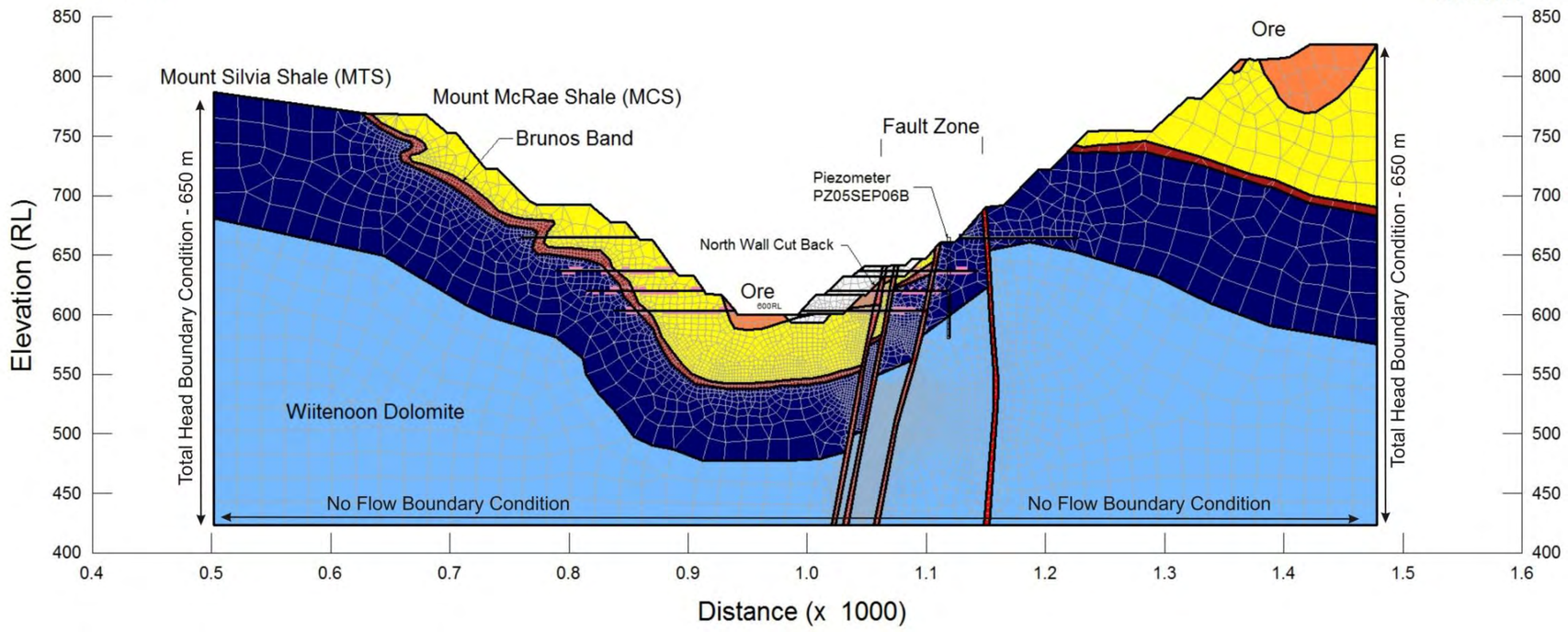

Figure 6-3 - Model domain with respective pit wall cut backs.

6.3.3 **Meshing**

Meshing of a model's geometry can simply be defined as subdividing a region or domain into a number of small pieces or "elements". Finite element numerical models fundamentally rely on the ability to describe a behaviour or set of actions at any specified node within a designated geometry. Once individual nodal computations have been completed the model acts to reconnect all of these elements to provide an overall response for the system in question.

It is therefore important to consider the required meshing constraints (size and shape) when creating the basic model geometry. This can be primarily determined by establishing the level of detail required from an analysis. For example, simulation of drawdown around a well screen aims to answer a vastly different set of questions compared with investigations into leakage through an earth dam. For this reason significantly different element (mesh) sizes are applied within a model. This allows the software to accurately depict the level of detail proposed in the scope of a project. As this SEP model represents a landform with close to 1 km in horizontal extent it would not be practical to apply a metre scale meshing pattern across its entirety. The calculations required at each node across the model would be excessive, and require an extremely long processing time.

Meshing properties in finite element models are not simply constrained to square geometries but instead utilise a mixture of triangular and quadrangular elements which is designed to best accommodate the models regional variability (Doulati Ardejani et al., 2003). The global element (mesh) size was defined at 20 m throughout areas of the model that were not subjected to ongoing changes to input parameters (e.g. far field WF aquifer with constant head). Complex meshing layouts (intricate polygon shapes) were generally avoided by ensuring model regions were constructed from simple geometric shapes.

In areas around of particular interest such as horizontal drain holes, fault zones and Brunos Band the mesh was constrained to an element size of approximately ≤ 2 m. This allows for increased accuracy in areas of fundamental importance (lithological contacts, structural complexities and changing conductivity values) to the model outputs while not created issues with processing requirements. The final meshing layout can be seen as a transparent layer in Figure 6-2 with the variable element sized; evident from the larger outer elements to the confined inner elements where the majority of detailed analysis is to be conducted.

6.3.4 Hydraulic Characteristics

Basic hydraulic parameters (Hydraulic Conductivity, Storativity and Specific Yields) were sourced for the respective geological units (Table 6-1). These were generated from a collaboration of works relating to the Mount Tom Price site from RTIO Hydrogeological personnel as well as studies and modelling carried out over the past 15 years by groundwater consultancies Aquaterra and Ultramafics Pty Ltd.

For any kind of numerical analysis it is of the utmost importance to ensure accuracy is not compromised when defining input parameters. The final outputs and subsequent results obtained from any analysis are only as reliable as the input data that is supplied in the first instance. For this reason a great deal of time and resources has been put into generating the most accurate input values for use in this finite element seepage analysis.

Table 6-1 - Hydraulic properties utilised in numerical modelling.

Unit	Hydraulic Conductivity (m/day)	Specific Yield	Storativity
Ore	3	0.05	$2.0x10^{-4}$
Mount McRae Shale	0.01	N/A	$2.0x10^{-4}$
Brunos Band	17	0.01	$2.0x10^{-4}$
Mount Silva Shale	0.01	0.001	$1.8\ x10^{-5}$
Wittenoom Formation	7	0.003	$3.1\ x10^{-4}$
Fault Zones	0.5	N/A	N/A
Drain Holes	60	N/A	N/A

Choosing the correct hydraulic function is the first step to creating a sound foundation to any model. Seep/w provides a number of possibilities when defining hydraulic conductivity functions. Saturated/unsaturated hydraulic functions have been selected for use in the analysis. This allows for regions within the model to respond to changes in the potentiometric surface as evolution of the groundwater table take place through time. Figure 6-4 shows the saturated/unsaturated hydraulic conductivity functions used in the Seep/w analysis for the respective lithologies outlined in Table 6-1. These functions utilise the relationship between a materials hydraulic conductivity (K_x) in m/day and negative pore water pressure (otherwise known as matric suction) in kPa. In addition to the hydraulic conductivity function a Volumetric Water Content function (Figure 6-5) is required for transient analysis. This function controls the amount of water that is released from storage when the system has a

drainage component applied and determined the time required for steady state conditions to be reached.

Generally rapid drainage is achieved through the presence of a) small specific yields; and b) steepness of the function. Therefore two materials have the same specific yield (the volume of water released as a result of passive gravity drainage) then the steepness of the respective function will determine which material will show the quicker response to drainage.

The specific hydraulic flow characteristics used to represent the passive horizontal drainholes will be discussed in increased detail in section 6.3.6 below. Special attention has been places on the best method to represent these structures due to the nature of the two dimensional analysis.

A thoroughly useful feature within the Seep/W software is the ability to include flux meters throughout the model domain (Figure 6-6). This allows for specific flow rates to be monitored within any material and graphed for analysis. A total of eleven flux meters were installed throughout the SEP model geometry. These were located within areas of fundamental hydrogeological significance such as the intersections of high conductivity lithologies (Brunos Band and fault zones) and across the beginning and end of horizontal drainhole within the northern wall. Flux rates were recorded during model simulations before being analysed to identify the influence horizontal drainhole activations had on the flow dynamics within the system. Special attention was paid to the flow rates in respective levels of drainholes as well areas of seepage shown to exist with the lower pit walls.

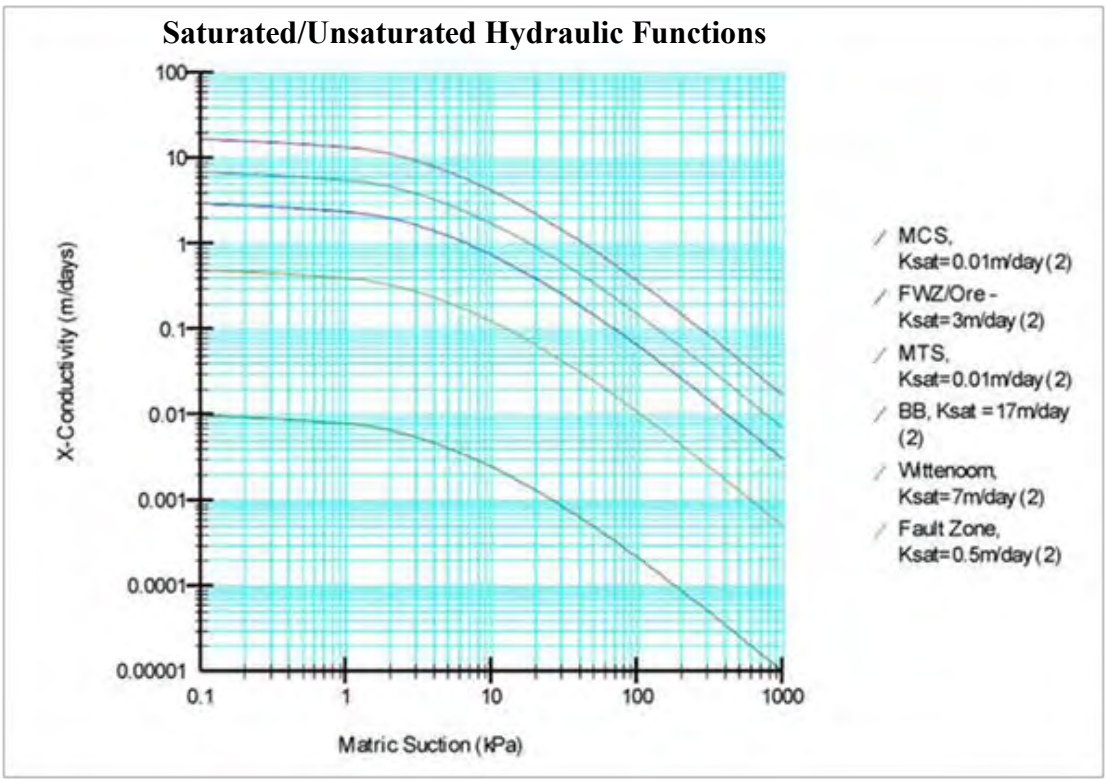

Figure 6-4 - Saturated/unsaturated hydraulic conductivity functions generated for SEP Seep/W modelling.

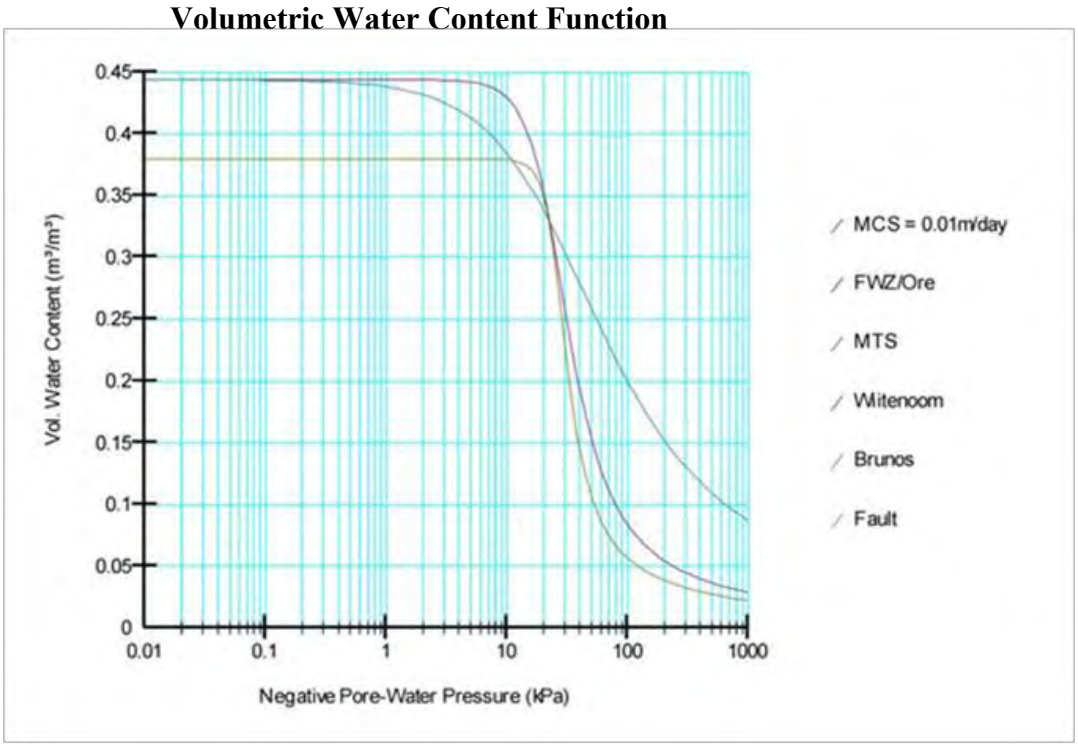

Figure 6-5 - Volumetric water content function generated for SEP Seep/W modelling.

6.3.5 Boundary Conditions

As with hydraulic functions, boundary conditions play an extremely important role in creating an accurate and meaningful numerical model. Results are generated in direct response to designated initial boundary conditions; therefore without them it is not possible to obtain a solution. To generate flow within a model a hydraulic gradient need to be developed, this is the total head difference between two points or some specified rate of flow into or out of the system. The solution is effectively the response inside the problem domain to the specified conditions on the boundary (Geo-slope_International, 2007).

As complex as the high order mathematics is, to represent a given physical situation in a numerical model all finite element equations just prior to solving for the unknowns ultimately simplify down to:

Equation 6-3

$$(K)\{X\} = \{A\}$$

Where:

$[K]$ = a matrix of coefficients related to geometry and materials properties,

$\{X\}$ = a vector of unknowns which are often called the field variables, and

$\{A\}$ = a vector of actions at the nodes (points).

More specifically for a seepage analysis the equation is:

Equation 6-4

$$(K)\,\{H\} = \{Q\}$$

Where:

$\{H\}$ = a vector of the total hydraulic heads at the nodes, and

$\{Q\}$ = a vector of the flow quantities at the node.

The prime objective of this computation is to solve for the unknown factors in the equation; for a seepage analysis this is the total hydraulic head at each node. The unknowns will be computed relative to the H values specified at some nodes and/or the specified Q values at some other nodes. Therefore for any analysis to be operational at least one H or Q value must be specified. These values can fundamentally be established by identifying what information

or data is available and what is required. If there is an initial head value available it can be included which will allow for the respective flow rate to be calculated and vice versa. In doing this the model has some defined boundary conditions of which to basis the calculations from (Geo-slope_International, 2007). These are formally known as Total Head (H) and Total Flux (Q) boundary conditions.

A third important behaviour (in addition to H and Q) that needs to be fully understood when working on the fundamentals of boundary condition application is how to represent a situation when neither H nor Q is specified at a node. In this case the computed Q is zero. A "seepage face" is a boundary condition that can be utilised when this situation arises. It can be assumed that the pore-water pressure is zero (H equals elevation) at the location where the seepage face develops, however the size of the seepage face that will exist is not known. To put this into a physical context, what it means is that the groundwater flow coming towards a node is the same as that leaving the node. Alternatively this mean can represent a condition where no flow is entering or leaving the system at these nodes. Water leaves or enters the system only at nodes where H or a non-zero Q has been specified. At all nodes without a specified condition, Q is always zero (Geo-slope_International, 2007).

The numerical model created for this study has been designed to analysis the conceptual flow dynamics and time dependant drawdown of the potentiometric surface using passive horizontal drain holes within the SEP utilised several types of boundary conditions. Initially a total head boundary condition was incorporated for the widest extents of the model. This boundary was allocated total head of 650 mAHD (Figure 6-2), as this reflects the recorded localised ground water level indicated by the mine piezometric monitoring network. This value can also be validated through previous work carried out by (RTIO, 2008, Preston, 1995, Rozlapa, 2008). Although previously noted (section 4.3), the regional ground water gradient extends from a high point to the west of the SEP to a low south/south east of the pit (Figure 4-1); this study has been directed towards a localised analysis of the controlling flow mechanisms acting within the walls. For this reason the external total head boundary conditions have been set at a uniform level. The base of the model domain does not have an allocated boundary condition (Figure 6-2) and is therefore assigned a default no flow boundary which, as the name suggests does not permit flow across it in any direction.

To establish a hydraulic gradient to drive flow within the model domain, an internal total head boundary was placed beneath the central base of the pit floor at a level 595mAHD (Figure 6-6). This was chosen to represent the effects of in pit dewatering bores acting to

lower the potentiometric surface of the ore body aquifer. There will be some influence placed on the underlying WF however this is primarily focused on limiting recharged as opposed to drawdown of the aquifer.

To allow the release of water from the model (as a result of the installed gravity drainage) a potential seepage face was allocated at the ends of the drainholes as they daylight in the pit walls. Seepage faces are illustrated in Figure 6-6 as light blue lines on the pit wall. This figure was generated during a transient simulation where the lower most drain holes have been activated.

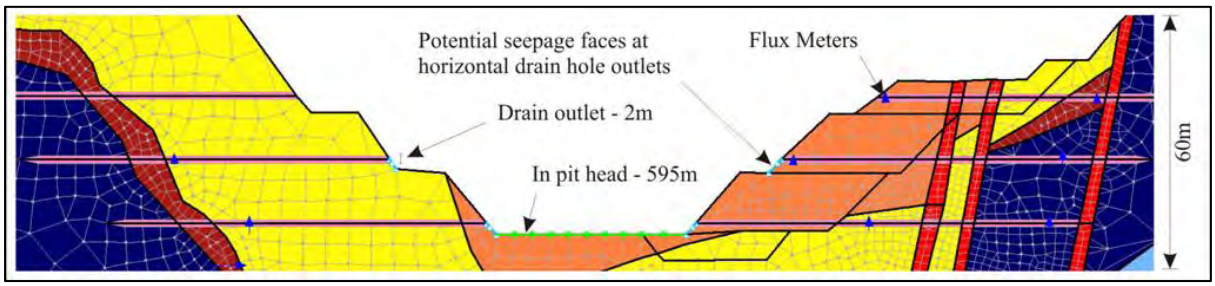

Figure 6-6 - Detailed view of in pit model setup including constrained mesh, boundary conditions (seepages faces and in pit head), flux meters and dimensions of drainhole outlets.

6.3.6 **Drainholes**

Horizontal drain holes have been included within both northern and southern walls of the SEP pit for this analysis. A total of four levels of drainage have been modelled at the following elevations: 605 mRL, 625 mRL, 645 mRL and 665 mRL (Figure 6-2). A naming convention based on the respective elevations of each drainage level has been adopted to simplify discussions. The top level of drains at 665 mRL are known as first level which progressed down to the drains at 605 mRL which are known as fourth Level drains.

Special considerations need to be made when deriving hydraulic conductivity functions for drain holes within a two dimensional analysis. The drains are effectively depicted as extending infinitely, both in and out of the section by virtue of the model setup. This is obviously not an accurate representation of reality and therefore needs to be accounted for in the hydraulic function.

The horizontal drainholes have been modelled very simply as a line intersecting the surrounding geology within the wall rock. To allow a hydraulic conductivity value to these lines interface elements were applied to the “drainhole lines”. Interference elements vary from the region type geological representation used for the rest of the model as it allows

greater control in assigning meshing components and therefore accuracy in analysis. The interface elements were assigned a total thickness of 2 m (Figure 6-6) to a) make the drains visible; b) improve the discretisation; and c) facilitate addition/removal of the drains. The area of the simulated drains is therefore 2 m^2 (thickness of 1 m each side of drainhole line within the model).

As discussed, the drain area was selected to be 2 m^2; consequently, it was necessary to "scale" the hydraulic conductivity so that simulated drains had an equivalent capacity taking into account the 25m spacing that are currently utilised in horizontal drainhole installations within the SEP. An estimation of the flow properties of the drain can be attained by using a pipe flow equation. The Bernoulli equation (Fetter, 1994: pg 133) for pipe flow (Equation 6-5) states that the pressure drop that occurs from point A (p_A) to point B (p_B) as result of viscous head loss for water flowing through a closed pipe of constant diameter D and velocity V (by continuity):

Equation 6-5

$$p_B = p_A - \rho g \left(dz + f \frac{L}{D} \frac{V^2}{2g} \right)$$

Where:

L = Pipe length between points A and B,

dz = Change in pipe elevation (zB – zA),

f = Friction factor of pipe,

V = Velocity,

g = Gravitational constant.

The conventional hydraulic gradient for water flow can be obtained as:

Equation 6-6

$$\frac{p_A}{\rho g} - \frac{p_B}{\rho g} - (z_B - z_A) = f \frac{L}{D} \frac{V^2}{2g}$$

Which leads to;

Equation 6-7

$$\frac{\left(h_{pA} + z_A\right) - \left(h_{pA} + z_{\boldsymbol{B}}\right)}{L} = i = \frac{f}{D}\frac{V^2}{2g}$$

Where the subscript p indicates a pressure head and the sum of the pressure head and elevation (head) is equal to the total head. The left hand side of this equation is the hydraulic gradient i. The velocity can be solved as:

Equation 6-8

$$V = \sqrt{\frac{iD2g}{f}}$$

Multiplying the velocity by the area of the pipe gives the flow capacity:

Equation 6-9

$$Q = \frac{\pi D^2}{4}\sqrt{\frac{iD2g}{f}}$$

The Moody Chart (Moody, 1944) indicates a friction factor of f = 0.1 assuming turbulent flow and rough pipe. This was deemed to be the closest realistic value for an uncased drainhole drilled into a hard rock environment. Using a hydraulic gradient of 0.3 (discussed in Section 6.5) and D = 0.11 m (4.5 inches) produces a flow capacity of 0.024 m^3/s, which is equal to 2089 m^3/day. Normalising the flow capacity for the 25 m spacing that are currently in use for the horizontal drainhole installations gives 2089m^3/day/25 m = 83.6 m^3/day/m. From Darcy's Law (Equation 6-10), the hydraulic conductivity required to give the simulated drain an equivalent capacity is:

Equation 6-10

$$K = \frac{Q}{iA} = \frac{2089\ m^3}{[0.3(2\ m^2)]} = 139\ m/day$$

Alternatively, it could be assumed that the maximum measured flow rates are reflective of the flow capacity given the 25 m spacing (i.e. the spacing is accounted for in the measured flow rates). Using Darcy's Law directly and an approximated measured peak flow rate of 40

m^3/day yields K = 12944 m/day, calculated using the actual area of the drain (D = 4.5 inches/11 cm; A = 0.0103 m^2). In order for $Q_{measured} = Q_{modelled}$ under the same gradient, the hydraulic conductivity is $K_{modelled}$ = 12,944 m/day, ($A_{pipe}/A_{modeled}$) = 12,944 m/day (0.0103/2) = 66 m/day. This value is lower than the value calculated from the pipe flow equations; a potential reasoning for this response it to the drains not reaching the maximum flow capacity at the time of installation.

Using these calculations as a guide, a „conservative' value of 60 m/day was selected for saturated hydraulic conductivity of the drain material. The drains were initially not assigned a hydraulic conductivity function for simplicity; however, the unrestricted flow capacity caused the drains to „wick' water, which altered the long-term steady-state head distribution. Realistically, the drain flow capacity would be expected to decrease when operating under negative pore-water pressures; consequently, a constant function was assigned to the drain materials to limit the capacity when the pore-water pressures were negative.

6.4 Analyses

A total of six stages of analysis (both steady state and transient) were undertaken to determine the groundwater flow mechanisms and their responses to installed drainage. Each type of analysis has been outlined below, giving a brief introduction into the respective applications for this study.

6.4.1 Steady State Analysis

When any physical scenario is modelling mathematically by way of finite element (or otherwise) the first step in an analysis is to establish the equilibrium conditions for a given point in time. To achieve this, a steady state analysis was carried out to determine the initial hydrogeological conditions for the SEP pit walls. An advantage in carrying out a steady state analysis is that the output can be calibrated against known conditions that already exist and have been recorded. Abundant potentiometric data for the pit has proved beneficial as the equilibrium groundwater level can be calibrated against real life data.

An additional requirement for conducting a steady state analysis of a given scenario is that it provides a parent analysis for which a time dependant Transient Analysis can be initiated. Without a base line equilibrium position it is not possible to analysis a responses to changes in the flow dynamics of a system.

6.4.2 Transient Analysis

A transient analysis by definition means one input variable is always changing. This is primarily a result of the changing boundary condition imposed on a model and the computations working to establish the duration of time required for the material (rock or soil) to respond to such changes and reach equilibrium (steady state).

The specific requirement for a transient groundwater analysis in this study has been to constrain the mechanisms controlling flow within the wall rock and their time dependant sensitivity to alterations within the system. This has been especially difficult due to the complex hydrogeological conditions present within the wall rock and the many variable present within the analysis.

As mentioned previously, a transient analysis requires a specified set of initial conditions which are provided by the initial (parent) steady state analysis. It should be noted that all transient analyses were simulated for a duration of 180 days. This duration was selected in response to initial drainage trials showing yields reaching a near equilibrium states within this period.

6.4.3 Breakdown of Analysis Schedule

Below is a list of the components that make up the numerical analysis. Each stage of simulation has been outlined and labelled according to the previous stages drawn from.

1) Steady-state analysis of existing pit geometry with no drains;

2a) Steady-state analysis with 3 levels of drains installed (requires no initial conditions);

2b) Transient analysis with 3 levels of drains installed (with the initial conditions defined by (2a));

3a) Steady-state analysis with 4 levels of drains activated (requires no initial conditions)

3b) Transient analysis with 4 levels of drains activated (with initial conditions defined (2a)).

4) Steady-state analysis pit cut back with 4 levels of drains activated (requires no initial conditions)

6.5 Outputs and Results

6.5.1 Steady State No Drains

This analysis is designed to provide a background understanding of the equilibrium hydrogeological conditions present within the SEP prior to the installation of any horizontal drainholes. The results of this simulation have shown some fundamental flow mechanisms acting within the northern wall. It should be noted that for ease of description, the faults represented within the following models will be referred to as Fault 1 (left hand or southern side) through to Fault 4 (right hand or northern side).

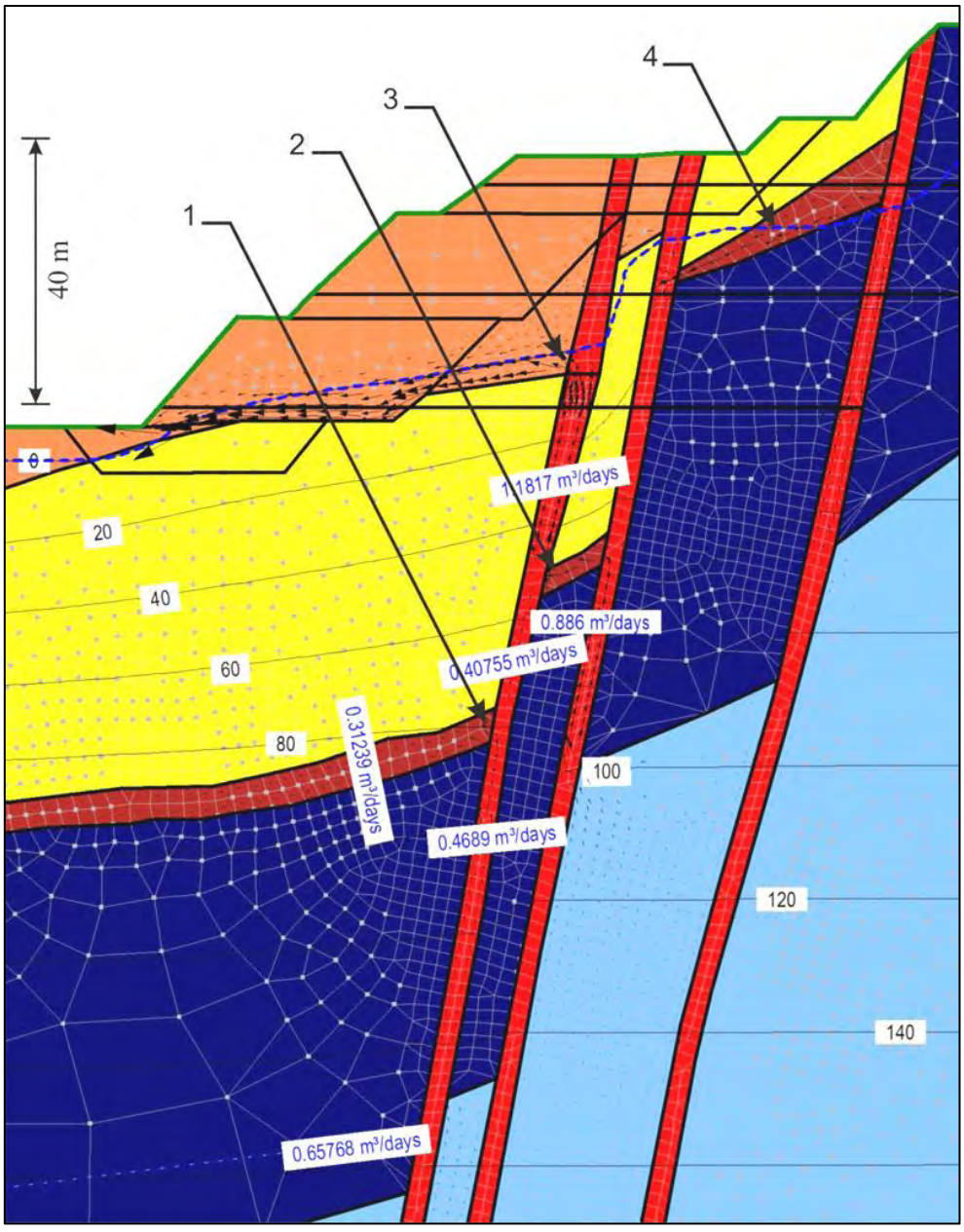

Figure 6-7 - Steady-State flow dynamics showing groundwater transport within the northern wall from the underlying Wittenoom Dolomite along the Faults to the base of the pit.

Figure 6-7 illustrates a magnified view of the steady state output profile located at the base of the northern wall for the resultant analysis. To outline what has been highlighted in the figure; the numbers attached to isolines indicate the pressure head in twenty metre intervals within the slope. The influence of the MCS and MTS as aquitards confining Brunos Band and the WF respectively can be seen as there is a marked steepening of the pressure head gradient (see 80 m – 100 m isolines) across these lithologies.

There are a number of flux sections included in this section of the model to allow the hypothesis of flow to be quantified by visualising the flow rates at designated locations. One flux section traces through the WF from the left (south) boundary up to Fault 1 (traverses a length of 5000 m), while the other sections cut across the faults in a four locations as indicated in Figure 6-7.

Flow vectors are represented by the directional arrows and increase proportionally with increasing flow rates in the simulation. This allows for quick reference of flow paths when looking at model outputs. As seen in Figure 6-7 the highest flow rates occur within the ore body as flows from the underlying WF have travelled up preferential flow paths before converging on the impermeable MCS and flowing towards the base of the bit. A more in depth description of these processes is outlined in the following paragraphs.

The faults have been modelled as being generally less than 10 m wide. Water travels primarily up three of the four faults and into the ore deposit – the ore deposit acts as a receptor of water flowing through the faults. Faults 1 and 2 are transporting 0.47 m^3/day and 0.89 m^3/day, respectively, while only 0.66 m^3/day is flowing across all 5000 m of the WF. These flow rates clearly demonstrate that the faults impose a significant control on the groundwater flow system.

A portion of the water flowing through Fault 1 flows into Brunos Band (Figure 6-7: Point 1), leaving 0.41 m^3/day continuing up the fault. This divergence of flow is of relevance to the greater flow dynamics and will be discussed is analyses to follow. The significant portion of the water in Fault 2 flows into Brunos Band and back into Fault 1 (Figure 6-7: Point 2), resulting in 1.18 m^3/day of water continuing up Fault 1. Water has the tendency to flow from Fault 2 across Brunos Band to Fault 1 because the “discharge point” of Fault 1which has been defined as the intersection with the Ore (Figure 6-7: Point 3), as this has a relatively high conductivity in comparison with the adjacent MCS. In addition to this a lower elevation (607 mRL) than the intersection of Fault 2 and the ore (670 mRL) promotes the release of water

from Fault 1. Incidentally, the same flow pattern occurs between Faults 3 and 2 (Figure 6-7: Point 4). Fault 4 (not shown in the figure) does not intersect any of the preferential flow paths and therefore is not imposing any significant control on the flow system.

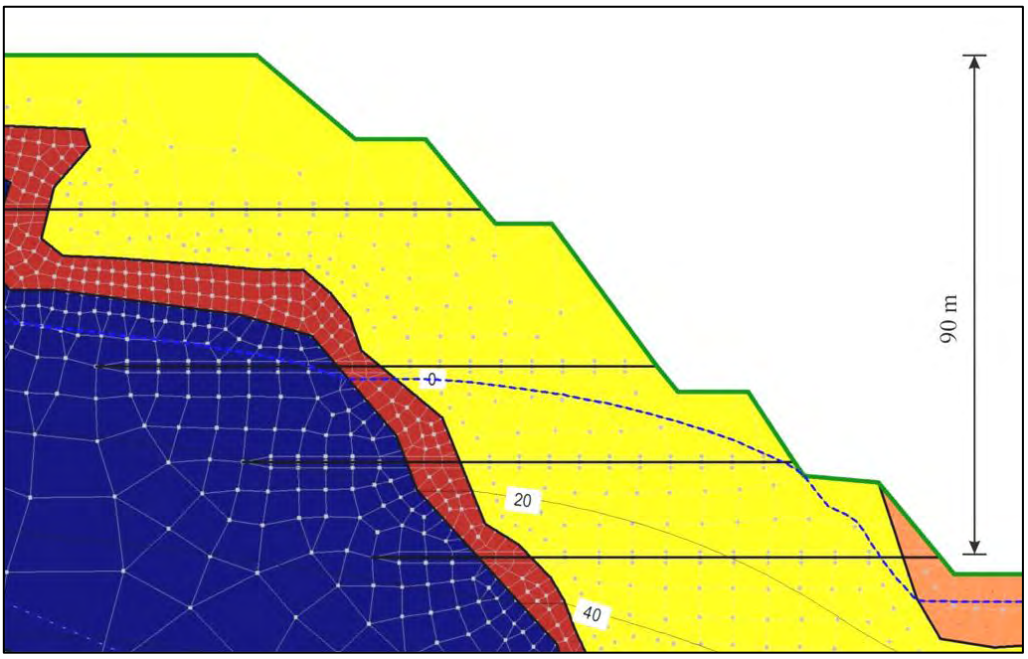

Figure 6-8 - Southern Wall phreatic surface for Steady State analysis with no drains activated.

The third and fourth levels of drains on the south side, which are approximately 100 m long as indicated by drilling records, have a steady-state head distribution without the drains present as shown in Figure 6-8.

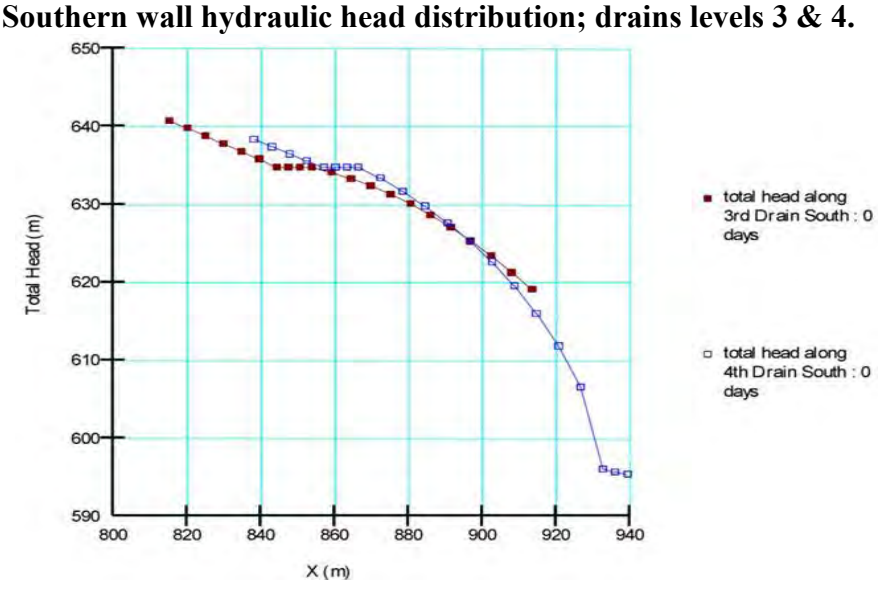

Figure 6-9 - Hydraulic head distributions for drain levels 3 and 4.

The respective hydraulic head distributions for the third and fourth level drains have been plotted in relation to their lengths in Figure 6-9, which closely follows the profile of the phreatic surface in Figure 6-8 as one would expect. It can therefore be assumed that this head distribution will act as a driving force to promote flow along the horizontal drains at the time of the installation; the x-hydraulic gradients can be calculated at the third drain level as:

Equation 6-11

$$\frac{619 - 640.8\ \text{m}}{100\ \text{m}} = -0.22$$

The x-hydraulic gradient for the fourth drain level is calculated as follows;

Equation 6-12

$$\frac{595.4 - 638.4\text{m}}{100\text{m}} = -0.43$$

The average hydraulic gradient can therefore be calculated as:

Equation 6-13

$$\frac{0.22 + 0.43}{2} = 0.325 \ \ = 0.3$$

(This value was utilised when constraining the hydraulic conductivity functions/flow properties for the drains as discussed in section 6.3.6).

As mentioned previously having an understanding of the pre drainage equilibrium flow conditions that are acting within the walls of the pit will provide an initial condition to work from in further analyses.

6.5.2 Steady-State Analysis: Activation of 3 Levels of Drains

This Steady-State analysis has been undertaken to determine the influence that the upper three levels of horizontal drains have on the SEP equilibrium groundwater flow conditions. This has the additional benefit of allowing comparisons to be made as the site conditions evolve. Figure 6-10 illustrates these flow dynamics in the vicinity of the SEPFZ (Faults 1- 4) before and after installation of the second and third level of drains.

The third level of drains was installed at an approximately elevation of 620 mRL. The first level of drains (665 mRL) is shown to be ineffective at this stage in the history of operations

as a result of the lowered (650 mAHD) far-field regional groundwater table. The fourth and lowest level of drains was assumed to not be installed at this stage of analysis to enable each stage of progression to be closely documented.

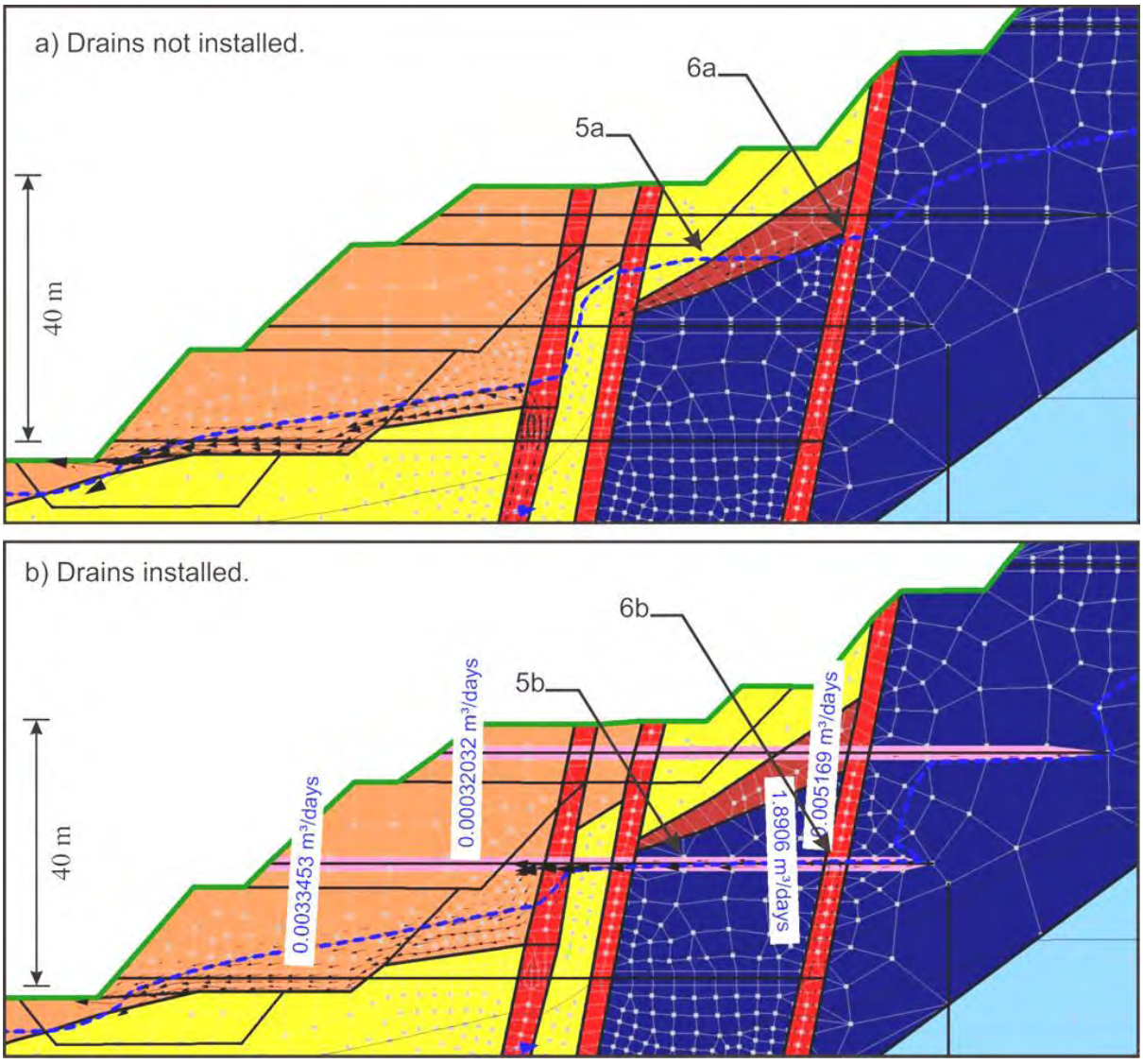

Figure 6-10 - Influence of north wall drain hole installations on phreatic surface, a comparison between Steady-State analyses.

A comparison between the two analyses suggests that the third level drains have a fairly significant effect on the phreatic surface behind Fault 2. This has been illustrated by the respective positions at Figure 6-10: Point 5a and Point 5b. The location of structural features has an important influence at this time in the simulation. The intersection of Fault 2 by the third level drainhole should be noted, as this creates what is effectively a "shortcut" for the flow of groundwater as it is able to migrate from Fault 2 into the drain prior to reaching high conductivity ore material which is situated at a higher elevation (~630 mRL).

Deeper within the wall the third level drain acts to transports water from Fault 3 (Figure 6-10: Point 6b) into the ore. This is a much shorter course of drainage in relation to the existing route that required flow to travel along Brunos Band (Figure 6-10: Point 6a) and into Fault 2. This increases the cumulative flow rate along the level three drainhole into the ore to ~1.9 m^3/day (as shown by flux meter in Figure 6-10b). Consequently, the "perched" water table in the ore (overlying the low K shale) that was identified in the previous analysis rises slightly as a result of the drains installation. Finally, as with the first level drains, the flow within the level two drainhole is reduced to no more than a trickle due to the majority of water travelling within the lower drain.

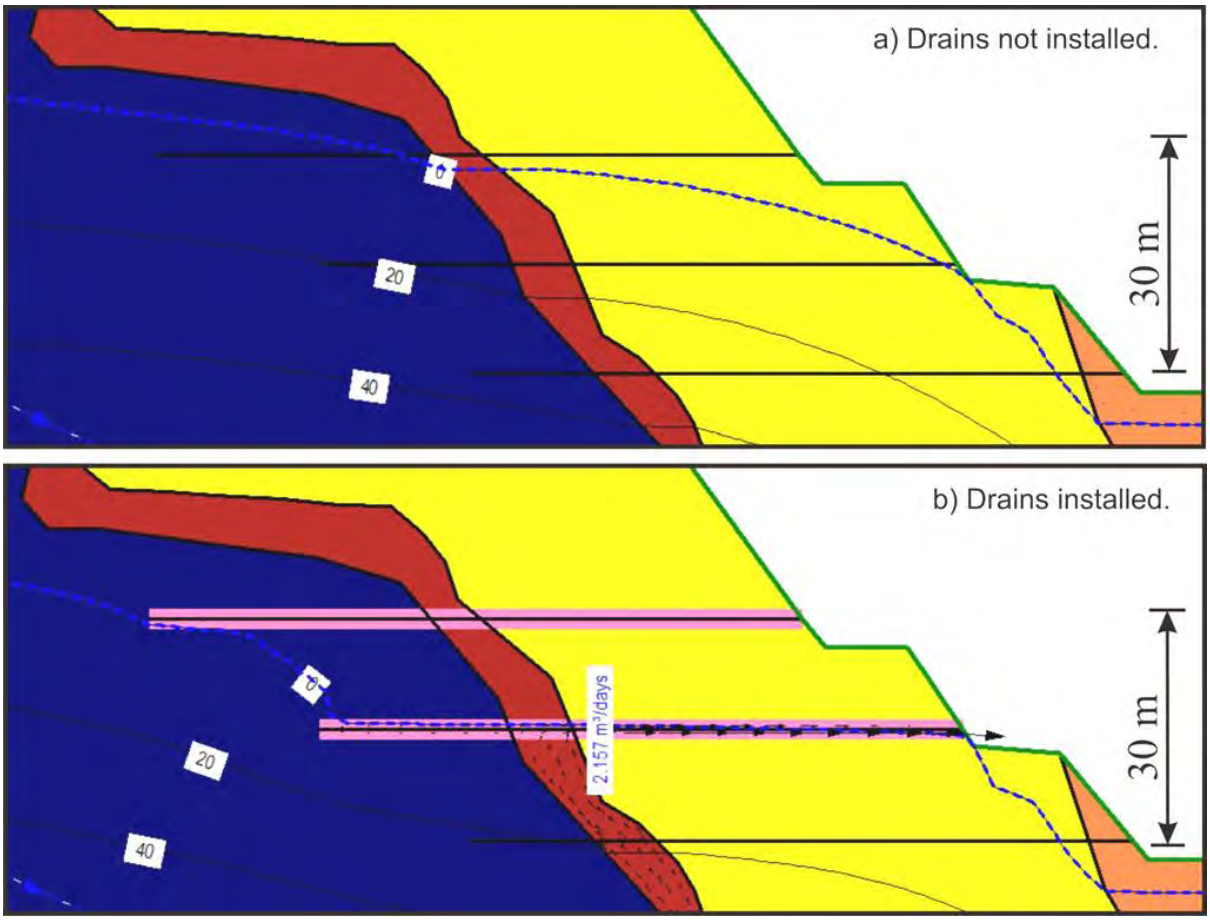

Figure 6-11 - Influence of south wall drain hole installations on phreatic surface, a comparison between Steady-State analyses.

As previously mentioned the southern side of the pit was modelled to represent the flow dynamics within the walls where structural features play a less influential role in the hydrogeological regime.

Figure 6-11 shows the results of the two steady state analyses both with and without horizontal drains in place on the south pit walls of the SEP. The total head at the intersection

point of Brunos Band and the third level of horizontal drains is approximately 625 m, which can be equated to a pressure head of 0 m as it is located at the same elevation. This is shown by the third level drain on the South side as it controls the location of the phreatic surface with a consistent pressure head along its length. As the zone above the drain is drained and becomes un-saturated and the phreatic surface moves towards the end of the drain as illustrated when comparing Figure 6-11 a) no drains with Figure 6-11 b) installed drains. A small level of ongoing recharge is also represented by flow vectors in Figure 6-11 (b) as water is transported up Brunos Band from Fault 1 on the northern side (which intersects Wittenoom Dolomite) to the lower drains.

6.5.3 Transient Analysis: Activation of 3 Levels of Drains

A transient analysis has been undertaken to simulate the time dependant response of the system to the activation of both the second and third levels of drains around the pit. As a consequence of including assumptions with respect to matric suction and storativity values while developing hydraulic conductivity material functions for the model it is not viable to achieve real time results from the analysis. As alluded to in previous sections, the accuracy of any numerical results will be constrained to the quality of input data therefore the results are being treated as conceptual as opposed to absolute.

Additions to the initial boundary conditions from previous Steady-State analysis include a "Potential Seepage Face". This has been applied to the discharge point at the end of each respective drain throughout the transient analysis. The run time of the model has been set for a duration of 180 days. To allow for progressive analysis throughout this time frame a total of fifteen time steps were utilised. These have been assigned to have an exponential time step sequence with an initial increment of one day. The results of the transient analyses were compared to physical observations to determine if the mechanisms controlling the drainage are being captured by the numerical simulations.

The predominant driving force within the walls of the pit is the large hydraulic gradient established along the length of the drains (refer to section 6.3.6), which originates from the hydraulic head of 650 mAHD making up the regional groundwater table. This response is therefore most noticeable within the first few days at the completion of the drainhole installation as the head-time relationship is one of exponential decay; consequently, it takes a long time to reach steady-state.

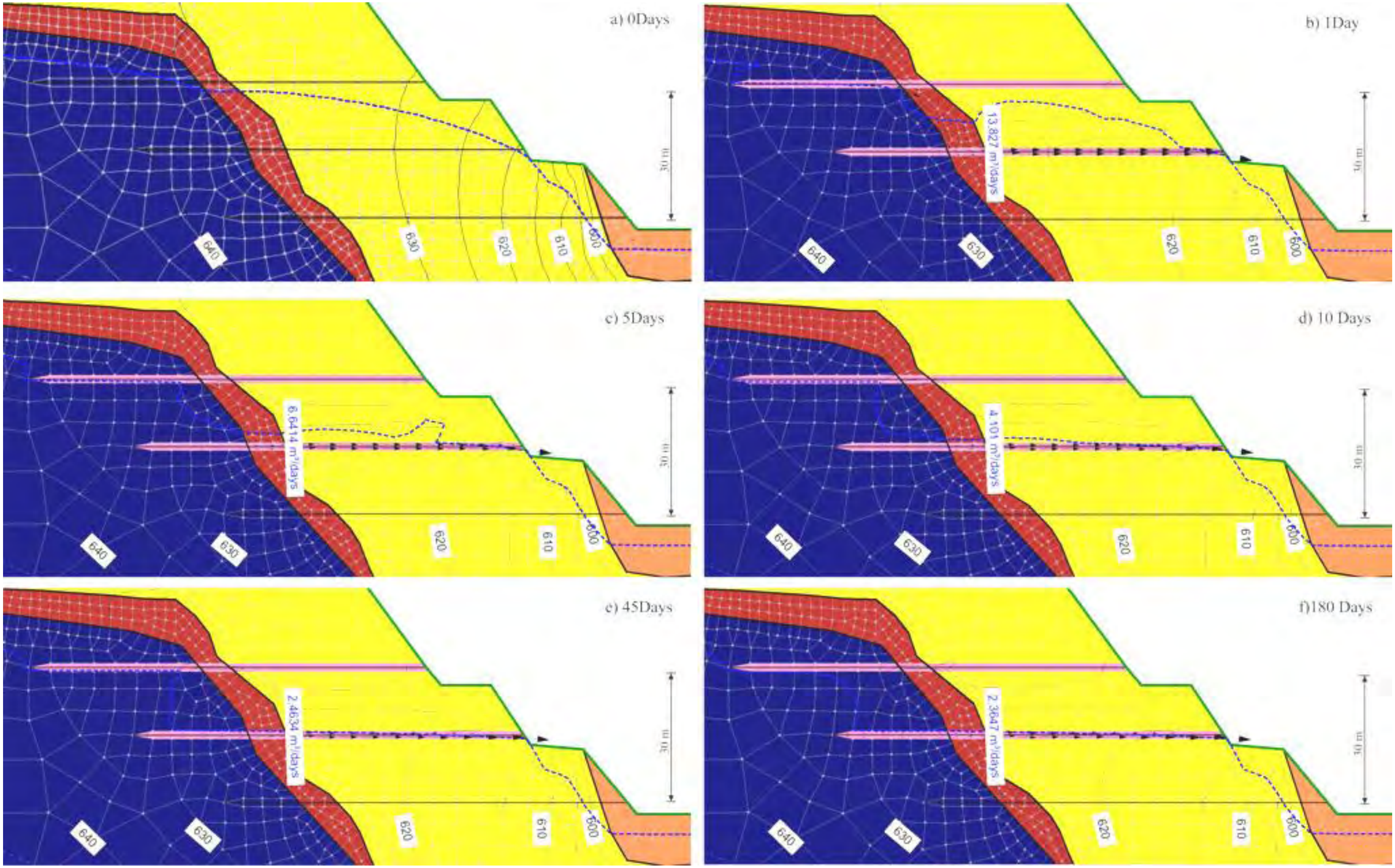

Figure 6-12 - Southern wall, transient progression of three level drain activation. Note: Total head contours have been labelled in 10m intervals.

The influence of the hydraulic gradient on drainage is most simply represented when observing the response of the Southern wall drainholes as they are not manipulated with the complication of structural features; this is a common theme in all simulations. Figure 6-12 shows Brunos Band draining to an unsaturated state before the MCS. As water enters the overlying second level drain it is transported into Brunos Band before migrating down into the third level drain.

Figure 6-13 shows the flow rate progression along this third level drain. The drain flows at around 15 m^3/day and then rapidly diminishes over the first week, reaching a near steady-state flow rate by around day 60. This can be seen by comparing the phreatic surface (represented by the blue line Figure 6-11b) from the steady-state simulation with the transient drawdown in Figure 6-12. Graphing flow along a drain can only be achieved when water travels along the entirety of a drains length and is discharged at the pit face. This flow behaviour is present within the lower southern wall drains as a result of the encapsulating MCS. This is not possible within the current northern wall drain installations due to the groundwater re-infiltrating in to the high conductivity ore (Figure 6-14). This inhibits the ability to record a a full data set and therefore the creation of a graph illustrating flow rate.

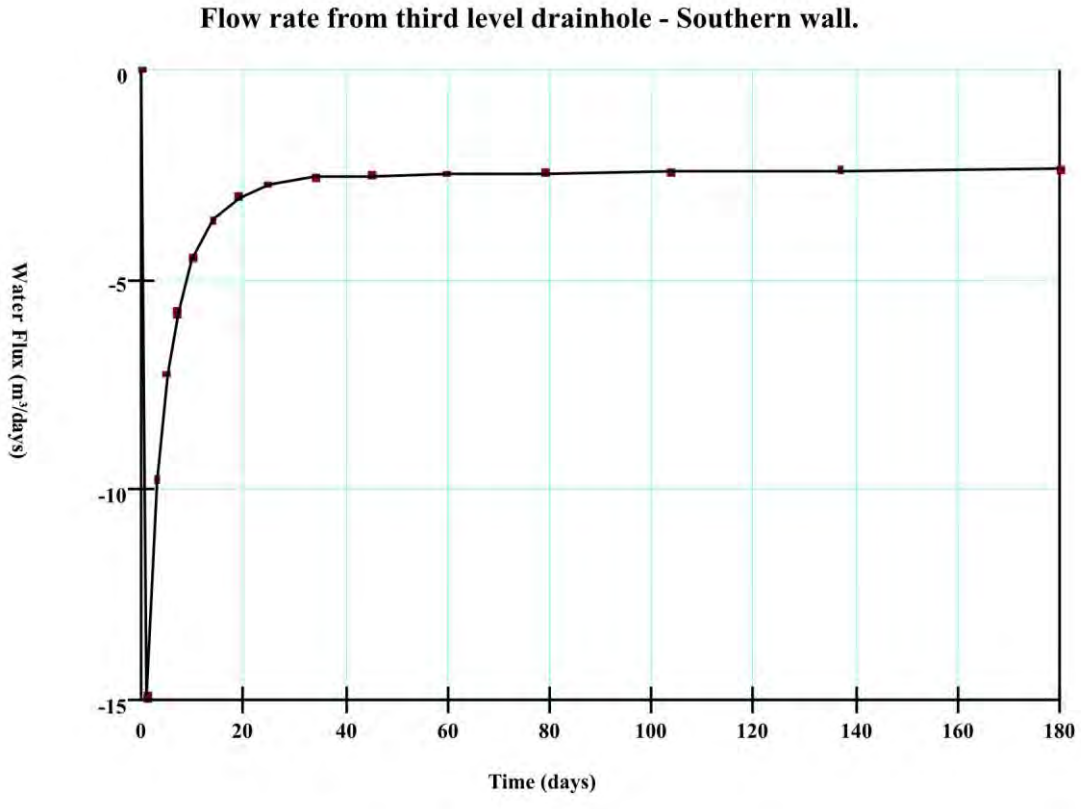

Figure 6-13 - Flow rate of third level drain during transient analysis.

The drains on the northern side of the pit do not experience the same high flow rates seen in the southern wall drains at the time of installation due to a lack of initial hydraulic gradient. This can be confirmed by comparison of the respective flow rates for each time interval in Figure 6-12 and Figure 6-14.

In addition to a reduced hydraulic gradient, much of the water that travels down the northern drains re-infiltrates into the high conductivity ore and migrates to the pumping wells at the base of the pit (Figure 6-14). A similar flow path to this has been mentioned in Steady-state analysis 6.5.2. As a consequence, the phreatic surface initially rises in the ore as a result of the majority of the water from the faults being diverted down the drains. The third level drains contributes largely to the drawdown of the phreatic surface as it intersects the upward flowing water in the second and third faults (as do the second level drains) at the lowest elevation in the system.

Areas where the MCS is the abundant lithology in both the Northern and Southern wall drains have shown a lag in the drainage rate when compared to the surrounding lithologies. This is to be expected due to the reduced hydraulic conductivity, and is illustrated by a perched zone of saturation in the rockmass throughout the early stages of the transient analysis, most noticeably in the Southern wall.

To summarise, the key observations from this transient analysis:

- Within the southern pit wall Brunos Band transports water from the upper drain and Fault 1 to lowest level of installed drains (which is this case is the third level drains).
- The lowest level of drains will always transport the greatest amount of water as a result of having the largest available hydraulic head.
- Within the northern pit wall the lowest level of drains provides a “preferential” pathway for water flowing through the complex structural setting of faults and the high conductivity Brunos Band.

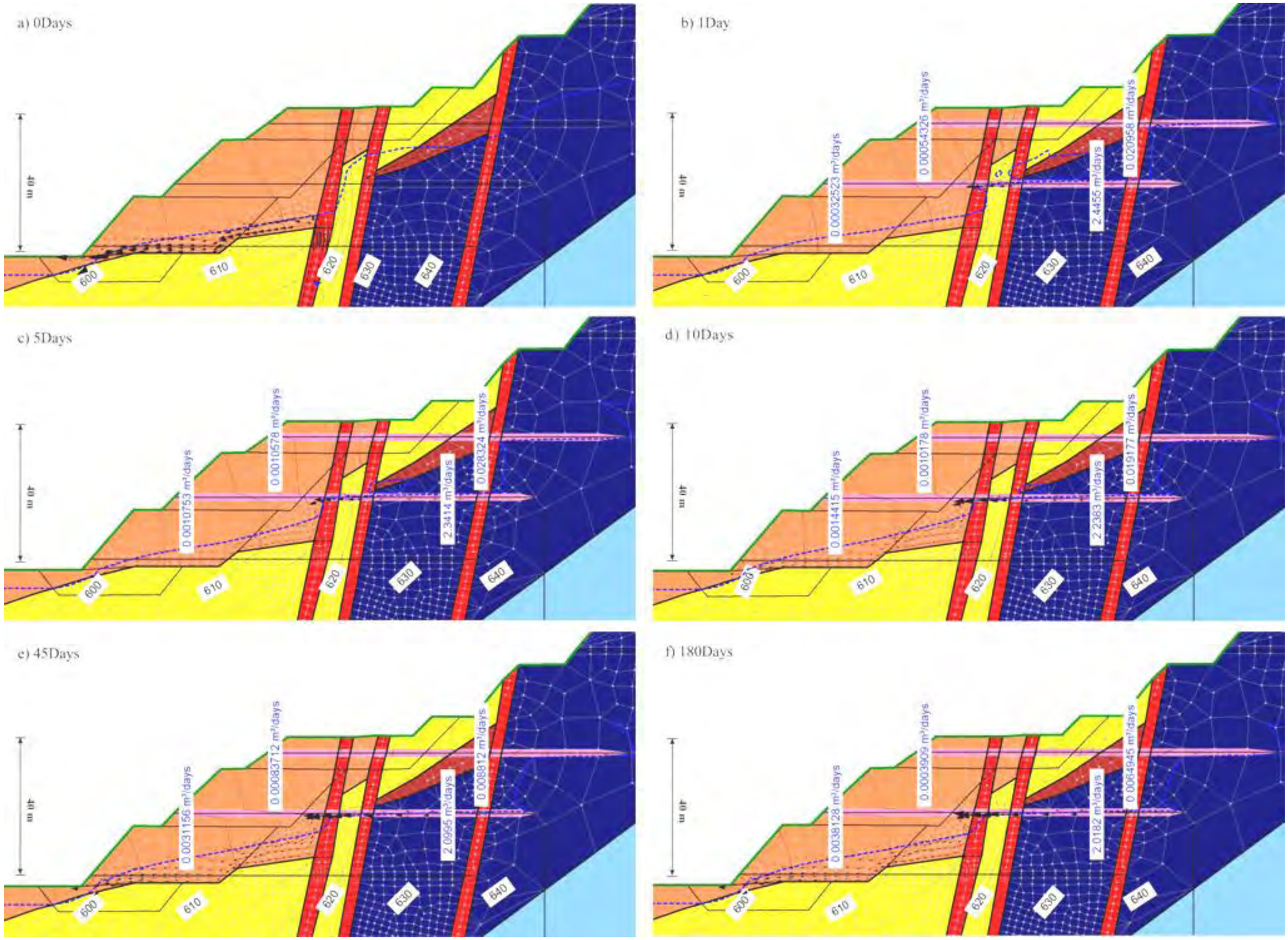

Figure 6-14- Northern wall, transient progression of three level drain activation. Note: Total head contours have been labelled in 10m intervals.

6.6 Steady-State Analysis: Activation of Fourth Level Drains

Similar to the previous three stages of analysis this final simulation of the current geometry examines the impact installation of the fourth level drains has on the system. As with the second and third level installations, the steady state analysis has been included to illustrate the equilibrium conditions. Independent observations have been made for the South and North wall reactions to these drains.

Each additional level of drainage must initially transport the overlying water in storage. Once this is complete, the majority of water transported by the drain originates from the northern faults and transported up Brunos Band; that provides the primary recharge to the southern wall with approximately 3.5m^3/day. This is evidenced by the steady-state flow rates in Brunos Band and the drain (Figure 6-15). Note that successively lower drains must carry more water because the distance of Brunos Band between the southern drains and Fault one is reduced. In other words, the hydraulic gradient is increasing (compare steady-state flow rate through drain three and drain four in Figure 6-11 and Figure 6-15, respectively). Flow along the drain is not released at the pit wall in its entirety due to the intersection of ore at the pit face. As with previous scenarios on the Northern wall re-infiltration of water into the ore will be directed to the dewatering bores in the base of the pit.

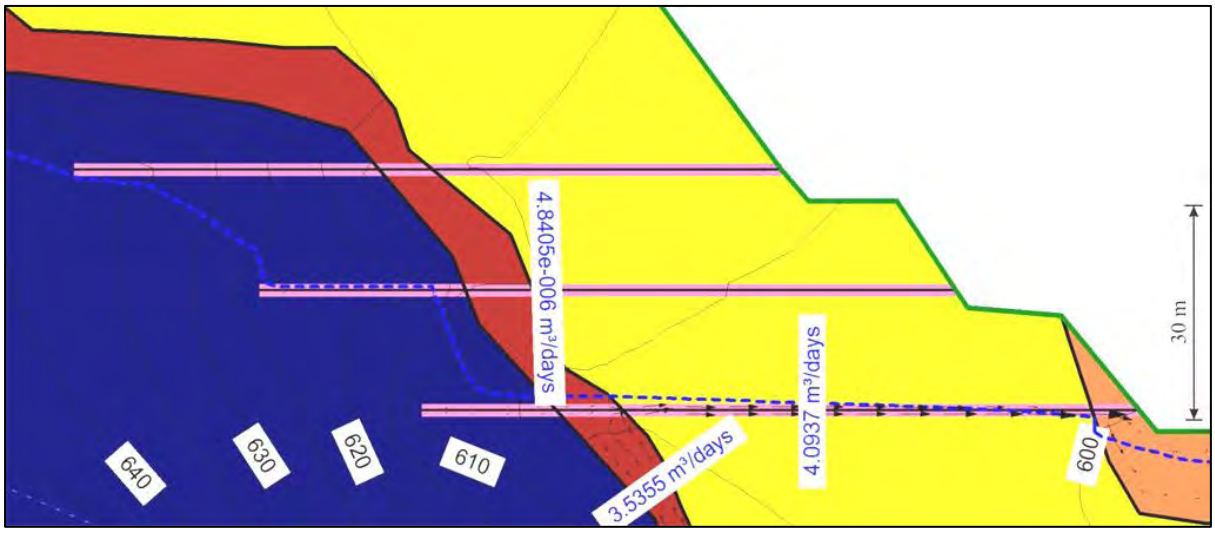

Figure 6-15 - Southern wall phreatic surface for Steady State analysis with four levels of drains activated.

The northern wall behaves in the same manner as its southern counterpart with the upper drains being rendered ineffective at the time of a lower drainage installation. Figure 6-16

reinforces the concept of diminishing flow rates. The phreatic surface rises gradually with depth into the wall rock. As the overlying rockmass becomes fully depressurised the phreatic surface would be expected to align with the drain in its entirety. Flux meters suggest approximately 3.5 m^3/day of water enters the fourth level drain from Fault 3. Additional water is transported down the fault from the overlying drains, resulting in a flow rate of 4.5 m^3/day towards the outlet. Additional contributions from Faults one and two increase the total flow rates up to approximately 6.4 m^3/day. The steep hydraulic gradient, emphasised at the end of the drain results in a steady-state flow rate of sufficient volume that a seepage face develops at the ore face which has not been observed in previous analysis.

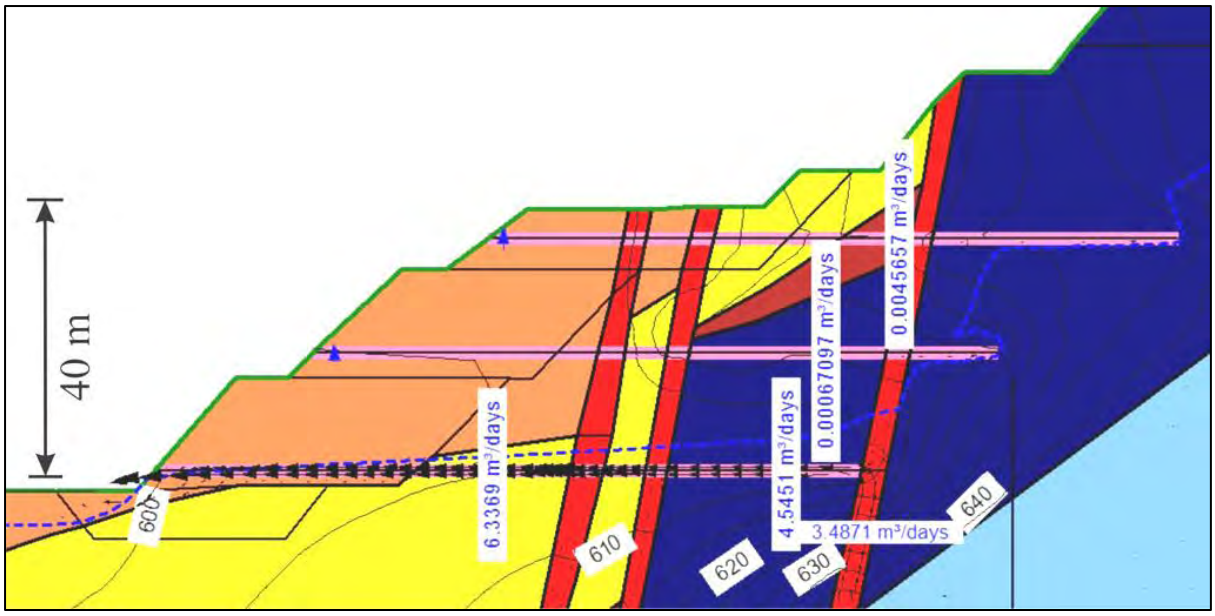

Figure 6-16 - Northern wall phreatic surface for Steady State analysis with four levels of drains activated.

6.6.1 Transient Analysis: Activation of Fourth Level Drains

The installation of fourth level drains has shown a detailed time dependant reaction of the low conductivity MCS to drainage (Figure 6-18). As noted on a number of occasions, previously lower level drainage outweighs the effects of its predecessors as the majority of flow is directed to the lowest point in the system with maximum hydraulic head. This concept has been confirmed as the flow rate along a respective third level drain in the southern wall rapidly decays over the initial days until flow all but stopping (Figure 6-17). As mentioned in section 6.5.2, a graph can only be created in the instance of water travelling the entire length of the drain. The water re-infiltrates into the ore material therefore it is not possible to create a graph for this scenario. Alternatively, flow rates measures within the model using flux

meters during transient analysis indicates that on the first day after installation the flow rate into the fourth drain was approximately 20 m^3/day (Figure 6-18a).

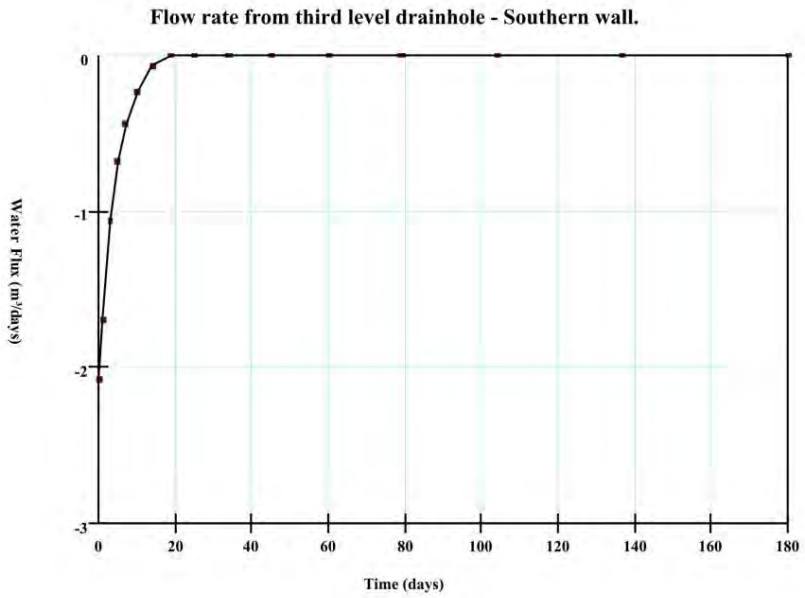

Figure 6-17 - Flow rate of third level drain after fourth level installation during transient analysis.

The changing flow paths develop with every level of installation, water collected by third level of drains is now flowing down Brunos Band and into the fourth level drains. Of particular note, one day after installation a gradient reversal causes water to flow from the third level drain back into Brunos band and down the lower fourth level drain (Figure 6-18a).

The most noticeable difference in the outputs of this transient analysis is the slower reaction of the phreatic surface to drainage. This is to be expected as a result of the low conductivity MCS (being at least an order of magnitude lower than the drains). Brunos Band aids in drainage deep within the wall leaving the section toward the face to drain at its own rate. A defined region of elevated pressure head. This may become an issue in time sensitive drainage scenarios in future if cut backs are planned within a close time periods. Figure 6-18d shows a prominent elevated region that takes a further three weeks until it the phreatic surface is aligned with the drain level.

The response of the northern pit wall (Figure 6-19) follows more closely to previous transient simulations in terms of the phreatic surface. Faults 1 and 2 exhibit a rapid response to the drain installation with only a small lag in the “intermediate” MCS between the two structures (Figure 6-19 a and b). The multiple recharge points have been covered in the steady-state

analysis with respective flow rates discussed. A more gradual decline in flow along the drains persists in comparison with the southern wall. This can be attributed to the ongoing inflow from the fault zones averaging out the flow rate rather than simply having a surge from drainage overlying strata before dealing with a single recharge source.

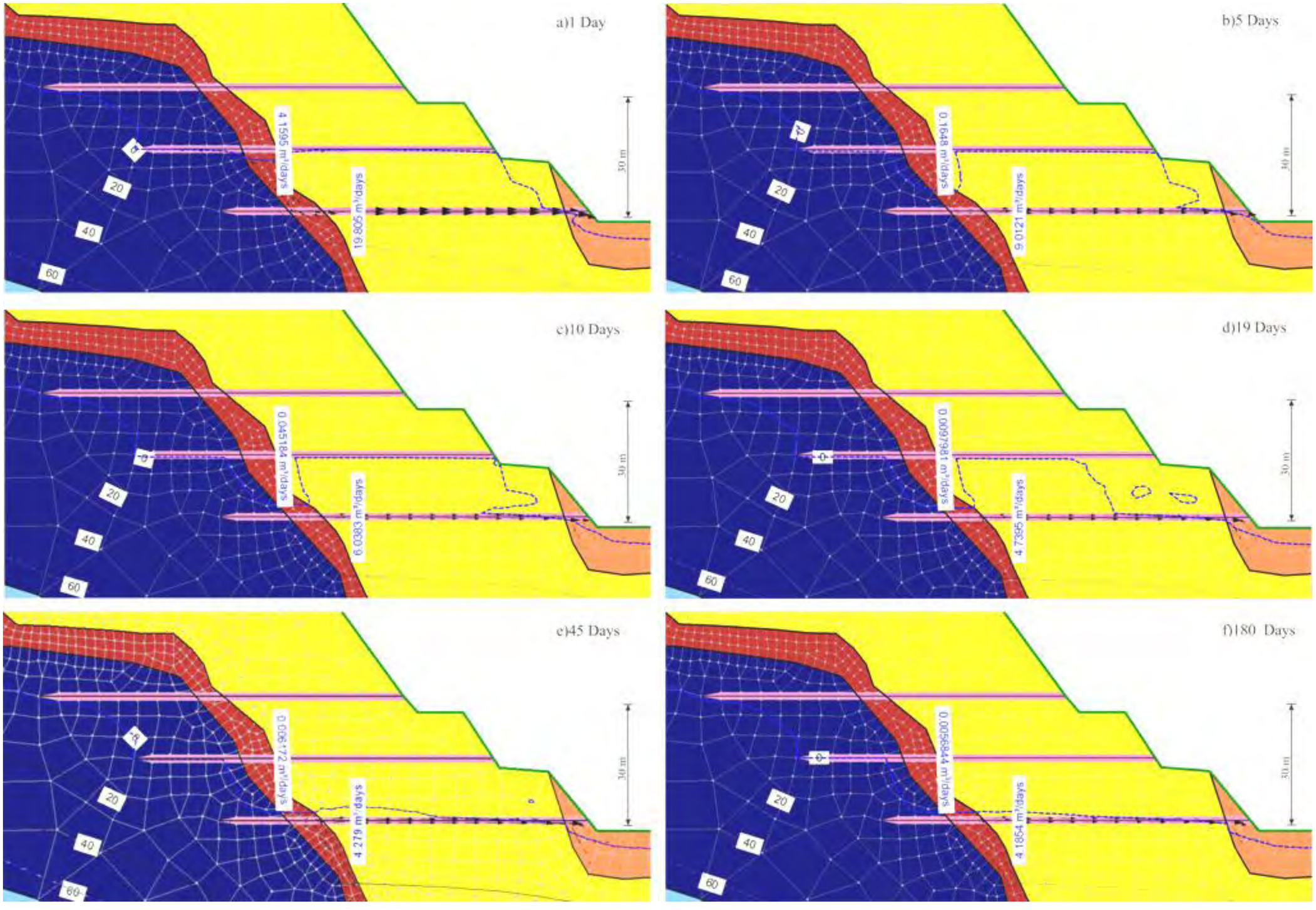

Figure 6-18 - Southern wall, transient progression of four level drain activation. Note: Total head contours have been labelled in 10m intervals.

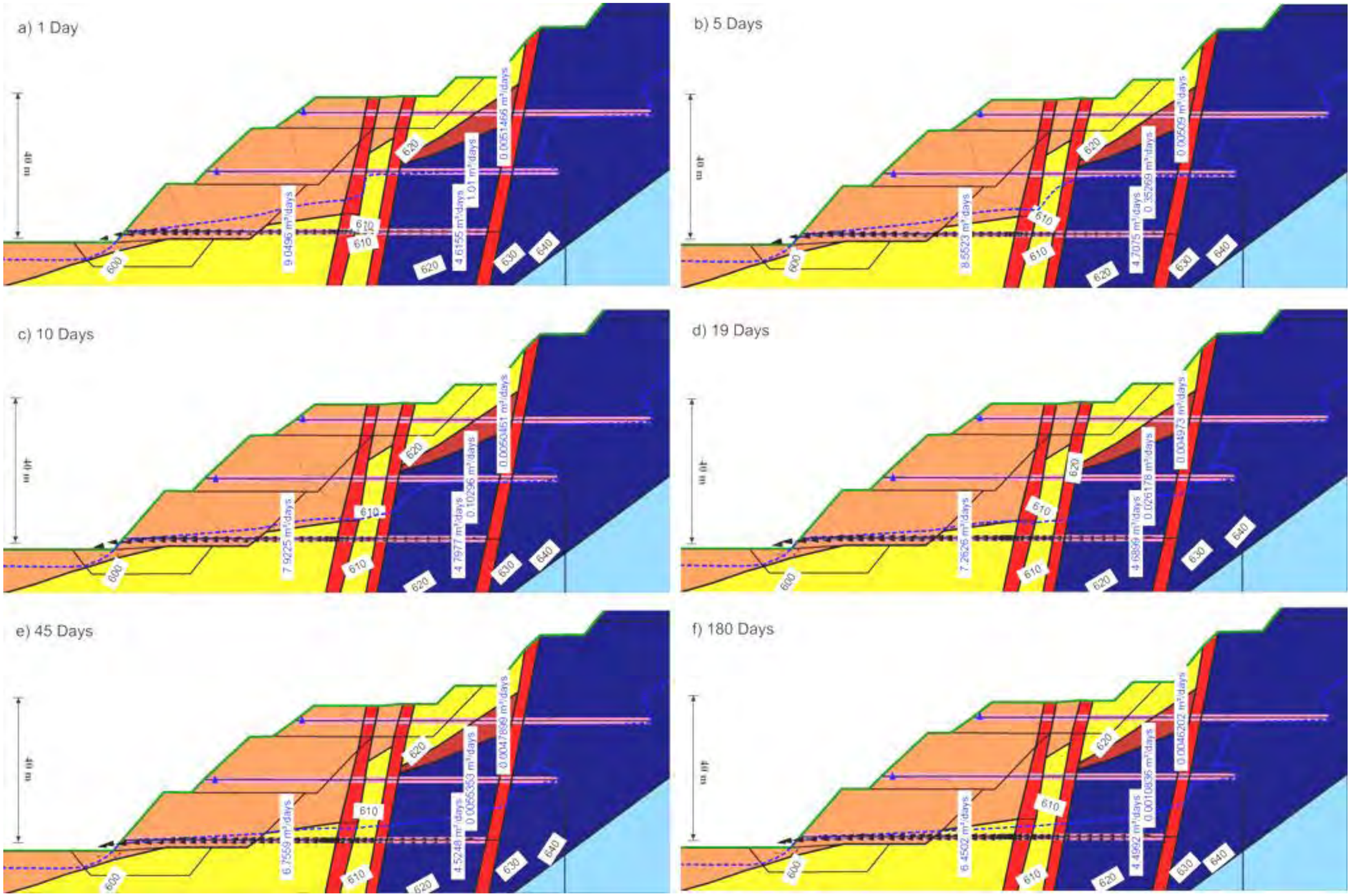

Figure 6-19 - Northern wall, transient progression of four level drain activation. Note: Total head contours have been labelled in 10m intervals.

Calibration of analyses

Although the model has been based around obtaining a conceptual understanding of the flow mechanisms present with the pit walls of the SEP a high level of accuracy has been emphasised throughout. As a means of calibration a hydrograph from a piezometer located within close proximity to the modelled section was selected. Piezometer PZ05SEP06-B was identified as having an extensive record of hydraulic head data with real time responses to the drainage installations that have occurred within the site historically. With the availability of such valuable data a replica of the piezometer was included in the fourth level transient analysis in an attempt to illustrate the modelled wall rock response to drainage installations. The monitoring bore was modelled to a depth of 80 m from the 660 mRL bench (Figure 6-20). According to the bore log (Appendix C) a 50 mm PVC pipe made up the piezometer with a slotted screen extending from 44 - 80 m. For the simplicity of the model a single node was selected as a monitoring point which has been highlighted by the red circle as the bore log does not show intersection with the WF.

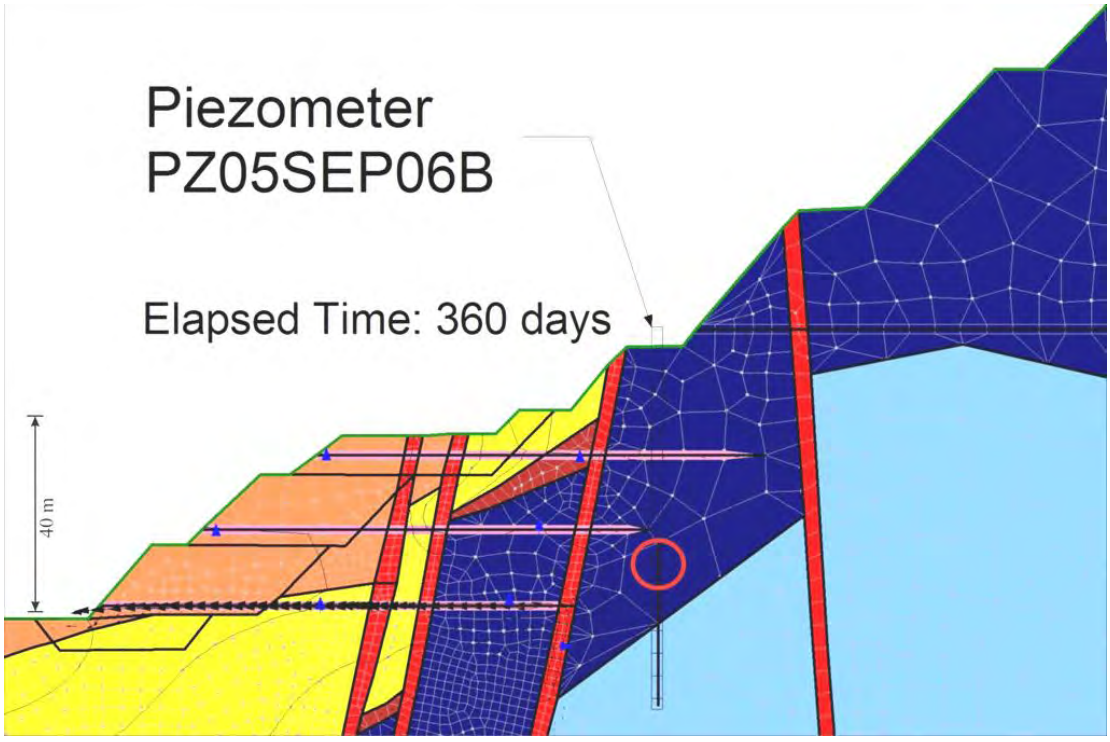

Figure 6-20 - Location of piezometer in numerical model.

Figure 6-21 shows the measured response of the phreatic surface within the wall rock. Annotations supplied by RTIO personnel provide an insight into the site conditions over the graphed time period. One of the key observations to be taken from this is the large drop in water level as a response to horizontal holes HD06SEP30 and HD06SEP32. Although these

holes were located in the northwest corner of the pit it is the conceptual nature of the response that is of interest in this case.

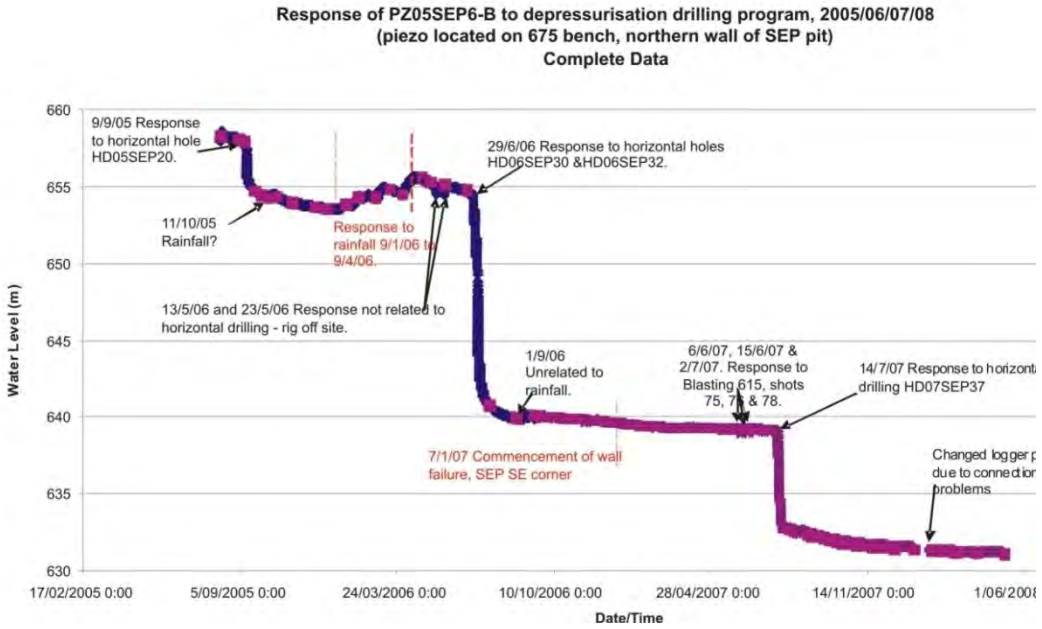

Figure 6-21 - Hydrograph showing response of north wall piezometer to drainhole installations (RTIO, 2008).

Figure 6-22 shows the simulated response for piezometer PZ05SEP6-B during the transient analysis. The steep drop in water level after installation of associated horizontal drainholes has been replicated in the model. Although the initial head was not at the same height as the real time monitoring data the shape of drainage response has been captured. This suggests that the conceptual groundwater model is responding in a similar manner to that of the rockmass on site.

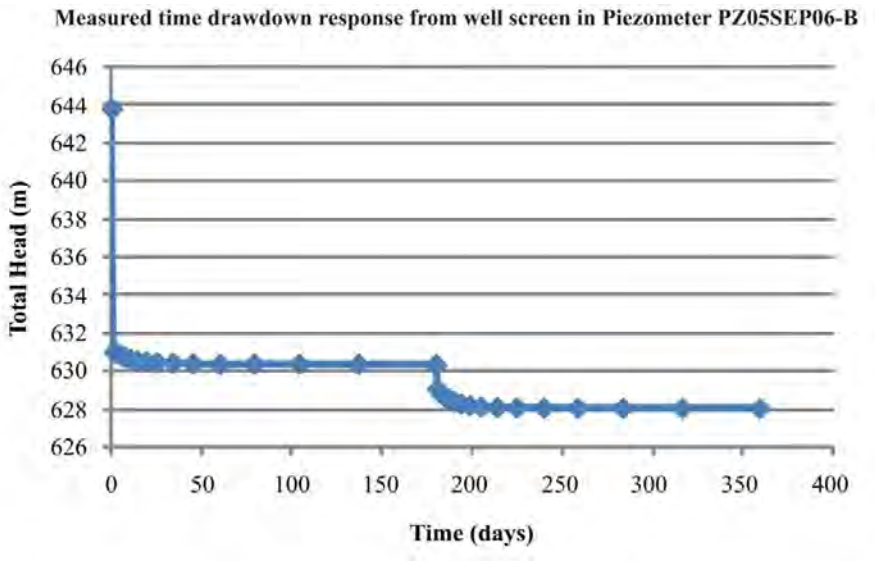

Figure 6-22 - Modelled piezometer response to show calibration of model to real time data.

6.6.2 Steady-state Analysis: Pit Cutback with Fourth Level Drains Activated

Pit floor cutbacks have been designed to optimise the SEP and ensure maximum recovery of remaining high grade ore. In light of this, an additional steady-state simulation has been undertaken to analysis the likely hydrogeological response. A number of potential issues were identified prior to running the model recovery. These include reduction in effective length of the previously installed horizontal drainholes and proximity of the phreatic surface to the refined pit wall. If passive horizontal drainage proved inadequate to provide the level of required depressurisation and/or sufficient buffer for unforeseen storm events or a hiatus in pit floor dewatering alternative methods would require investigation.

Figure 6-23 represents the refined pit geometry with the pit floor at approximately 590 mRL. Pit designs at the time of model conception indicated this as being a likely pit shell layout, but since this time further revisions have been made with a final pit floor level of 570 mRL. It must be reinforced that this is a conceptual representation of the pit walls response to drainage with associated flow mechanisms being examined. Although this model does not depict the final design it will provide sufficient insight into any potential complications cutting back of the drainholes will have.

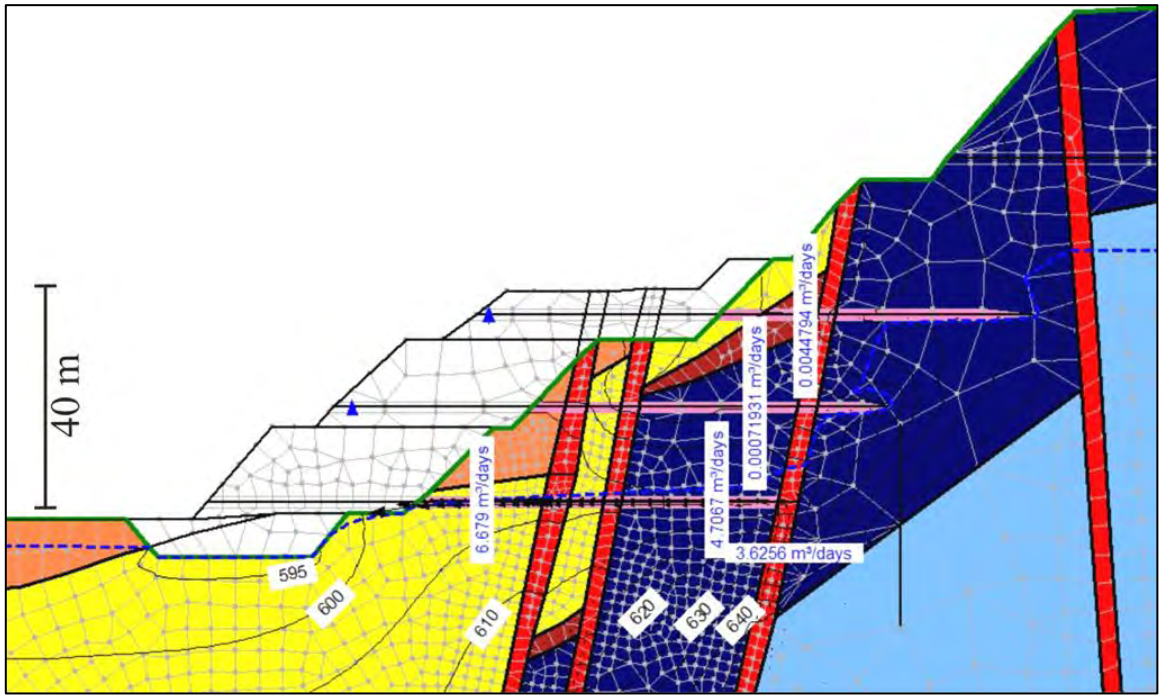

Figure 6-23 - Steady-state analysis with pit wall cut back and four levels of installed drainage

The Steady-state solution for the scenario has shown that similar preferential flow paths acting within the wall rock. The phreatic surface appears to remain at a slight inclination to

the drainhole which has been shown throughout previous analysis (section 6.6.1) and is likely a response to the low conductivity shale member (MTS) that requires a longer period to reach its full drainage potential. The total head contours demonstrate a rapid increase in gradient after the drainholes terminate in the wall rock making an exaggerated/bulb shaped cone of depression as the drains contribute to pumping wells in the base of the pit. The phreatic surface follows a similar profile, rising up at the end of each drainage level. This had been initially predicted prior to the commencement of numerical modelling.

6.7 Conclusions

Limiting time constraints have meant that a real time drainage analysis has been unable to be carried out during this study. Instead the use of a conceptual analysis has provided a much greater understanding as to the current flow dynamics and controlling mechanisms acting within the pit walls of the SEP. As noted, the use of numerical models is often best confined to providing a conceptual based solution to real world scenarios due to the use of varied assumptions and anisotropy within the materials would not allow for a true and accurate representation of the site. Instead having a clear understanding of the likely flow dynamics allows for greater focus in future dewatering/depressurisation infrastructure and monitoring requirements.

There are a number of key observations regarding groundwater flow dynamics within the SEP system that can be taken from the previous six stages of analysis:

1. The location of the phreatic surface prior to drain installation is governed in large part by the fault system (SEPFZ) and the high-conductivity materials. Groundwater is directed up the faults and discharges into the high-conductivity ore material on the northern side of the pit. This creates a perched water table on top of the MCS before being removed from the base of the pit using the installed dewatering bores.

2. Fault 1 plays a significant role in the transportation of groundwater flow and from the underlying Wittenoom Dolomite, it acts to control the location of the phreatic surface with the southern pit wall because water preferentially flows along and up the relatively high conductivity Brunos Band (k_x = 17m/day) and into the surrounding lithologies.

3. The steady-state flow rate of water entering the third drain on the southern side of the pit is approximately 2.16 m^3/day (Figure 6-11). This same volume of water is

exiting the drain at the pit wall due to the drain being bounded by low conductivity MCS within the southern wall.

4. In contrast, the third drain on the northern side has approximately 1.9 $m^{3/}$day entering the drain near Fault three but no water exiting the drain at the pit wall (Figure 6-10). The presence of the high-conductivity ore material promotes groundwater downward percolation from the drain into the ore. As noted above, this process would keep the perched water table south of Fault two elevated because water would not discharge at the pit wall.

5. As noted in Figure 6-21, the blasting process is likely to promote fracture development in the MCS as a result of high energy explosions. The possibility of an increased hydraulic conductivity zone near the face of the pit wall would promote downward percolation before reaching the pit wall (similar to responses seen on the northern side). Consequently, piezometric measurements may indicate continued drawdown despite the fact that only a small quantity (possibly none) of water is discharging at the pit wall. This hypothesis could be used as an explanation to a possible lack of seepage from the southern wall drains despite their conceptually modelled effectiveness in lowering of the phreatic surface.

6. The model demonstrates that the drains are only effective in lowering the water level near the pit face on the northern side if the drain intersects the fault before the fault intersects any the high-conductivity ore material. Furthermore, re-infiltration or percolation from the upper drains, which are tapped into Faults three and four, re-infiltrates into the ore, maintaining elevated water levels in the ore.

7. Calibration through the comparison of real time site based monitoring data and that of a replicated piezometer in the model (transient analysis of the fourth level drain installation) have shown similar drawdown responses. This would suggest that the model has accurately captured the conceptual flow dynamics acting within the wall as a response to the installation of passive horizontal drainholes.

8. The effects of planned pit wall cutbacks within the SEP were simulated using a steady-state analysis (Figure 6-23). The effectiveness of the currently installed horizontal drainhole does not appear to be compromised. This is due to the lowermost drains having the greatest influence on the drawdown of the phreatic surface. Potential issues had been identified as the length of the drainholes will be reduced in

the wall rock. The flow rates shown by flux meters in the model suggested this wasn't going to be a key factor in their performance.

9. Results obtains from the conceptual groundwater analysis have satisfied the initial hypothesis outline the research proposal by illustrating " a measureable decline in the pore pressure levels within the wall rock in response to the installation of passive horizontal drainholes".

Chapter 7: Geotechnical Stability Modelling

7.1 Introduction

The use of parametric modelling has been recognised for a number of decades as one of the most effective methods in assessing slope stability. In this study, numerical limit equilibrium analysis has been utilised to provide a means of measuring the influence passive horizontal drainholes have on the SEP northern pit wall. The second hypotheses developed in this research mentioned that the installation of passive horizontal drain holes would result in lowering of the phreatic surface within the wall rock. This should therefore be reflected by an increase in the two dimensional factor of safety based on available geological and geotechnical models.

In addition to the passive horizontal drainage being undertaken as part of this study, both a geotechnical review and detailed design study relating to the upcoming SEP pit development has been completed. Geotechnical Consultants "Xamine Consulting Ltd" released findings from a geotechnical review early in the first quarter of 2008. "MiningOne Consultants Ltd" were responsible for the design of the SEP pit cutbacks and associated sensitivity analysis. This work was completed in January 2009. Both reports contained a large amount of highly detailed geotechnical analysis relating to the same localities as this research. Fortunately, a visit to MiningOne's head office in Melbourne was conducted during December 2008. This allowed for correspondence with experienced personnel during of their development of the rockmass model. This also allowed for an understanding of the fundamental geotechnical data to be obtained, with emphasis on anisotropy within the rockmass and the role that structural features influence stability.

The sensitivity analysis included in this research is based on the rockmass model developed by MiningOne as it is believed to the most accurate and up to date available. This comprehensive dataset has been made available for this study (as mentioned in section 5.4.2) and has allowed for an initial representation of the anisotropic nature of the rockmass to be developed.

To maintain continuity with the conceptual nature of the hydrogeological numerical analysis a simple geotechnical sensitivity analysis has been undertaken. This will show the likely response of the rockmass to changes in the phreatic water levels, before and after the installation of the passive drainage.

7.2 Limit Equilibrium Sensitivity Analysis

Geotechnical engineers have been working for years in an attempt to ensure that slopes involved with or part of a development are deemed to be safe. Any non horizontal surface will have a component of gravity acting to force the rock/soil of the slope downwards. If the gravitational force is large enough, and can overcome the resistance offered by the shear strength of the material in question, a slope failure can occur. Stability assessments are achieved through the calculation of a Factor of Safety (FoS) for any given slope (natural, excavations or embankment structures) utilising material characteristics. As technology has rapidly developed over the last two decades a number of highly specialised numerical modelling software packages have been developed. These enable fast simulations for any given slope and associated material properties. For this study, RocScience Slide 5.0 has been chosen as the preferred limit equilibrium software package.

7.2.1 Factor of Safety

A FoS is able to be calculated for most slopes using Equation 7-1 where the shear strength of a material is divided by the shear stress required to maintain equilibrium within the slope (Fell et al., 2005).

Equation 7-1

$$FoS = \frac{Shear\ Strength\ of\ the\ Material}{Shear\ Stress\ required\ for\ equilibrium}$$

The output result is therefore numerical, the following scheme of interpretation being widely accepted be engineers. If the FoS was to result in a value of 1 or below then it is not deemed to be in an equilibrium state. This would infer that the slope in question is facing imminent failure. Results that exceed 1 are interrupted as stable in terms of slope equilibrium. It should be emphasised that the outputs from such analysis are only as accurate as the input data utilised in the simulation. If inadequacies are present in input data then the results can only be at best that accurate. A number of guidelines have been developed to provide a "buffer" or level of assurance for any given result. If the slope is designated to be developed for use in structural foundations as minimum FoS of 1.5 has to be achieved within the slope. WA mining regulations have guidelines for acceptable FoS and Probability of Failure (PoF) values for various scenarios. Ultimately the "level of risk" is determined by the owner and is a function of data uncertainty, risk to capital and risk to personnel and equipment. In addition to the considerations are made regarding a mines ability to manage the risk and associated

consequences. RTIO have developed an acceptance criteria for various slope scenarios as summarised in Table 7-1.

Table 7-1 - RTIO Acceptance Criteria for Slope Stability

Slope Scale	Acceptance Criteria	
	FoS (min) (Static)	PoF (max)
Bench	1.2	10% - 30%
Inter-ramp (no ramp)	1.2 - 1.3	5% - 10%
Inter-ramp (with ramp)	1.3	<5%
Overall	1.2 - 1.3	<5%

7.3 Model Setup

7.3.1 Geometry

The geometry utilised in this limit equilibrium numerical model has been based on the structural geology mapping carried out by Brockman Solutions. Similar to that of the hydrogeological modelling in Chapter 6, it is only necessary to include a level of complexity that fulfils the requirements of a proposed analysis without creating unnecessary detail. There is a common dialect between geological details and engineering understanding. “A model is an aid to thought, rather than a substitute for thinking” (Starfield and Cundall, 1988).

A geological cross section was created by Brockman Solutions, after extensive structural mapping. This has been exported as a base layer into Slide to create a background for the model geometry. This image was scaled according to ensure no distortion had taken place.

The geological units represented in the model were streamlined for use in the analysis. The major lithologies located within the pit shell were all incorporated (DG, FWZ, MCS, MTS). The WT has been omitted and instead the MTS has been extended through to the base of the model section. This has due to the WT not outcropping significantly close to the pit shell, it was therefore deemed not to play an influential role in the stability of the slope.

Faults have been represented as their own unique lithology, without making any differentiation to what country rock they had intersected. This was preferred as fault structures have shown (in previous studies) to be key zones of weakness. Tension cracks have been documented in the head scarps of documented historic failures (de Graaf, 2009) and observed during a site visit made in May 2008. In response to this, tension cracks have been incorporated into the lower haul road (known as the Pineapple ramp) accessing the pit. This is represented by the bench at 640 mRL in the cross section (Figure 7-1).

An outline of the typical geometry used in this analysis has been included in Figure 7-1, it shows only the northern half of the pit. This is due to recommendations made in the geotechnical review undertaken by Xamine Consulting Services (2008), mentioned in section 7.1. Zones of potential instability within the northern high wall were highlighted. The hydrogeological complexities within this region add to the elaborate geomechanical model of the pit creating an elevated risk to stability.

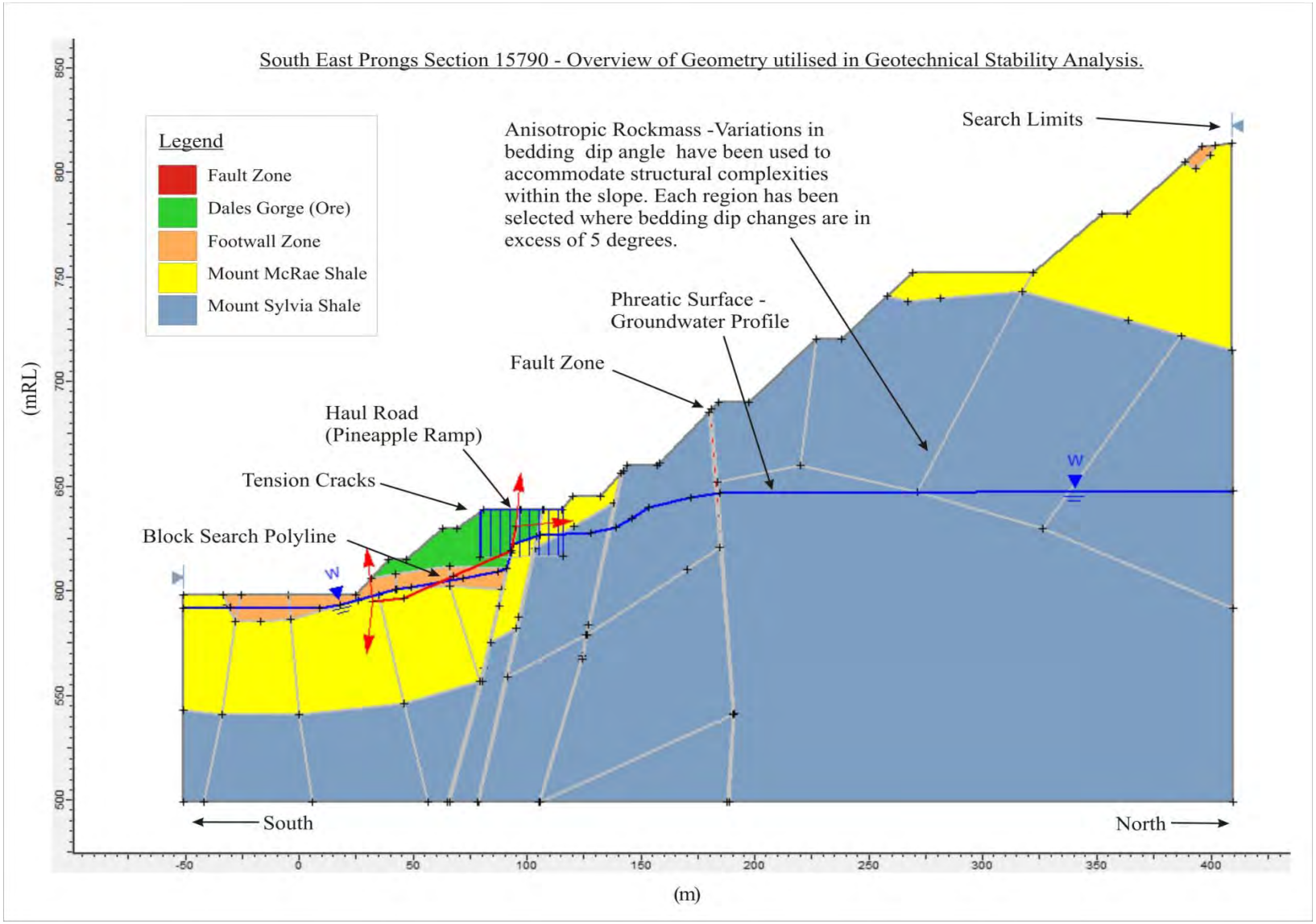

Figure 7-1 - Slide 5.0 Limit Equilibrium Sensitivity Model Setup Geometry

7.3.2 Material Properties and Anisotropic Strengths

Due to structural complexities within the SEP (section 5.2) it has been considered only logical to incorporate anisotropic strengths within the rockmass characteristics of the model. Investigations into previous failures with the SEP and greater Mount Tom Price operations, it has been established that the most common failure mechanisms are dominated by potential sliding along structures. These incorporate major faults and shale bands as well as smaller scale bedding planes. The numerical analysis has been designed to replicate such behaviours as listed below:

- Major structures such as faults have been were represented by specific thin layers of weak material in the model; and
- As mentioned above variations in bedding dip have been accommodated using the anisotropic rock-mass strength function within the software.

An "Anisotropic Linear" function (Slide version 5.038 or later) allows for variability in dip angles (as a result of fold progressions) to be accommodated within the model geometry. Each lithology has been divided into zones, each having comparatively consistent bedding dips; not exceeding a five degree range. Once respective domains have been established within the model the respective material propertied are assigned. The specific bedding dips are accommodated using variations in theta angle where required.

The "Anisotropic Linear" strength function allows for allocation of specific details of influential within each respective analysis:

- The definition of both maximum and minimum strength parameters (bedding and rock mass);
- Designations of bedding dip angles throughout rock mass, for example the specific failure path dip at the point where the minimum shear strength will occur; and
- Tolerances for stated dip angles. This is especially used when attempting to simulate a range of dips resulting from variations in altered bedding planes.

Trial analyses carried out by MiningOne (as part of the aforementioned SEP cutback design study) determined an appropriate set of dip tolerance values that have been adopted for use in this study. These are commonly referred to as "A" and "B" angles. To replicate the most realistic failure paths within the rockmass (whereby failures follow bedding where possible before breaking out through the rockmass) it has was deemed that angles of A=5° and B=10°

are most appropriate. An illustrative example of this concept has been included in Figure 7-2 (MiningOne Consultants Pty Ltd, 2009).

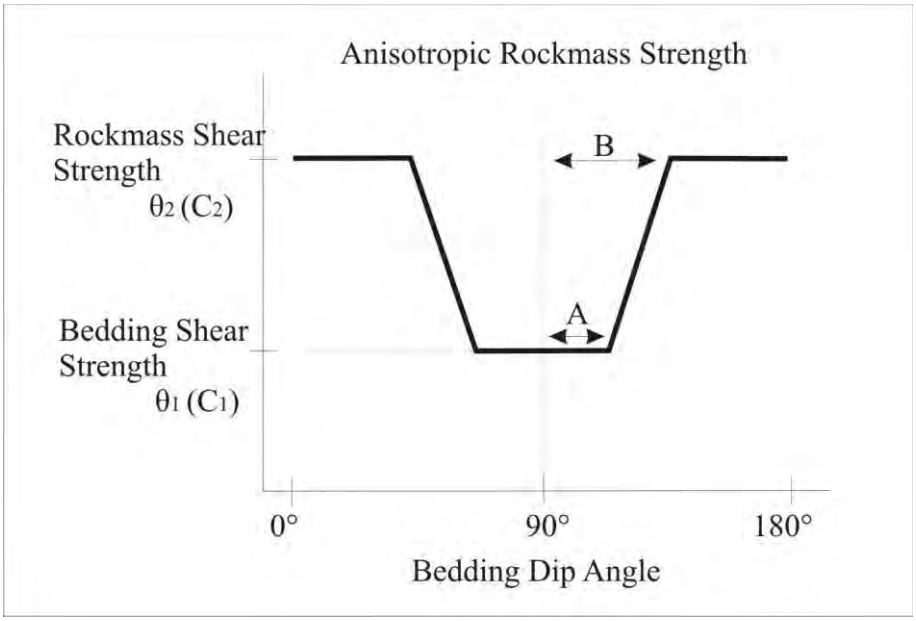

Figure 7-2 - Illustration of rockmass and bedding strengths in relation to bedding dip angle.

The effects of the "A" angle are summarised as follows. The smaller the angle the more restricted the failure paths would become. The will be increases in the respective FoS values as a result of increase shearing through the rock mass. Alternatively, greater "A" angles produce circular type failures, more frequently observed in unconsolidated materials. This results from weaknesses within bedding shear strength, irrespective of the dip (MiningOne Consultants Pty Ltd, 2009).

- Angle "A" is used to specify the range of tolerance both above and below the bedding dip angle. This is where the minimum or bedding strength is applied within the model;
- Angle "B" is used to specify the range of tolerance both above and below the bedding dip angle. This is where the maximum or rock mass strength is applied within the model;

It should be noted that when failure-path angles occur between the stated "A and B" values an intermediate strength condition is calculated within Slide. This acts as an estimate between the maximum rock mass strength and minimum bedding strengths.

Table 7-2 summarises the anisotropic strength characteristics that have been utilised in the limit equilibrium model for this analysis. Two separate strength conditions have been included in the sensitivity analysis. This allows the model to determine whether changes in phreatic surface are the dominant factors in stability, or if rockmass strength plays a more influential role. The "rock mass" strength applies to shear across bedding and is derived from the inputs in Appendix B.

Disturbance Factor

Calculations of rock mass strength using the Hoek-Brown method (Wyllie and Mah, 2006) require a Disturbance Factor (D). This factor is typically in the range of 0 to 1. It is included to accommodate shallow disturbances relating to blasting and stress relief by lowering the strength of the rockmass. MiningOne Consultants (2009) have recommended the use of a D=0.7 after being specified in the Hoek-Brown criterion as a suitable value for use in large open-pit mines with good blasting practices. It has been noted by MiningOne Consultants Ltd (2009) that the use of such a D has predicted large scale failure in slope that is otherwise stable. Typically a D such as this is only applicable to shallow failure analysis (~30 m) within the excavation. In light of this a level of understanding has been applied to the associated results.

Table 7-2 - Rock mass strength – anisotropic strength combinations

Strand	Strength type	Unit Weight (kN/m^3)	Shear through rock mass		Shear along bedding	
			cohesion	friction	cohesion	friction *
DG (ore)	Conservative (D=0.7)	35	215 kPa	25°	0	30° – 35°
	Typical (D=0)		370 kPa	36°	0	30° – 35°
FWZ	Conservative (D=0.7)	32	160 kPa	22°	0	30° – 35°
	Typical (D=0)		290 kPa	33°	0	30° – 35°
MCS	Conservative (D=0.7)	22	135 kPa	25°	0	30° – 35°
	Typical (D=0)		240 kPa	36°	0	30° – 35°
MTS	Conservative (D=0.7)	22	145 kPa	26°	0	33° – 38°
	Typical (D=0)		250 kPa	37°	0	33° – 38°

** NOTE: Range of bedding friction angles applied to north wall (Table 52-Appendix B). This table is intended to highlight the combination of rock mass strength parameters used for the two strength types.*

7.3.3 Method of Analysis

RocScience Slide Version 5 is designed to compute the static limit equilibrium stability of slopes using various methods of slices. This allows for both deterministic (factor of safety) and probabilistic (probability of failure) analyses can be computed.

The preferred method of analysis for this study was Generalised Limit Equilibrium (GLE)/ Morgenstern-Price. This was selected as a result of its rigorous nature in satisfying both force and moment equilibrium. It is commonly applied to scenarios where non-circular failure paths are present. This method also accounts for groundwater (hydrostatic pressures) in slopes (Rocscience Inc, 2006), which is the fundamental reason for carrying out this analysis; to constraint the effects of the passive horizontal drain holes within the slope.

7.3.4 Failure Path Search

To establish the global minimum failure surface within the SEP pit slope a "block search" method was utilised throughout all sensitivity analysis. This allows for non linear failure paths to be simulated which have been determined as the most likely form of failure surface to be expected within the wall rock.

An optimisation function has been included in the model, these acts to vary the initial non linear failure path to perform addition search routine (random walking) to determine the lowest critical FoS within the slope (Rocscience Inc, 2006). This function is especially useful when anlaysing failures that break out along both weaknesses in bedding strength as well as the rock mass strength of the lithology in question.

Specific locations of the failure surfaces were outlined using Slide's non-circular "block search polyline" method of assigning search paths. The idea behind this was to follow bedding layers where possible and allow the software to determine breakout points where required. An example of a "block search polyline" is illustrated in Figure 7-1; the arrows at each end identify the range in which a failure surface can be established.

7.4 Analyses

A total of eight stages of analysis have been undertaken as part of the two dimensional limit equilibrium sensitivity modelling component of this research. As noted in the research hypothesis, geotechnical sensitivity analysis has been undertaken in an attempt to further determine the effectiveness of horizontal drainhole installations. A lowering of the phreatic surface within the wall rock has been observed in Chapter Six. Sensitivity analysis is

conducted to determine whether this can be reflected by “an increase in the two dimensional factor of safety based on available geological and geotechnical models”.

The respective trials have been designed to investigate both the effect of rockmass strength (through the incorporation of two strength conditions) as well as the influence of changing pore pressure profiles within the slope, resulting from installed drainage measures. An outline of each set of analyses has been included below.

7.4.1 Trial 1a/1b - Estimated groundwater table prior to numerical modelling with original pit wall geometry

An initial pair of analyses has been undertaken utilising an approximated groundwater table prior to numerical groundwater modelling. These approximated phreatic surface levels are based on monitoring data but have simply been projected using a generic drawdown curve from the base of the pit. This simulation will act as a base line scenario to compare previous stability analysis with recent simulations carried out as part of this research, utilising a modelled phreatic surface.

7.4.2 Trial 2a/2b - Steady-State groundwater table with original pit wall geometry

To establish an equilibrium stability condition for the slope, the steady-state phreatic surface discussed in section 6.5.1 was imported into Slide. This was incorporated within the original pit slope geometry to represent the external boundary for analysis. An equilibrium solution allows for future trials to be compared as this effectively acts as a benchmark for the stability of the slope.

7.4.3 Trial 3a/3b - Groundwater table from four levels of drain activation using original pit wall geometry

The transient phreatic surface obtained from the analysis discussed in section 6.6.1 was utilised in this stage of stability analysis. This transient groundwater table allows for what are the most advanced drainage conditions that can be achieved using the current methods of depressurisation. Results obtains from this analysis should indicate the “best case” stability outcomes of all the trials as it highlights the greatest potential drawdown from the horizontal drainholes.

7.4.4 Trial 4a/4b - Groundwater table from four levels of drain activation using optimised pit wall geometry

The final stage of limit equilibrium analyses undertaken in this study incorporates the transient groundwater table generated from four levels of horizontal drainhole activation. The geometry reflects that of the planned cutbacks to the northern wall of the SEP (as current at

the time research was initiation). This was identified as an area of potential instabilities, as the phreatic surface is located closer to the pit wall. The two strength conditions for the rockmass will be modelled with the outcome signifying what should be the lowest FoS from these trials.

7.5 Outputs and Results

The results from the eight trials have been grouped with respect to their strength characteristics to allow for clarity in discussion. Trial series "a" refers to the conservative strength parameter that utilised a disturbance factor of 0.7. Trial series "b" represents the typical rock mass strengths for the site. The importance of having multiple variables in a sensitivity analysis must again be stressed. Having both changes in groundwater level and strength parameters provides an accurate understanding as to what conditions a slope is more sensitive to.

Output figures for Trials "1a-4a" are included in Figure 7-3 and combined with a summary of the FoS results in Table 7-3 give an overview of the stability analysis. Changes to the groundwater profile within the pre-cutback geometries (1a and 1b) show a similar output within this section. The key difference is that the assumed groundwater profile creates a saturated base to the DG lithology.

Table 7-3 - Geotechnical Sensitivity Results Summary - Conservative Strength.

Trial Number	**1a**	**2a**	**3a**	**4a**
Strength type	Conservative (D=0.7)	Conservative (D=0.7)	Conservative (D=0.7)	Conservative (D=0.7)
Geometry	Pre Cutback	Pre Cutback	Pre Cutback	Cutback
Groundwater Table	Originally Assumed GW Profile	Steady State GW Profile	4 Levels of Drain Activation	4 Levels of Drain Activation
Factor of Safety	1.42	1.49	1.60	1.32

** NOTE: Specific strength conditions for the respective materials can be found in Table 7-2*

Experience gained through the study of previous analyses of similar sections (Xamine Consulting Services, 2008, MiningOne Consultants Pty Ltd, 2009) has shown that groundwater plays a pivotal role in the stability of lower slopes containing DG and FWZ lithologies due to weaknesses in shear strength along bedding. Due to lower dip angles within this particular slope section (as a result of the multiple fault sets of the SEPFZ offsetting the F3 syncline) the respective FoS values are not at a critical level.

The global minimum failures have broken out along the modelled tension cracks within the Pineapple Ramp haul road. These are of a multiple bench scale magnitude and as indicated by Eggers, (2008) the basal slip surface has occurred along the FWZ/MCS contact. In reality this occurs along a known shale band weakness, although this particular shale band has not been included in the model geometry.

Results from Trial 3a have shown an increase in the simulated FoS values to 1.60. An elevated level of stability is to be expected in the scenario. The lowering of the groundwater profile through the activation of four levels of passive horizontal drainage can be attributed to this result. To compliment the lowering of the groundwater table the tension cracks were simulated as being dry. This combination of geometry (pre-cutback) and groundwater profile would be most representative of the current conditions within the SEP pit, all drains are operational and pit optimisation is yet to commence.

The final analyses undertaken using conservative strength characteristics yielded a notable result. The fundamental aim of trial (4a) was to forward predict the stability of the slope once wall optimisation is completed. A FoS of 1.32 (Table 7-3) is well within the equilibrium stability condition for a slope and the RTIO acceptance criteria for slope stability.

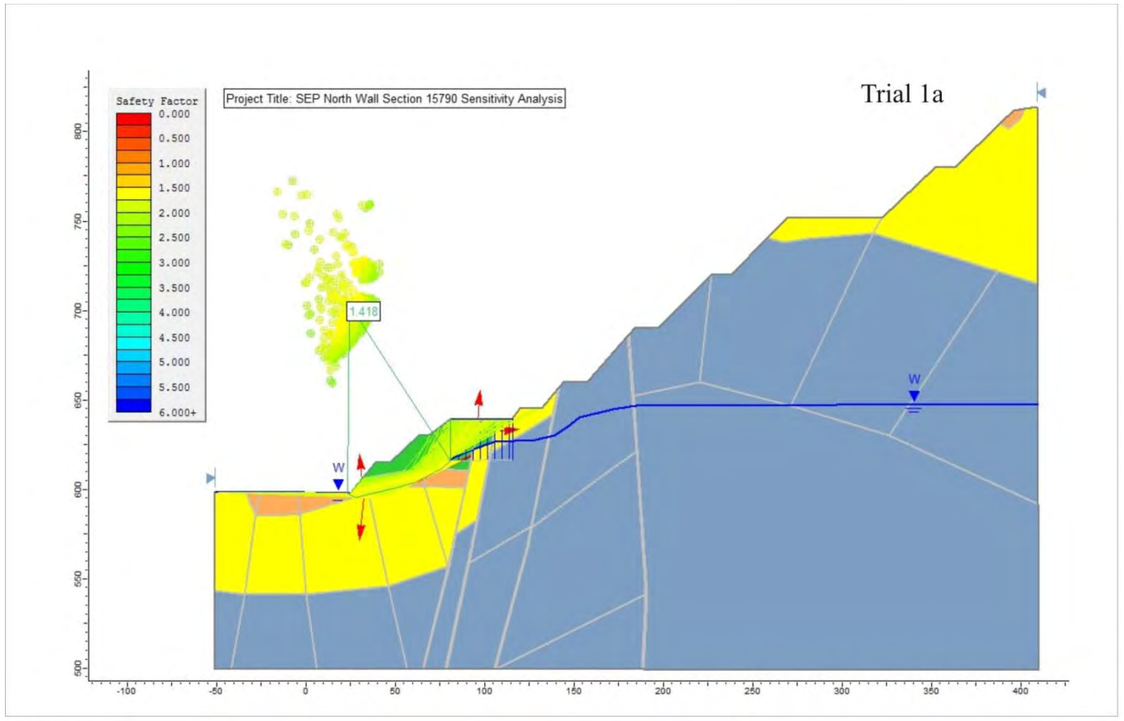

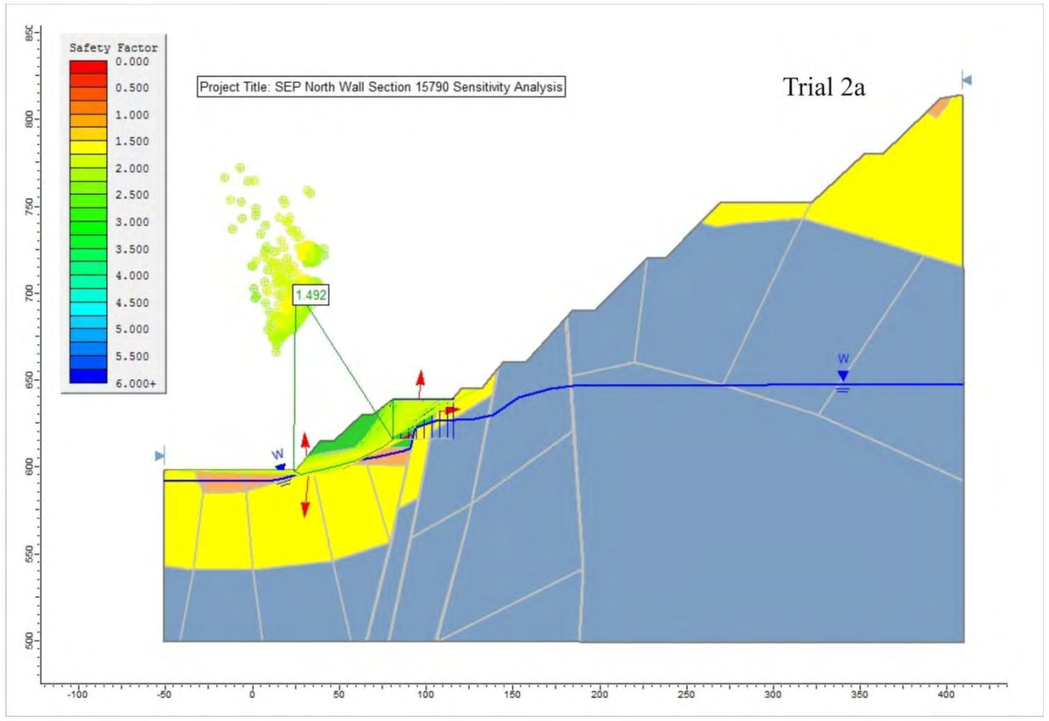

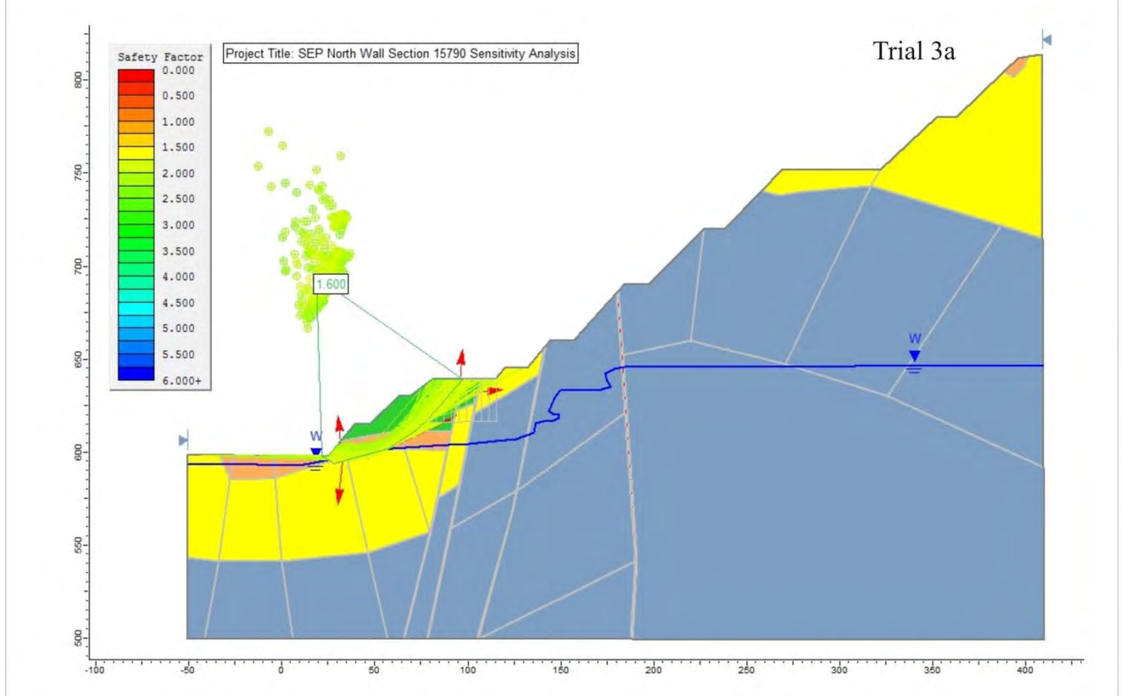

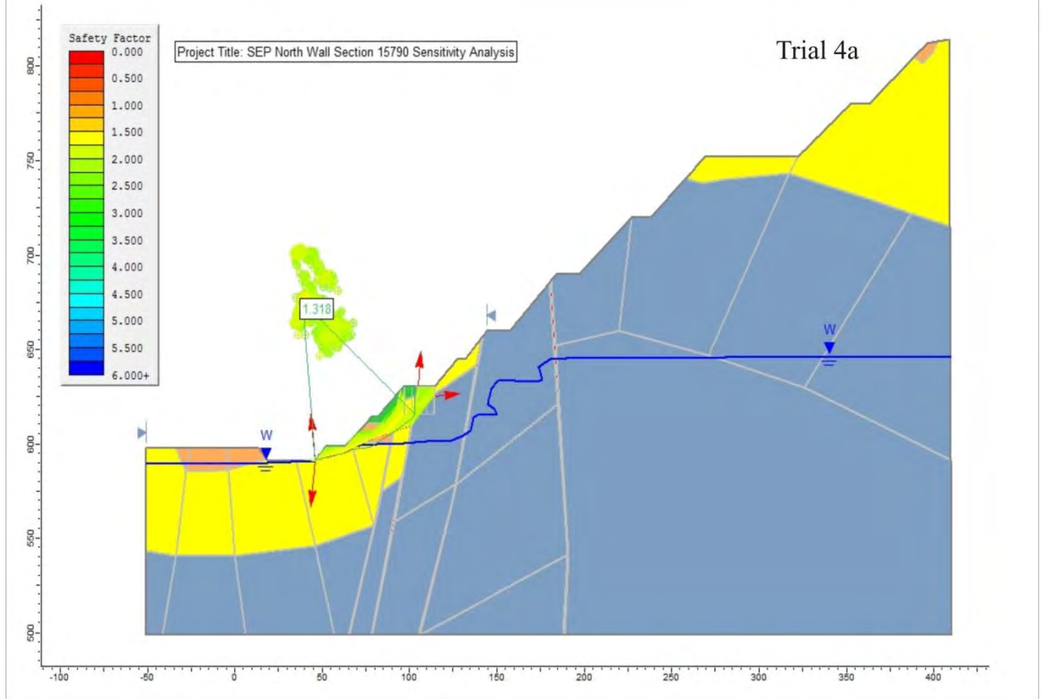

Figure 7-3 - SEP Section 15790 Sensitivity Analysis Outputs for Conservative Strength Parameters - Trials "1a-4a" as outlined in Summary Table 7-3.

The important message to take from this is that this section was initially selected to provide the most complex hydrogeological conditions within the northern wall and not necessarily the highest risk geotechnically.

The groundwater profile has been modelled to daylight at the toe of the slope along the FWZ/MCS contact in response to the significant permeability differences. Recharge potential of the fault zones has been discussed in section 6.6.1. This could prove to be a serious risk to stability of the wall in steeper dipping sections without further drainage installations. The current horizontal drains will require a buffer period to allow sufficient time to reduce pore pressure and lower the phreatic surface within the MCS. This may provide justification for an alternative active drainage system to be investigated. The magnitude of the predicted global minimum failure surface has remained consistent throughout each trial to a multiple bench scale. Although the block polyline search was located in this region, additional trials were run prior to finalising this surface. This ensures that most accurate representation of the geometry was possible.

Output results for sensitivity Trials "1b-4b" have been included in Table 7-4 with the resultant illustrations in Figure 7-4. Global minimum failure surfaces have remained reasonable constant with the increase in rockmass strength resulting from the absence of a disturbance factor. A query has been run throughout all analysis to limit the mapping of failure surfaces to a maximum FoS of 2.3. If results from Trial "a" and Trial "b" are compared it is apparent that the number of surface is greatly reduced which is to be expected. The global minimum values have increased throughout with no values beneath 1.60 which was the best result obtained from Trial "a". The increased FoS values reflects the influence rock mass strength has on the stability of the slope independent of groundwater level.

Table 7-4 - Geotechnical Sensitivity Results Summary - Typical Strength.

Trial Number	**1b**	**2b**	**3b**	**4b**
Strength type	Typical (D=0)	Typical (D=0)	Typical (D=0)	Typical (D=0)
Geometry	Pre Cutback	Pre Cutback	Pre Cutback	Cutback
Groundwater Table	Originally Assumed GW Profile	Steady State GW Profile	4 Levels of Drain Activation	4 Levels of Drain Activation
Factor of Safety	1.70	1.77	2.23	1.68

** NOTE: Specific strength conditions for the respective materials can be found in Table 7-2*

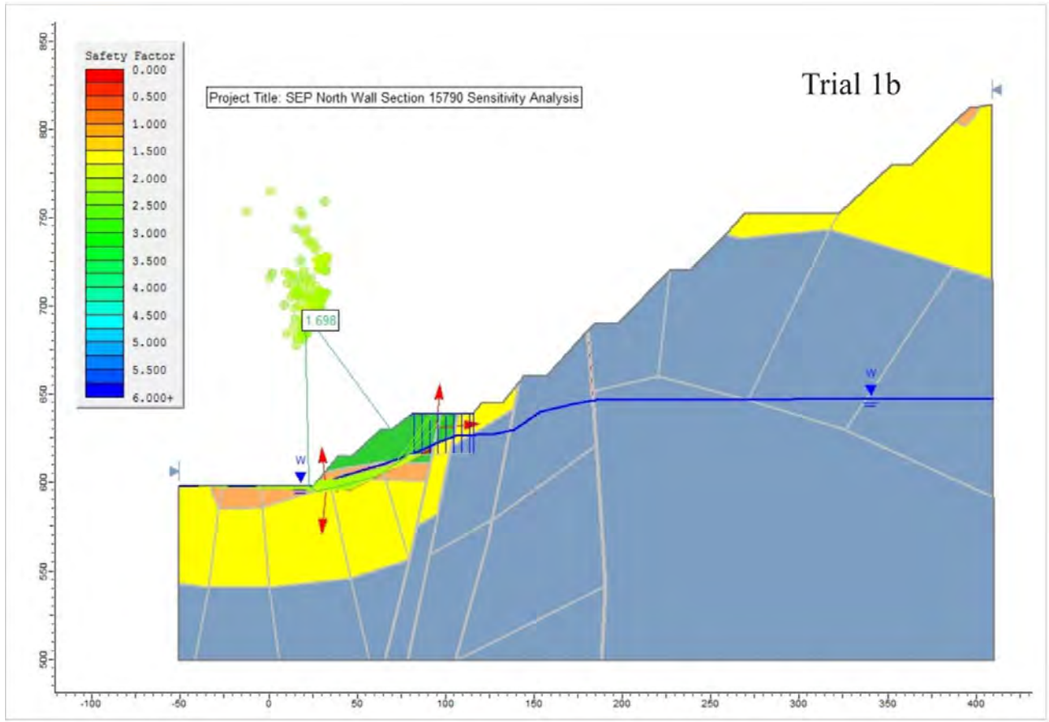

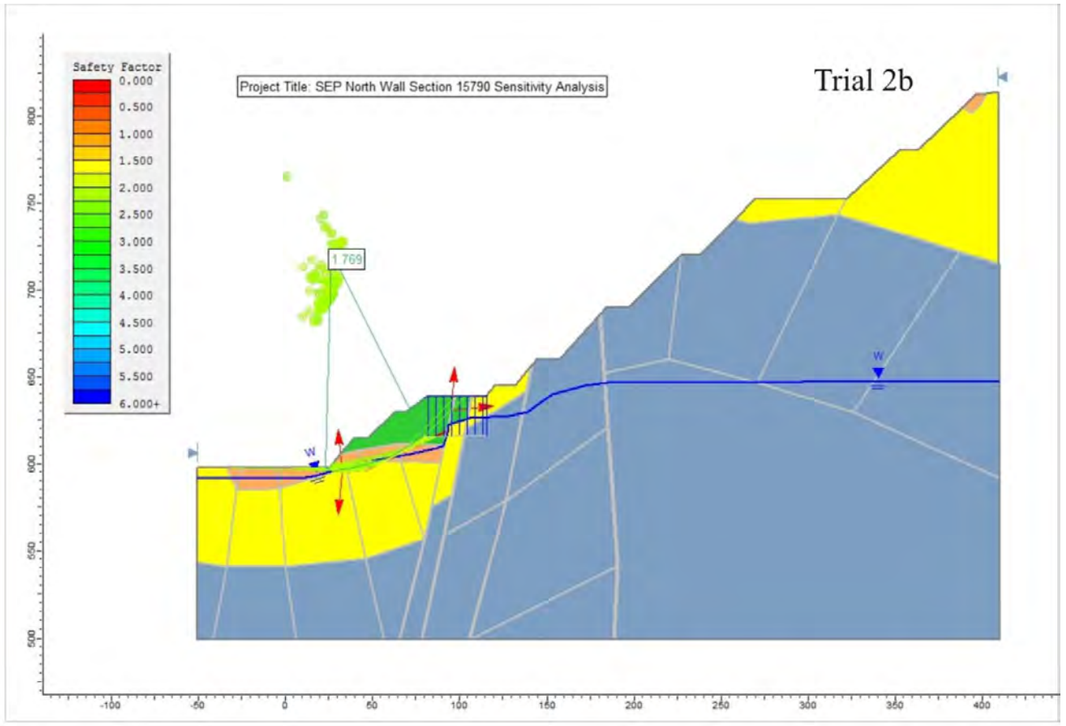

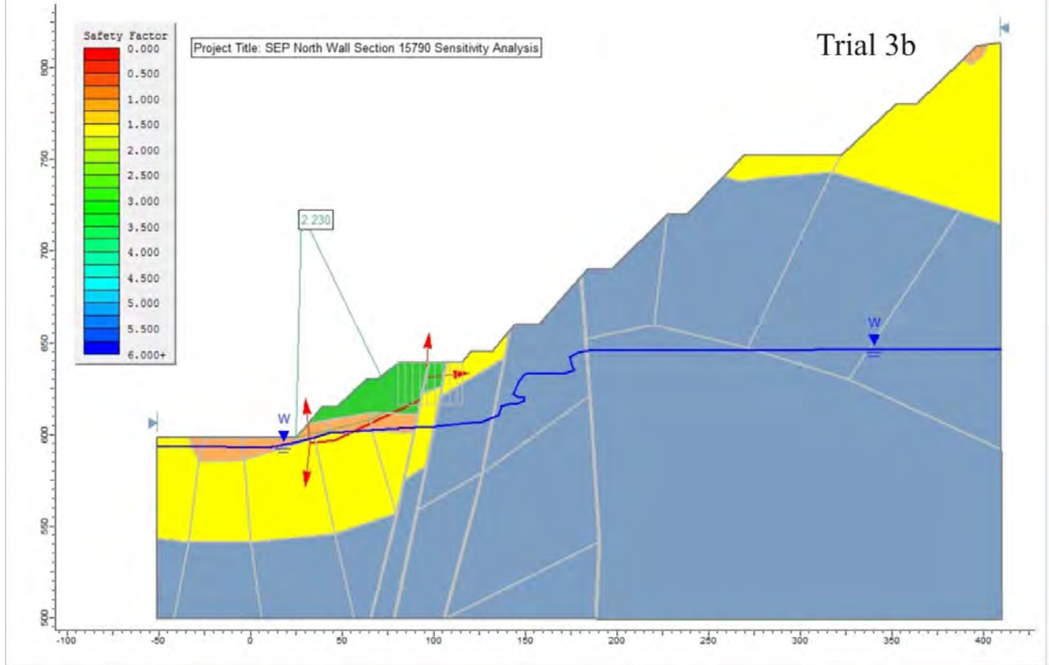

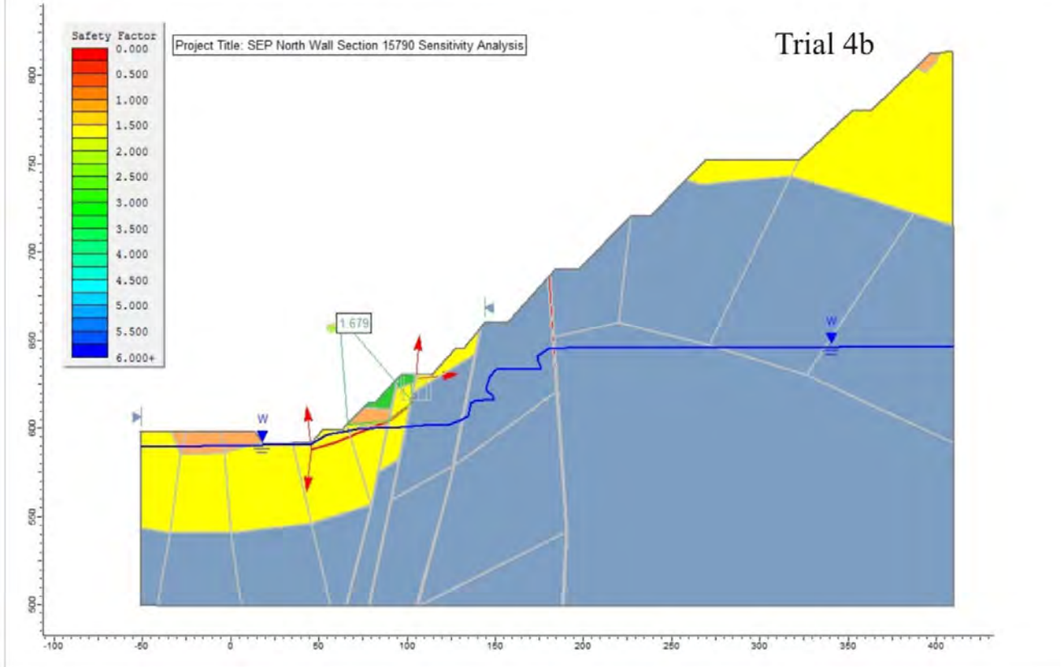

Figure 7-4 - SEP Section 15790 Sensitivity Analysis Outputs for Conservative Strength Parameters - Trials "1a-4a" as outlined in Summary Table 7-4

7.6 Conclusion

Initial model geometry for the RocScience Slide analysis was based on the geological cross sections developed by Brockman Solutions, (2008). Progressive bedding dip angles resulting from the prominent F3 syncline structure have been accommodated with an anisotropic rockmass model to depict the northern wall of section 15790. Slide can accommodate such variability through its "Anisotropic Linear Function". Failure paths searches were defined by way of a block search polyline which allows specific release angles of a failure to be designated.

To provide an accurate understanding of the sensitivities within the rock mass two strength characteristics have been utilised. This encompasses both a typical strength condition that reflects the "standard" strength of the rockmass. A conservative strength condition has also been included. This incorporates the use of a disturbance factor which accounts for blast damage and stress relief within the rockmass.

Detailed hydrogeological analysis (Chapter 6) has provided a series of conceptual groundwater profiles that have been utilised in these simulations. The key difference in the modelled phreatic surface compare to those used in previous analysis is that it shows compassion to variations in permeability between units and the surrounding structural complexities.

A number of key outcomes have been achieved as a result of the geotechnical parametric study:

1. Projected groundwater profiles that are based on monitoring data and a generic drawdown cone from the base of the pit have shown to provide unnecessarily low FoS results. This occurs as the lower DG and FWZ members have shown weaknesses in bedding shear strength which is exacerbated when saturated.
2. The majority of basal failure surfaces identified within this analysis have incorporated a release along the FWZ/MCS contact. The magnitude of such failures appears to be in the multiple bench scale.
3. The current pit geometry with four levels of activated horizontal drainage provides an adequate level of stability within the pit wall. This is confirmed as trials conducted under both strength conditions yielded FoS values ≥ 1.60.

4. As cutbacks are conducted to optimise the pit shell a significant reduction in FoS has been predicted from these analysis. This has occurred due to the groundwater profile running along the FWZ/MCS contact, as the MCS effectively behaves as a confining layer. The relative low permeability of the MCS inhibits the rapid drawdown in response to activation of horizontal drains. The recharge potential of the SEPFZ is likely to overcome the drainage potential of a passive system and therefore an alternative system of drainage should be investigated.

5. All simulations undertaken as part of this geotechnical sensitivity analysis have illustrated the importance of bedding shear strength to the resultant FoS values. It should be emphasised however that values generated as part of this analysis may well prove to be optimistic when compared to adjacent sections. The 15790 section has been selected for its hydrogeological complexities and as a result does not contain the steep bedding dips that are present elsewhere in the pit. Further analysis should be undertaken on such sections with a developed understanding of the groundwater profiles present within the pit walls.

6. At the completion of this geotechnical sensitivity analysis of the SEP northern wall the hypothesis derived for this study can be confirmed after comparisons between trials 1a/1b and 1c. A reduction in the phreatic surface (and associated pore water pressure) within the wall rock has been reflected by a lowering in the respective FoS values for the slope.

Chapter 8: Discussion

Discussion of primary results has been incorporated in the respective hydrogeological and geotechnical modelling chapters. A number of concepts have been identified as a result of this research. Key questions will be discussed below with reference to examples and case studies from the literature.

8.1 How do the numerical modelling outcomes influence the current understanding of hydrogeological conditions within the SEP?

A revised understanding of the hydrogeological conditions within the SEP has confirmed the presence of a leaky confined aquifer system, instead of the previously accepted confined bath tub model. The finite element numerical model developed as part of this research reflects the leaky confined status of the ore body aquifer within the SEP. The leaky confined aquifer was initially defined after standpipe piezometer monitoring boreholes were installed through the base of the impermeable MCS pit shell, providing a previously unavailable insight into groundwater conditions (RTIO, 2009a).

The confined bath tub style hydrogeological model would have sufficed during early stages of pit cutbacks. FoS improvements were able to be achieved through dewatering bores situated in the base of the pit. Relatively high hydraulic conductivity rates (3 m/day) of the DG and mineralised FWZ members allowed for rapid drawdown of the phreatic surface to be achieved. Passive horizontal drainholes installed over a series of four benches (levels 605mRL, 625mRL, 645mRL and 665mRL) aided in this drawdown by extending the cone of depression created by the dewatering bores.

Currently the ore body aquifer can be successfully dewatered via the vertical pumping wells with the aid of horizontal drainholes for depressurisation. For future mine development a buffer of dewatered rock 15 m vertical and 25 m horizontal from the pit face is required (Xamine Consulting Services, 2008). The pit cut backs have been designed to terminate within the MCS (Figure 6-23). Due to the MCS acting as a confining layer, the vertical bores will no longer be able to dewater with a rapid drawdown response.

This is in part due to the bores (e.g. WB07SEP01) penetrating the MSC. Pumping of these bores therefore yields leakage from the underlying WF aquifer. Due to the regional groundwater table, lowering of the phreatic surface beyond ~590 m AHD will require

prolonged pumping. It is important that these considerations are incorporated in the planned pit cutbacks.

Flow mechanisms identified through conceptual numerical modelling have shown that preferential recharge is encouraged along a path of least resistance (Figure 6-7). Groundwater from the underlying WF aquifer is transported vertically up fault structures. The faults within the SEPFZ provide recharge to the upper aquifer, where intersection with Brunos Band occurs at the top of the MTS. Water is able to flow sub- horizontally towards the pit walls, assisted by the large F3 syncline, as the associated bedding dips towards the centre of the pit, as discussed in section 5.2. This provides justification to the recognised high yields within Brunos Band as identified in the horizontal drilling logs and spatial groundwater analysis in section 6.2.

Horizontal drain holes have shown large variations in yield; absolutely dry to 30 L/s. Numerical modelling has shown that horizontal drain holes have acted to provide an outlet for upwelling groundwater that has been transported (as a result of far field pressure head) up the fault zones and along the broken cherty material of Brunos Band. The path of least resistance is altered by the installation of the drain holes. Groundwater is released into the aquifer via transportation through the relatively impermeable MCS towards the pit face.

Flow along the horizontal drainage holes appears to be unobstructed with high yields being recorded over the first days after installations, before proceeding to weep for the coming weeks. This was noted in the results from the numerical model (Figure 8-1) and has been observed in the field by site based hydrogeological personnel. In some instances, where the pit face is currently intersecting the FWZ or DG members, flow from a drainhole may only reach the surface during the initial high flow period. Once these yields have begun waning, it appears that the relative high permeability of the ore body permits re-infiltration from the uncased drain hole. This allows for either recharge of the ore body aquifer or creation of what is effectively a small perched water table. This is likely to be eliminated during planned pit cutbacks as the final wall is to be located within the MCS. This should result in the majority of groundwater yields reaching the hole's collar at the pit face, this then allows for proper routing and removal of the drained water.

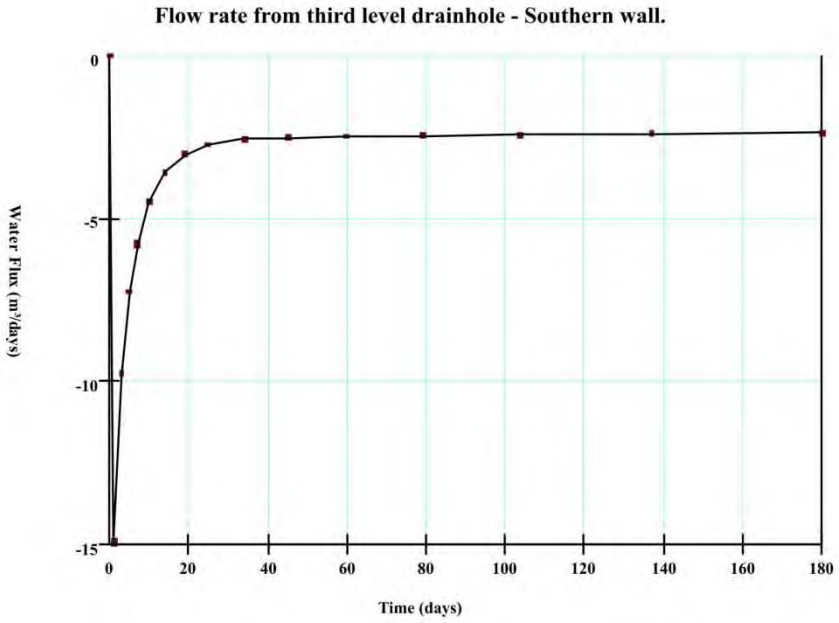

Figure 8-1 - Plot of flow rate versus time for horizontal drain hole in numerical model

A series of multi level vibrating wire piezometers could be installed in strategic locations within the northern wall of the SEP pit. This will provide valuable data to enable the evaluation of structural and hydrogeological interactions. A proposed installation plan has been included in Appendix C, including justifications for each specified monitoring point.

The recharge potential of the high conductivity units within the wall rock can be constrained as concentrated monitoring along lithological units allows measured flow rates. This includes an assessment of groundwater transport within the northern wall along strike (SEPFZ) especially in the problematic Bullnose area. Flow into and throughout Brunos Band can also be further understood as this has been identified as one of the fundamental routes for groundwater to reach the pit face.

This information will provide insight relating to which faults are acting as barriers to flow and which respond as conduits. As noted by Rozlapa, (2008) the dolerite dykes often weather to an impermeable clay material where water flow is severely limited. A similar condition can develop if gauge develops in fault zones. This occurs as a result of country rock being ground into small particles by fault movements before binding together to create an impermeable layer. These lithologies will be prime causes for the development of compartmentalisation within the wall rock. A number of potential compartmentalisation

zones have been identified as a result of site based data analysis undertaken by RTIO personnel (RTIO, 2008).

It is entirely possible for there to be substantial variability within the groundwater flow of the SEPFZ. Data from the proposed VWP program would allow for refinement of future models enabling more accurate prediction of drainage rates. The lack of specific hydrogeological knowledge relating to the SEPFZ in particular is a principal reason for not creating a real time draw down response model. During development of a numerical model the more assumptions made regarding input parameters the less accurate the outputs can be (Harmen et al., 2007).

In locations where compartmentalisation is identified, depressurisation will become more critical in maintaining the integrity of adjacent slopes. To mitigate the effects of elevated pore water pressure in areas of compartmentalisation, drainage systems should be designed on a case specific basis. Impermeable layers will not promote high yields from installed passive horizontal drainholes (as simulated in the conceptual model for section 15790). This is due to constraints as water released from high permeability material will be confined where drainholes intersect. Forward planning will therefore be required to allow depressurisation of targeted zones within the allocated time frames prior to advances in pit wall optimisation.

8.2 Is the current method of uniform horizontal drain spacing the most effective and efficient use of resources?

The current procedure within the SEP is to install horizontal drainholes at approximately 25 m spacing. Drilling records suggest that initial installations between 2005 and 2007 were limited to a depth of ~102 m. The most recent holes installed throughout 2008 and the first quarter of 2009 have been extended to depths in excess of 150 m in an attempt to alleviate the effects of known compartmentalisation within the northwest corner of the pit.

Yields from horizontal drain holes extending in excess of approximately 150 m should be closely monitored in comparison to equivalent holes of only 100 m in length. Brown (1981) identifies that a limiting factor in horizontal drain holes is their effectiveness at depths greater than approximately 150 m. As suggested by (Rahardjo et al., 2003: pg 296) a reduced number of drain holes installed at targeted locations of known water bearing structures is likely to provide the same level of effectiveness with a largely reduced outlay of initial time and resources.

Ahlbom et al., (1991) as in (Forth, 2004) highlight the effects of rockmass tightening as an important consideration when planning deep drainage system. Complications resulting from a materials specific coefficient of consolidation can severely limit the effectiveness of these holes. Tightening of a rockmass with depth reduces the available void space for groundwater, limiting both storativity and transmissivity. Flow in these areas is promoted through secondary fracture flow developed within structural features. To effectively target these structures a detailed understanding of the rockmass is required.

With a sound understanding of the recharge sources to such zones it could be beneficial to investigate alternative methods of drainage. Minimising recharge, be it flow through the fault zones along strike or from the underlying WF, will reduce the required level of depressurisation within the slope by intersecting groundwater closer to the source. As progressive cutbacks take place, the volume of the ore body aquifer (currently the highest priority in terms of dewatering maintenance) will be reduced. This will make it difficult to lower the phreatic surface and the subsequent pore water pressures using the current drainage systems as they primarily rely on abstraction from upper aquifer.

The proposed refinements to the hydrogeological model within the SEP (in relation to recharge to the ore body aquifer) as a result of the numerical groundwater modelling have lead to some suggested amendments to the current depressurisation system. A feasibility study into the use of vertical pumping wells around the north western perimeter of the SEP pit would be a logical next step. This will ensure the ongoing stability of the identified high risk slopes of the SEP as per geotechnical review presented by Xamine Consulting Services during the first quarter of 2008.

Installation of vertical pumping wells designed to intersect the WF behind the MTS contact (depth approximately $\leq$ 150 m) with the northern wall would mean recharge could be cut off to the high permeability faults that act to supply over lying lithologies and structures. Drains that are currently free flowing are not the ultimate concern. Areas that do not yield water and subsequently develop high pore water pressures will benefit from a vertical depressurisation program. The zone of influence of proposed vertical wells will combine with the current central dewatering bores, to create a wider cone of depression, emphasised within the northern pit wall.

As noted in the conceptual flow model, recharge to the southern wall is driven by the far field head (~650 mAHD) in the WF aquifer. This hydraulic head allows groundwater to be

transported along Brunos Band to high conductivity lithologies prior to discharge. “Pinching” and loss of stratigraphy (Tyler and Thorne, 1990) at the base of the pit has allowed the WF to be located closer to the pit shell than it otherwise would be. Mount Tom Price hydrogeologic records (Campbell, 2008) mention an encounter with substantial artesian pressure at the time of lowering the central dewatering bore, such experience would align with the proposed flow conditions in this study.

By reducing the recharge potential to the leaky confined DG aquifer and surrounding intermediate lithologies of the MTS and MCS (which have proven notoriously difficult to drain under the current system) would mean that pit wall pore pressure will be minimised through the later stages of the SEP pit floor cutbacks. Additional benefits resulting from the installation of vertical pumping wells include reduced operational downtime that would be required for horizontal drainholes to be installed. Respective drawdown rates will also be faster which will achieve the Xamine Consulting Services (2008) recommended 15m vertical 25m horizontal phreatic surface buffer. More responsive drawdown rates will promote faster advances in pit cutbacks, ultimately reducing abstraction costs.

Finally, the level of compartmentalisation will be reduced as a result of less recharge. Areas of ongoing compartmentalisation can be addressed with targeted drainhole installation. Fold hinges and fault intersections would be the ideal targets for these holes as noted by Campbell, (2008) as being a predominant water bearing structure; this would also ensure fewer dry holes.

8.3 How could the groundwater model be further constrained to increase accuracy of output simulations?

A lack of detailed understanding regarding the hydrogeological interactions of structural features has been highlighted throughout this research as a limiting factor in the development of models to give an absolute result. It is a fundamental requirement to constrain the behaviours before any more detailed hydrogeological drainage modelling can be undertaken. Similarly, a detailed review of the storativity and specific yield values for the local lithologies is required. At present the available data would suggest that many rock types respond identically however this would be surprising given the local environment.

It is important to reiterate that the volumetric water content functions have a considerable impact on the transient response of a flow system to a change in conditions. Volumetric water content functions work to define the ability of a rock material in terms of both the rate and

volume of water which can be released from a system. Steep volumetric water content functions with an associated small specific yield (as the case with this analysis, Figure 8-2) generate a more rapid response than gently steepening slopes (volumetric water content) with a large specific yield. Utilising the current storativity and specific yield estimates the draw down is very high as shown by the time required to reach an equilibrium yield. (Figure 8-1).

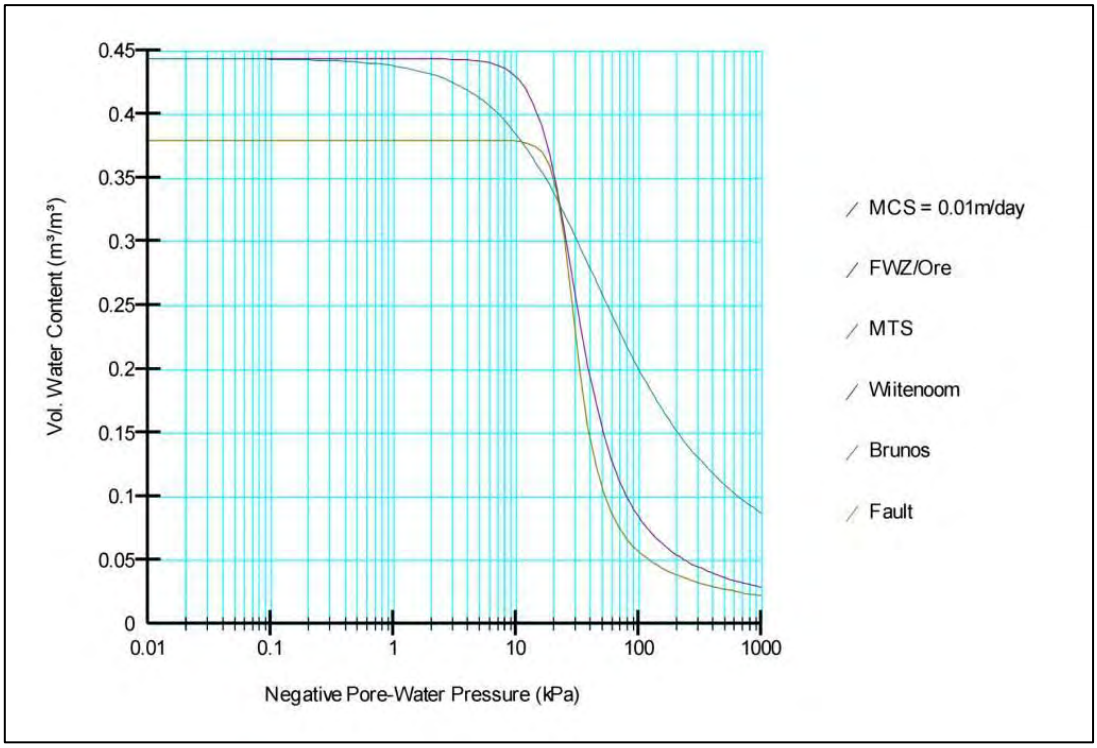

Figure 8-2 - Volumetric Water Content functions used in transient analysis for this study.

Refinement to boundary conditions in future models could include precipitation/infiltration and recharge as well as the effects of in pit dewatering bores currently in use. This model was constructed under the "worst case" conditions assuming all fault zones act as flow conduits which in reality is potentially incorrect. This methodology was selected to provide insight into the wall rock flow dynamics as an initial investigation with limitations in the data set.

The initial model has aimed to provide a primary understanding of the flow dynamics within the northern wall as a greater potential for wall rock instabilities has been identified in this region. To accommodate the regional structural asymmetry of the SEP future models could investigate the influence of unique boundary conditions for the northern and southern walls. The extensional nature of the southern wall is likely to be responsible for the majority of free flowing drain hole installations and associated higher yields. The northern wall however is a

compressional environment which reflects the concept of rockmass tightening with depth (Forth, 2004).

An interesting future trial could be conducted to assess the influence of surface recharge to the system once the primary hydraulic functions have been finalised. By extending both the northern and southern extents of the model and applying no flow conditions to these boundaries a recharge function could be applied along the ground surface. This would provide a more fundamentally correct approach to defining the far field total head parameters and allow for model calibration with known climatic data. This would allow for the entire system to respond to future cutbacks within the pit and dewatering works. The regional water table within the model would reflect the ongoing pumping from dewatering bores and adjust accordingly. At present the total head is specified as opposed to being simulated. This is evident as it remains constant throughout all of the transient analysis which impacts on the flow rates and temporal response of the system.

8.4 How can study outcomes from this research be applied to other scenarios/ deposits within RTIO operations?

The importance of having a detailed understanding of subsurface conditions have been emphasised as a result of this research. Mount Tom Price was the first of the RTIO operations to begin mining below the groundwater table in 1994 and appears to have initially misunderstood the complexities of the hydrogeological environment. Hedley and Domahidy (2007) mention the fact that groundwater was only considered a resource for consumption and to benefit production during the early stages of mine development. As the demand for primary resources has increased over the past few decades mines have been forced to extend to much greater depths in order to achieve maximum ore recovery. Steepening of pit walls and optimisation of mine design is becoming increasingly important (Harmen et al., 2007). Decreasing failure risks associated with steepening pit walls is directly proportional to installation of effective drainage systems (Mandzic, 1992). Mine designers now have a greater appreciated for the requirements of pit development below the groundwater table.

RTIO deposits that are earmarked to extend below the groundwater table include Brockman 4, Mount Tom Price Section 10 (Turner Syncline), Hope Downs and 4 East Extension (Paraburdoo). These deposits can benefit from conducting detailed dewatering feasibility investigations to assist in the designation of appropriate infrastructure. Hall (2003) emphasises the need to allocate adequate lead time to drawdown the groundwater table and

associated pore water pressures prior to pit excavation. This will reduce future production delays that may be encountered if dewatering and depressurisation fall behind schedule as is the case with the SEP.

Preferential flow paths identified in the conceptual modelling component of this research can be used as a case study to identify potential zones of significance for depressurisation. The response of the SEP passive horizontal drainage system has been highly beneficial throughout the current pit developments. However, there is a risk to the future success of the horizontal depressurisation program as drainholes have the potential to divert groundwater into the pit. Similar scenarios that are encountered in future operations could benefit from an alternative depressurisation scheme. Such installations would be straight forward when based around a comprehensive groundwater model.

Finite element numerical modelling based on a comprehensive data set and conducted with a parametric field study provides a valuable tool to assist in the forward prediction of drainage characteristics in a variety of unique environments (Rahardjo et al., 2003). The principle benefit associated with this approach is that it provides a cost effective and timely simulation to allow for successful future pit designs (Geo-slope_International, 2007).

Chapter 9: Conclusions

9.1 Thesis Objectives

The principal hypotheses of this thesis are that:

- There will be a measurable decline in pit wall piezometric pressures following installation of the horizontal drainage systems.
- This will also be reflected by an increase in the two dimensional factor of safety based on available geological and geotechnical models.
- A predictive model can be developed to improve slope stability (and hence mine safety) by strategically planned drainage measures in advance of pit floor lowering.

This study has combined an understanding of the localised hydrogeological conditions within the SEP with knowledge of the geotechnical characteristics of the rock mass to determine whether the current level of depressurisation within the pit is adequate in providing suitable pit slope stability for ongoing operations within the area.

9.2 Significance of Study

The Hamersley Province in Western Australia is an extensive area of BIF. Enrichment mechanisms (Taylor et al., 2001) particularly within the Brockman and Marra Mamba Iron Formations have transformed these formations into highly enriched iron ore sequences that are laterally persistent and can extend to great depths (~400 m).

The Brockman Iron Formation (DG1-3) holds the majority of high grade deposits with iron grades in excess of 64% comprised of enriched hematite, goethite and limonite with minor amounts of magnetite. These are most extensively deposited within the Mount Tom Price and Mount Newman regions.

Within the open pit mining industry, pits depths are increasingly being deepened as the easily accessible surface ore has been removed. This often involves excavating pit walls below the existing groundwater table, which can lead to instabilities within pit walls. Added to this is the timing and economic considerations which need to be accounted for in a working mine.

Located within the Mount Tom Price mine the SEP current pit floor (at the time of writing) is located at 600 mRL. The long term development plan for the western end of this pit includes a further 30 m of excavation to a final depth of 570 mRL. This currently poses a number of

stability issues that require resolution before any development can be undertaken. Additional issues include the location of the access ramp to the base of the pit.

The local hydrogeology of the Mount Tom Price area involves two main aquifer systems. The DG member of the Brockman Iron Formation with contributions from the upper mineralised section of FWZ make up the main semi confined aquifer within the area. The underlying low permeability MCS and MTS lithologies separate a secondary aquifer which is located within the WF. A dewatering program within Mount Tom Price has been ongoing since installation in 1994.

The SEP deposit is located within the fold nose of the Turner Syncline, it is of importance to the greater RTIO operations as a source of high grade hematite ore (>64% Fe). The structure of the SEP is unique in that the deposit lies in the base of a steeply dipping double plunging syncline that is intersected by the major Southern Batter Fault which runs parallel in strike to the Turner Syncline.

It has been noted that due to a lack of advanced dewatering within the SEP, passive horizontal drainage systems may not be able to provide a sufficient level of depressurisation in the available time frame. A primary focus has been placed on the SEP pits as operations have moved below the regional groundwater table, which is currently located at 597 mAHD.

Xamine Consulting Services (2008) and MiningOne (2009) have identified in respective geotechnical and design investigations for the proposed three stage long term mine plan, effective management of pore water pressures within the wall rock (especially the north wall) is essential through the current depressurisation system.

9.3 Conceptual Groundwater Flow Dynamics

The effectiveness of the current horizontal drainhole depressurisation system within the SEP was undertaken using a method of finite element numerical drawdown analysis. This provided a much greater understanding of the current flow dynamics and controlling mechanisms acting within the pit walls in both equilibrium and time dependant scenarios.

The key observations resulting from these investigations include:

- The complex structural setting within the northern wall of the SEP has shown to interact with high conductivity lithologies to promote preferential flow of groundwater from the underling WF aquifer. Recharge to the semi confined DG aquifer occurs as groundwater travels up shear zones within the SEPFZ before

migrating along Brunos Band. Where horizontal drainhole installations are present, water is then diverted toward the pit face. If ore units are intersected within the horizontal drain holes groundwater has been shown to reinfiltrate and form a perched groundwater table at the base of the pit on top of the confining MCS.

- The combination of vertical pumping wells for dewatering and passive horizontal drain holes for depressurisation has lead to generally positive responses in the drawdown of the SEP phreatic surface throughout pit developments to date. However, a number of compartmentalised zones have been identified within the Bullnose area and the western corners of the pit.
- An investigation into alternative methods of depressurisation has been recommended to ensure the ongoing management of pore water pressures within the northern pit wall during planned pit cut backs. Limiting recharge from the WF to the pit through stated preferential flow paths has been identified as a potential issue when the remaining DG aquifer is removed. Maintaining the proposed dewatering buffer will be difficult to achieve using the current system.
- Outputs from the conceptual analysis have been calibrated against real time site based monitoring data and have shown similar drawdown responses to horizontal drain hole installations. This confirms the model has accurately captured the influence of depressurisation drainage has on flow dynamics within the wall rock.
- Results obtained from the conceptual groundwater analysis have satisfied the initial hypothesis outline the research proposal by illustrating “a measureable decline in the pore pressure levels within the wall rock in response to the installation of passive horizontal drainholes”.

9.4 Limit Equilibrium Geotechnical Stability Modelling

A parametric geotechnical analysis was carried out to quantify the outputs portrayed in the conceptual groundwater analysis. Sensitivities within the anisotropic rock mass were assessed through a total of eight simulations utilising two strength characteristics and the generated groundwater profiles.

Fundamental outcomes resulting from this investigation include:

- The current pit geometry with four levels of activated horizontal drainage provides an adequate level of stability within the pit wall. This is confirmed as trials conducted

under both strength conditions yielded FoS values ≥ 1.60 which exceeds the RTIO acceptance criteria for slope stability.

- The majority of basal failure surfaces identified within this analysis have incorporated a release along the FWZ/MCS contact with magnitudes of such failures appearing to be of multiple bench scale.
- At the completion of this geotechnical sensitivity analysis the original hypothesis derived for this study can be confirmed as "a reduction in the phreatic surface (and associated pore water pressure) within the wall rock is reflected by a lowering in the respective FoS values for the slope".

9.5 Key Recommendations

- The importance of having a sound understanding of subsurface conditions has been emphasised throughout this study. The ability to design optimal pit shells for access and ore recovery as well as an effective dewatering and depressurisation system relies heavily on the a sound geological model. Further to this, time allocations to ensure forward planning deadlines are met can be significantly interrupted if adjustments to initial plans are required.
- As a result of this research a conceptual understanding of flow dynamics within structurally complex wall rock environment has been generated. This can be applied within future RTIO operations as a basis for forward prediction of potential dewatering and depressurisation requirements.
- It has been noted throughout the literature that there is an increasing dependency being placed on sophisticated numerical techniques to provide fundamental engineering solutions. It does not matter whether a problem has the benefit of a complete data set or whether widespread assumptions are included in a conceptual simulation. If there is a lack of basic conceptual understanding and emphasis placed on theoretical based analysis through solid engineering and geological precedent the reality of a solution has no means of being critiqued.

9.6 Recommendations for Future Work

- To constrain the influence of structural features on groundwater flow dynamics further monitoring instrumentation should be installed as suggested in the attached vibrating wire piezometer proposal.
- Further refinement of the Hamersley Group hydrogeological parameters should be undertaken to allow for increased accuracy in all analysis work. This is especially important with regards to storativity and specific yield values.
- Adjustments to the current Seep/w model through the inclusion of surface infiltration and aquifer recharge would provide a complete simulation of the dewatering process active within the area. This could therefore be applied as a base model for other sites comprising similar hydraulic characteristics with some simple changes to the initial input parameters. Additional improvements could be made by simulating the influence of a fifth level of horizontal drainage within the pit walls.

References

AHLBOM, K., ANDERSSON, J. E., NORDQVIST, R., LJUNGGREN, C., TIREN, S. & VOSS, C. (1991) Fjallveden study site - scope of activities and main results. Svensk Karnbrans-lehantering AB, Stockholm, SKB Technical Report 91-52.

ARYAFAR, A., ARDEJANI, F., SINGH, R. & SHOKRI, B. (2007) Prediction of Groundwater Inflow and Height of the Seepage Face in a Deep Open Pit Mine using Numerical Finite Element Model and Analytical Solutions. *IMWA Symposium 2007; Water in Mining Environments.* Cagliari, Italy.

ATKINSON, L. C. (2001) The Role and Mitigation of Groundwater in Slope Stability. IN HUSTRULID, W., MCCARTER, M. AND VAN ZYL, D. (Ed.) *Rock Slope Design Considerations.* SME.

BARLEY, M. E., PICKARD, A. L., HAGEMANN, S. G. & FOLKERT, S. L. (1999) Hydrothermal origin for the 2 billion year old Mount Tom Price giant iron ore deposit, Hamersley Province, Western Austrailia. *Mineralium Deposita,* 34**,** 784-789.

BARNES, G. E. (2000) *Soil Mechanic: Principal and Practice*, Macmillan.

BECKER, R. H. & CLAYTON, R. N. (1972) Carbon isotopic evidence for the origin of a banded iron-formation in Western Australia. *Geochimica et Cosmochimica Acta,* 36**,** 577-595.

BECKER, R. H. & CLAYTON, R. N. (1976) Oxygen isotope study of a Precambrian banded iron formation, Hamersley Range, Western Australia. *Geochimica et Cosmochimica Acta,* 40**,** 1153-1165.

BECKETT, K. (2007) Tom Price Mine Site Hydrology. Tom Price, Rio Tinto Iron Ore - Expansion Projects.

BELL, D. H. (1990) Nature, Occurance and Engineering Significance of Groundwater. *The New Zealand Geomechanics Society Symposium on "Groundwater and Seepage".* Auckland.

BELL, D. H. & PETTINGA, J. R. (1983) Presentation of Geological Data. IN BROWN, I. R. (Ed.) *Engineering for Dams and Canals.*

BLAKE, T. S. & BARLEY, M. E. (1992) Tectonic evolution of the Late Archaean to Early Proterozoic Mount Bruce Megasequence Set, Western Australia. *Tectonics,* 11**,** 1415-1425.

BLIGHT, G. E. (1980) The mechanics of unsaturated soils. *notes from a series of lectures delivered as part of course 270C at the University of California, Berkley.* Berkley.

BLOCKLEY, J. G., TEHNAS, I. J., MANDYCZEWSKY, A. & MORRIS, R. C. (1993) Proposed stratigraphic subdivisions of the Marra Mamba Iron Formation and the Lower Wittenoom Dolomite. Hamersley Group, Western Australia., Western Australia Geological Survey.

BROCKMAN SOLUTIONS PTY LTD (2007) Mt Tom Price, South East Prongs: Structural Geology Model. Vasse, WA.

BROWN, A. (1981) The Influence and Control of Groundwater in Large Slopes. *Third Annual Conference on Stability in Open Pit Mining.* Vancouver, BC., SME.

CAMPBELL, L. (2008) Personal Communication. Tom Price.

CIVIDINI, A. & GIODA, G. (2007) Back-Analysis Approach for the Design of Drainage Systems. *International Journal of Geomechanics,* 7**,** 325 - 332.

CORNFORTH, D. H. (2005) *Landslides in Practice; Investigation, Analysis and Remedial/Preventative Options in Soils,* New Jersey, John Wiley and Sons Inc.

CRAIG, R. F. (1997) *Soil Mechanics,* London, E & FN Spon.

CRONEY, D. & COLEMAN, J. D. (1960) Pore pressure and suction in soil, . *Pore Pressure and Suction in Soil* London, Road Research Laboratory, Department of Scientific and Industrial Research.

D'ACUNTO, B. & URCIUOLI, G. (2006) Groundwater regime in a slope stabilized by drain trenches. *Mathematical and Computer Modelling,* 43**,** 754-765.

DAS, B. M. (2002) *Principles of Geotechnical Engineering,* Pacific Grove, California, Brooks/Cole.

DE GRAAF, P. (2009) Personal Communication. Perth.

DEMING, D. (2002) *Introduction to Hydrogeology,* New York, McGaw Hill.

DEPARTMENT OF ENVIRONMENT (2004) "WA CRC FORGE EXTRACT" computer programme. *Surface Water Hydrology Series Report No HY20.* Government of Western Australia.

DOMAHIDY, G. (2008) Personal Communication. Perth.

DOULATI ARDEJANI, F., SINGH, R. N., BAAFI, E. & PORTER, I. (2003) A Finite Element Model to: 1. Predict Groundwater Inflow to Surface Mining Excavations. *Mine Water and the Environment,* 22**,** 31-38.

DUNCAN, A. C. (2003) Tom Price Marra Mamba South Deposit 2001, Structural and Stratigraphic Mapping., Hamersley Iron Pty Lfd.

EGGERS, M. (2008) Personal Communication. Sydney.

FELL, R., MACGREGOR, P., STAPLETON, D. & BELL, G. (2005) *Geotechnical Engineering of Dams,* London, Taylor and Francis Group plc.

FETTER, C. W. (1994) *Applied Hydrogeology,* Upper Sunday River, Prentice Hall.

FORTH, R. A. (2004) Groundwater and geotechnical aspects of deep excavations in Hong Kong. *Engineering Geology,* 72**,** 253-260.

FREDLUND, D. G. & RAHARDJO, H. (1993) *Soil Mechanics for Unsaturated Soils,* New York, John Wiley and Sons.

FREEZE, R. A. & CHERRY, J. A. (1979) Groundwater and Geotechnical Problems. IN FIRST (Ed.) *Groundwater.* Prentice Hall.

GEO-SLOPE_INTERNATIONAL (2007) Seep/W for finite element analysis.

GILHOME, W. R. (1975) *Mount Tom Price Iron Orebody, Hamersley Iron Province.*

HALL, J. (2003) The Practical Implementation of Dewatering and Depressurisation in Large Open Pits. *Fifth Large Open Pit Mining Conference.* Kalgoorlie, WA.

HAMERSLEY IRON PTY LTD (2000) Geology and Mineralogy of the Hamersley Province Iron Ores - Year 2000 update. Perth.

HARMEN, J., HORMAZABAL, E. & MARTINEZ, C. (2007) Fact and Fiction about Pit Slope Depressurisation. IN POTVIN, Y. (Ed.) *Slope Stability.* Perth,Wa.

HARMSWORTH, R. A. (1990).

HARMSWORTH, R. A., KNEESHAW, M., MORRIS, R. C., ROBINSON, C. J. & SHRIVASTAVA, P. K. (1990) *BIF-Derived Iron Ores of the Hamersley Province*.

HEDLEY, P. & DOMAHIDY, G. (2007) Hydrogeology, Hydrology and Hydrochemistry of the Pilbara Region. Perth, Rio Tinto Iron Ore Pty Ltd.

JEREMIC, B., CHENG, Z., TAIEBAT, M. & DAFALIAS, Y. (2008) Numerical simulation of fully saturated porous materials. *International Journal for Numerical and Analytical Methods in Geomechanics,* 32**,** 1635-1660.

KAUFFMAN, J. M. & VAN DELL, T. D. (1983) Integrating a groundwater data reconnaissance program into a mineral exploration program,. *Mining Engineering,* 35.

KIHM, J., KIM, J., SONG, S. & LEE, G. (2007) Three-dimensional numerical simulation of fully coupled groundwater flow and land deformation due to groundwater pumping in an unsaturated fluvial aquifer system. *Journal of Hydrology,* 335**,** 1- 14.

KRAPEZ, B. (1997) Sequence-stratigraphic concepts applied to the identification of depositional basins and global tectonic cycles. *Australian Journal of Earth Sciences,* 44**,** 1-36.

LI, P., LU, W., LONG, Y., YANG, Z. & LI, J. (2008) Seepage analysis in a fractured rock mass: The upper reservoir of Pushihe pumped-storage power station in China. *Engineering Geology,* 97**,** 53-62.

MACLEOD, W. N. (1966) The Geology and Iron Deposits of the Hamersley Range Area, Western Australia. *Western Australia Geological Survey Bulletin,* 117**,** 170.

MACLEOD, W. N., DE LA HUNTY, L. E., JONES, W. R. & HALLIGAN, R. (1963) A Prelimary report on the Hamersley Iron Province. North West Division: Western Australia Geological Survey.

MANDZIC, H. (1992) Mine water risk in open pit slope stability. *Mine Water and the Environment,* 11**,** 35-42.

MININGONE CONSULTANTS PTY LTD (2009) Tom Price - South East Prongs Pit Stage 3 Geotechnical Design For Rio Tinto Pty Ltd - DRAFT.

MOODY, L. F. (1944) Friction factors for pipe flow. *Transactions of the A.S.M.E,* 66**,** 671-684.

MORRIS, R. C. (1980) A Textural and Mineralogical Study of the Relationship of Iron Ore to Banded Iron-Formation in the Hamersley Iron Province of Western Australia. *Economic Geology,* 75**,** 184-209.

MORRIS, R. C. (1985) Genesis of iron ore in banded iron-formation in the Hamersley Iron Province of Western Australia. *Economic Geology,* 75**,** 184-209.

PARISEAU, W. G. (2007) *Design Analysis in Rock Mechanics,* Leiden, Taylor and Francis.

PELLS SULLIVAN MEYNINK PTY LTD (2005) South East Prong Pit, Tom Price: Geotechnical Review - DRAFT. Sydney.

PELLS SULLIVAN MEYNINK PTY LTD (2007) Tom Price Site Visit Report December 2006. Sydney.

POWELL, C. M., OLIVER, N. H. S., LI, Z. X., MARTIN, D. M. & J, R. (1999) Synorogenic hydrothermal origin for giant Hamersley iron oxide ore bodies. *Geology,* 27**,** 175-178.

POWERS, P. J., CORWIN, A. B., SCHMALL, P. C. & KAECK, W. E. (2007) *Construction Dewatering and Groundwater Control*, John Wiley and Sons, Inc.

PRESTON, M. J. R. (1995) Tom Price Hydrogeological Studies. Perth, Ultramafics Pty Ltd.

RAHARDJO, H., HRITZUK, K. J., LEONG, E. C. & REZAUR, R. B. (2003) Effectiveness of horizontal drains for slope stability. *Engineering Geology,* 69**,** 295-308.

RATHBONE, S. (2008) Personal Communication. Perth.

RIVERS, J. (1998) Mineralogy and geochemistry of carbonates from Tom Price Mine in Hamersley Group Rocks. *School of Earth Sciences.* Hobart, University of Tasmania.

ROBB, L. (2005) *Introduction to Ore-Forming Processes,* Oxford, Blackwell Science Ltd.

ROCSCIENCE INC (2006) Slide, 2D limit equilibrium slope stability for soil and rock slopes. Toronto.

ROSE, N. D. & HUNGR, O. (2007) Forecasting potential rock slope failure in open pit mines using the inverse-velocity method. *International Journal of Rock Mechanics and Mining Sciences,* 44**,** 308-320.

ROWE, J. & BEALE, G. (2007) Relieving the pressure; Core concepts and solutions in open pit water control. *Mining Magazine.*

ROZLAPA, K. (2008) Memorandum: Section 6 and South East Prongs Groundwater Modelling Progress Report 3. Perth, Aquaterra.

RTIO (2000) SEP Slope design Memorandum - Seepage faces and depressurisation. Tom Price.

RTIO (2008) Annual Aquifer Review. Tom Price, Rio Tinto Iron Ore.

RTIO (2009a) Hydrogeological Database. Tom Price.

RTIO (2009b) Tom Price Hydrogeology's response to failure mechanisms of SE slip, SEP. Tom Price.

RUTQVIST, J. & STEPHANSSON, O. (2003) The role of hydromechanical coupling in fractured rock engineering. *Hydrogeology Journal,* 11**,** 7-40.

SIMONSON, B. M. (2003) Origin and evolution of large Precambrian iron formations. *Geological Society of America***,** 231-244.

SIMONSON, B. M., HASSLER, S. W. & SCHUBEL, K. A. (1993) Lithology and proposed revisions in the stratigraphic nomenclature of the Wittenoom Formation (Dolomite) and overlying formations, Hamersley Group, Western Australia. *Professional Papers.* Western Australia Geological Survey.

SJOBERG, J. (1996) Large Scale Slope Stability In Open Pit Mining - A Review. Lulea, Lulea University of Technology, Division of Rock Mechanics.

SOLOMON, M. & GROVES, D. I. (1994) *The Geology and Origin of Australia's Mineral Deposits,* Oxford, Oxford University Press.

STARFIELD, A. M. & CUNDALL, P. A. (1988) Towards a methodology for rock mechanics modelling. *International Journal of Rock Mechanics and Mining Sciences & Geomechanics Abstracts,* 25**,** 99-106.

STEPHANSSON, O. (2003) Theme issue on hydromechanics in geology and geotechnics. *Hydrogeology Journal,* 11**,** 3-6.

SULLIVAN, T. D. (2007) Hydromechanical Coupling and Pit Slope Movements. IN POTVIN, Y. (Ed.) *Slope Stability.* Perth, WA.

TAYLOR, D., DALSTRA, H. J., HARDING, A. E., BROADBENT, G. C. & BARLEY, M. E. (2001) Genesis of High-Grade Hematite Orebodies of the Hamersley Province, Western Australia. *Economic Geology,* 96**,** 837-873.

THORNE, W. S., HAGEMANN, S. G. & BARLEY, M. (2004) Petrographic and geochemical evidence for hydrothermal evolution of the North Deposit, Mt Tom Price, Western Australia. *Mineralium Deposita,* 39**,** 766-783.

TRENDALL, A. F. & BLOCKLEY, J. G. (1970) The Iron Formations of the PreCambrian Group Western Australia: with special reference to the Crocidolite. *Western Australia Geological Survey Bulletin,* 119**,** 336.

TRENDALL, A. F., NELSON, D. R., DE LAETER, J. R. & HASSLER, S. W. (1998) Precise zircon U-Pb ages from the Marra Mamba Iron Formation and the Wittenoom

Formation, Hamersley Group, Western Australia. *Australian Journal of Earth Sciences,* 45**,** 137-142.

TSAO, T. M., WANG, M. K., CHEN, M. C., TAKEUCHI, Y., MATSUURA, S. & OCHIAI, H. (2005) A case study of the pore water pressure fluctuation on the slip surface using horizontal borehole works on drainage well. *Engineering Geology,* 78**,** 105-118.

TYLER, I. M. & THORNE, A. M. (1990) The northern margin of the Capricorn Orogeny, Western Australia - an example of an Early Proterozoic collision zone. *Journal of Structural Geology,* 12**,** 685-701.

WEBB, A. D., DICKENS, G. R. & OLIVER, N. H. S. (2003) From banded iron-formations to iron ore:Geochemical and mineralogical constraints from across the Hamersley Province, Western Australia. *Chemical Geology,* 197**,** 215-251.

WOODWARD, J. (2005) *An Introduction to Geotechnical Processes*, Spn Press.

WYLLIE, D. C. & MAH, C. W. (2006) *Rock Slope Engineering, Civil and Mining*, Spon Press.

XAMINE CONSULTING SERVICES (2008) Mt Tom Price Mine, South East Prongs Pit, Geotechnical Review with Design and Planning Recommendations and Adjustments.

Appendices

Appendix A: Structural Mapping data

- **SEPFZ Descriptions**

Appendix B: Geotechnical Data

- **Rockmass Characterisation Data**

Appendix C: Hydrogeological Monitoring Data

- **Piezometric Data and Hydrographs**
- **Dewatering Bore logs**
- **Horizontal Drainhole Drilling Logs**
- **Spatial Groundwater Analysis**
- **Proposed Vibrating Wire Piezometer Program**

Appendix D: Finite Element Numerical Model

- **Seep/W Drawdown Model**
- **Conceptual Transient Drawdown Videos**